URANIUM POTENTIAL OF THE CEMENT DISTRICT, SOUTHWESTERN OKLAHOMA

By

ROY FRANK ALLEN

Bachelor of Science

Texas A & M University

College Station, Texas

1974

Submitted to the Faculty of the Graduate College
of the Oklahoma State University
in partial fulfillment of the requirements
for the Degree of
MASTER OF SCIENCE
May, 1980

URANIUM POTENTIAL OF THE CEMENT DISTRICT,

SOUTHWESTERN OKLAHOMA

Thesis Approved:

Zuhair Al-Shaieb
Thesis Adviser

Douglas C. Kent

Gary J. Stewart

Norman N. Durham
Dean of the Graduate College

PREFACE

This thesis is concerned with the evaluation of the uranium potential of the Cement district, southwestern Oklahoma. The primary objective is to determine exploration targets of possible uranium mineralization. Examination of surface and subsurface radiometric anomalies, geochemical analyses of samples and a track-etch survey were utilized to determine the most favorable areas.

The author wishes to express his appreciation to his major adviser, Dr. Zuhair Al-Shaieb, and to the other committee members, Dr. Gary Stewart and Dr. Douglas Kent, for their assistance with the manuscript. Appreciation is also expressed to Dr. Richard Thomas for his valuable and stimulating assistance in the field and during preparation of the manuscript. The author wishes to thank Bendix Field Engineering, Inc. for funding during the study.

A note of thanks is given to Dr. Steve Tweedie for his assistance in the preparation of the Symap computer program. Thanks are also extended to Ms. Jeanne Vale for typing of the manuscript.

Special gratitude and thanks is expressed to my parents, Roy and Eva Jane Allen, for their understanding and support, and to my wife, Debbora, for her help in typing earlier drafts of the manuscript, her encouragement, and many sacrifices.

TABLE OF CONTENTS

LIST OF FIGURES

LIST OF PLATES

Plate

CHAPTER I

ABSTRACT

A detailed study of the uranium occurrence in the Cement district of southwestern Oklahoma was undertaken in order to delineate potentially favorable areas for uranium exploration. The only uranium ore body to have been mined commercially in Oklahoma to date was located at Cement. A number of additional surface and subsurface radiometric anomalies have been reported from the study area. One unique feature of the Cement district is the aureole of diagenetic alteration (expressed as marked changes in coloration and mineralogy) affecting the Permian sequence overlying the pre-Permian Cement Anticline. Six distinct diagenetic zones have been mapped in exposures of the Rush Springs Formation lying within or immediately adjacent to this alteration aureole. The diagenetic changes in this area are believed to be related to hydrocarbon micro-seepage, and the alteration aureole represents a favorable environment for the accumulation of uranium.

Computer-contoured data obtained from a track-etch (Alpha 2 detectors) survey (which measured the radon gas seepage from the sub-surface), combined with the distributions of geochemical, surface and subsurface radiometric, and ground water uranium anomalies, indicated that three localities within the study area are especially favorable for uranium accumulations.

CHAPTER II

INTRODUCTION

Although public and governmental acceptance of nuclear power plants is in a state of flux, future dependence on nuclear energy as a supplemental means of power generation during at least the next 20 years appears to be inevitable. Present economic trends have lowered the economic threshold of known uranium deposits. As a result, many deposits that were previously considered "uneconomic" have now become commercially viable ore bodies. In addition, uranium ore bodies located at depths of around 3,000 feet (1,000 m) are open to exploitation due to the technological development of *in-situ* leaching mining methods. The continued exploration of new and old uranium districts is necessary to insure the provision of the reserves needed to supply existing non-breeder nuclear power plants. To date the uranium deposit at Cement has been the only commercially mined ore body in Oklahoma. The deposit was mined in the mid-1950's. Since that time the price of uranium has increased five-fold. Uranium ground water and radiometric anomalies have been reported in the Cement district indicating that other possible economic deposits exist. This study was initiated to determine the uranium potential of the area.

Area of Investigation

The study area (Fig. 1) includes parts of Caddo and Grady Counties

in southwestern Oklahoma. The general shape of the area is rectangular. It measures 2 by 11 miles (3.22 km by 17.71 km), and has an approximate area of 22^2 miles (54.39^2 km). The surface outline of the study area parallels the axis of the subsurface Cement Anticline, and circumscribes the diagenetic alteration aureole within the red beds of the Rush Springs Formation overlying the anticline (Plate 1).

The town of Cement is located approximately in the center of the study area. The cities of Anadarko and Chickasha are located 8 miles (12.88 km) north and 9 miles (14.49 km) northeast of the study area, respectively. Three major highways intersect the study area. The H. E. Bailey Turnpike extends diagonally across the southeastern portion of the area, whilst Highway 19/277 trends east-west through the southern half of the area and connects the towns of Cement and Cyril. Highway 8 trends north-south through the western portion of the area and terminates at the town of Cyril.

In this portion of southwestern Oklahoma the mean average temperature ranges from the middle to lower 60's (degrees Fahrenheit; 18.3 to 16.1 degrees Centigrade). Average winter temperatures fall in the upper teens and twenties (degrees Fahrenheit; -8 to -4 degrees Centigrade) while summer highs of over 100°F (38°C) are common. The annual average precipitation is 28.1 inches (7.14 cm).

Purpose and Methodology

The purpose of the study outlined herein was the evaluation of the uranium mineralization and radiometric anomalies in the Cement district utilizing a variety of geologic, geochemical, and geophysical methods. The data obtained were used to outline specific areas considered

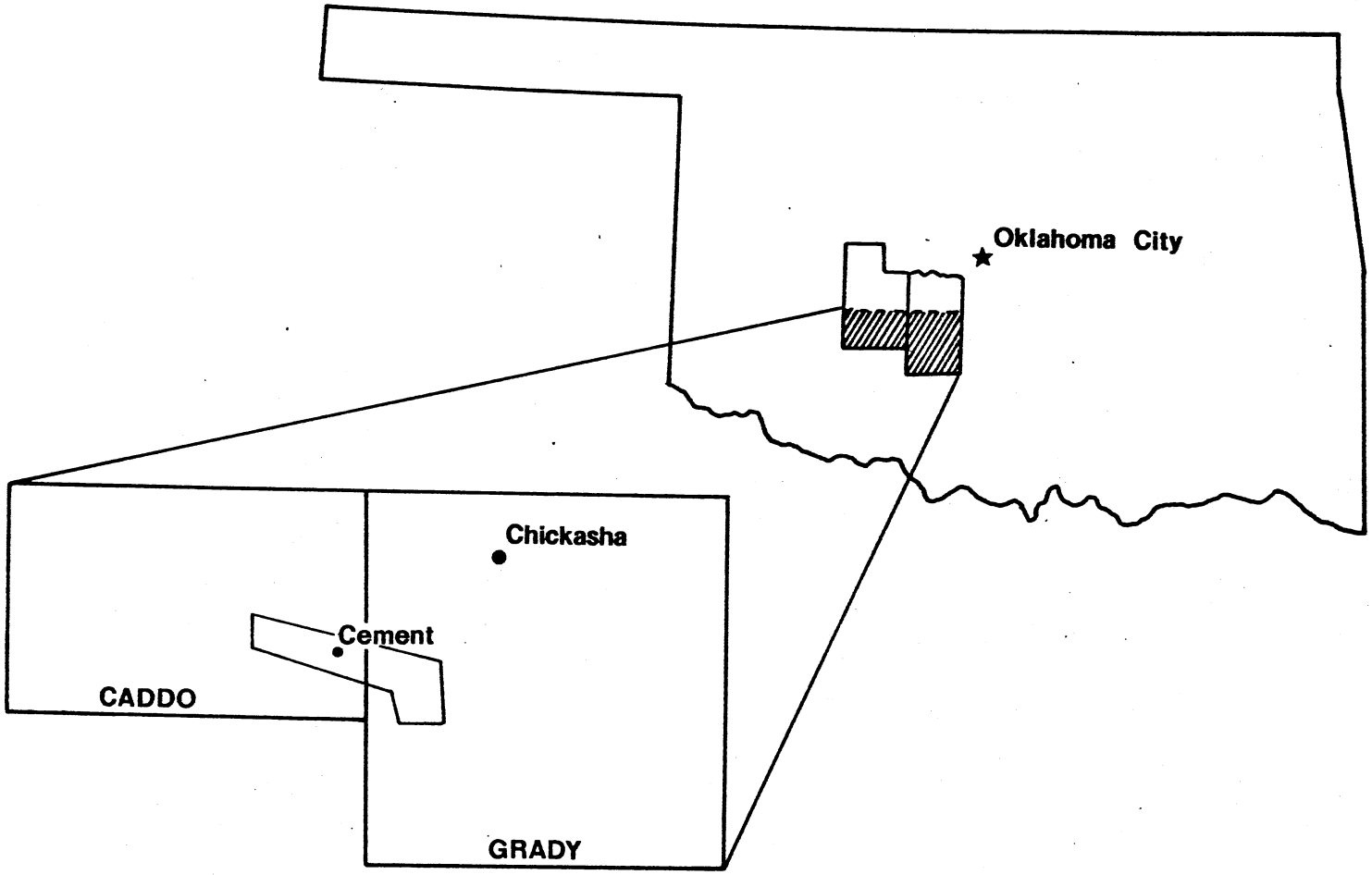

Fig. 1.--Index map of the study area.

favorable for the occurrence of uranium deposits.

The study involved eight main phases and these are briefly outlined below:

Phase One comprised the general geologic mapping of the area. During this mapping it became apparent that several distinct diagenetic "facies" existed within the Rush Springs Formation overlying the Cement Anticline.

Phase Two entailed detailed mapping of these coloration and cementation "facies" and resulted in the identification of six distinct diagenetic zones (Plate 2).

Phase Three involved locating previously reported surface radiometric anomalies and searching for new ones. A Scrintrex Model BGS-1s scintillation counter was used in a car-borne survey of the area.

Phase Four comprised the collection of rock, soil, and stream sediment samples from within the different alteration zones mapped in Phase Two. A total of 88 samples were collected (Plate 3).

In Phase Five these samples were analyzed using a variety of methods for a total of 30 elements (Appendix A). Uranium analysis was done by Uranium West Labs of Los Angeles, California, using delayed neutron-activation analysis. Analysis of the remaining 29 elements was done using a Perkin-Elmer 403 Atomic Absorption Spectrophotometer or a Philips PW 1540 X-Ray Fluorescence system. An Exploranium Model GR 410 Gamma-Ray Spectrometer was used at the geochemical sample locations shown in Plate 3. From the samples collected, 20 were selected for clay mineral analysis (Plate 3). A Philips X-Ray Diffraction machine was used for this purpose. Petrographic studies were also made of 20 other selected samples (Plate 3).

Phase Six entailed the utilization of Westinghouse Model 10411-AAR Alpha 2 Detectors in a track-etch survey. The data obtained from 150

detectors were used to construct a contour map of the values by means of a Symap Fortran program (Appendix E, Plate 13).

Phase Seven consisted of the examination of electric logs and gamma-ray logs from oil wells drilled in the area. This subsurface investigation was confined to the Permian sequence overlying the Cement Anticline and limited to a depth of 3,000 feet (1,000 m). Selected logs were used to construct nine cross sections through the area (Fig. 16; Plates 4 through 12).

Finally, Phase Eight entailed the evaluation of the data obtained and the delineation of the areas deemed most favorable for the occurrence of uranium deposits.

CHAPTER III

INTRODUCTION

Geologic Setting

The Permian sequence overlying the pre-Permian Cement Anticline is approximately 2,500 feet (760 m) thick. At the base of the Permian sequence is the Leonardian Wellington Formation which unconformably overlies the Upper Pennsylvanian Oscar Group, whilst the youngest member of the sequence is the Gaudalupean Cloud Chief Formation. The Late Paleozoic stratigraphic column used herein (Fig. 4) has been modified from Olmsted (1975). The formation subjected to the most detailed evaluation was the Rush Springs Formation because previous studies indicated that it constituted the most favorable environment for uranium accumulation.

Regional Tectonic Setting

The study area lies near the nose of the west-northwest to east-southeast trending Anadarko Basin and to the northeast of the eastern block of the Wichita Mountain Uplift (Fig. 2). Uplift of the Wichita Mountain block (Fig. 2) commenced in Early Pennsylvanian time and ended during the Wolfcampian Stage of the Permian Period. The early developmental phases of the southern Oklahoma aulacogen are reflected in the Cambrian igneous rocks of the Wichita Uplift. During the Cambrian period rifting was associated with the generation of both mafic and

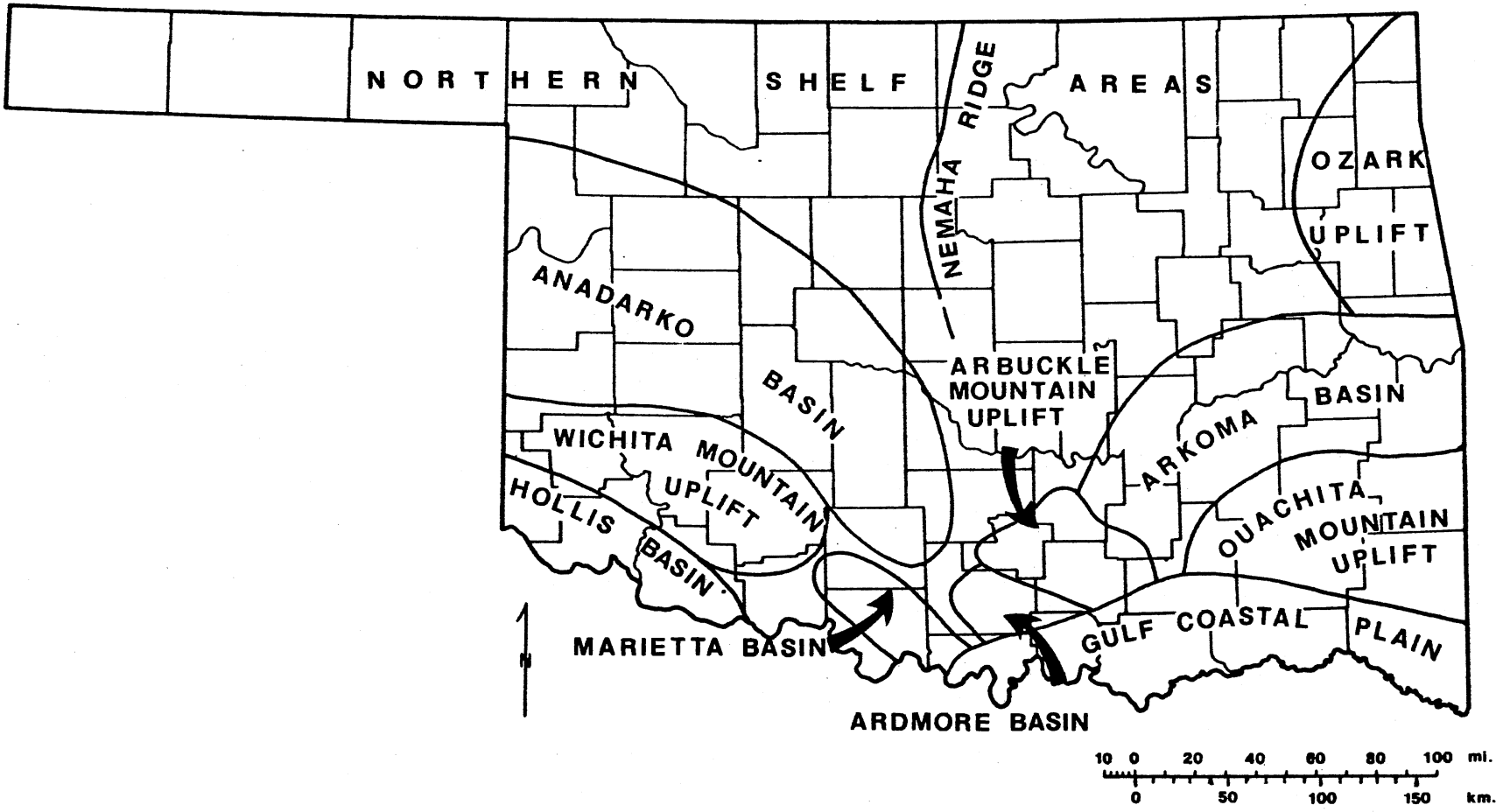

Fig. 2.--Major geologic provinces.

felsic extrusives and epizonal intrusives. The development of this rift system provided a suitable environment for the preservation of these volcanics (Al-Shaieb et al., 1977). Concomitant with the subsidence phase of aulacogen development was the deposition of a relatively thick Lower Paleozoic carbonate sequence together with interbedded shale and sandstone units. The formation of the Ouachita orogenic system (Fig. 2) involved a major compressional phase with related subduction according to the proponents of aulacogen development (Al-Shaieb et al., 1977). Associated with the Ouachita orogenic belt is the Anadarko Basin (Hansen, 1976) (Fig. 2). From Late Proterozoic to Middle Cambrian time the development of this basin was marked by extensional, graben-type tectonics and the emplacement of basic plutonic rocks (Hansen, 1976). Pennsylvanian through Permian time saw the final delineation and development of the Anadarko Basin. The igneous basement rock flooring the Anadarko Basin lies at depths of approximately 40,000 feet (12,000 m).

At the close of the Pennsylvanian the portion of southwestern Oklahoma, including the study area, was reduced to the proportions of a peneplain by erosion of the Wichita Mountain Uplift and the deposition of sediments in the Anadarko Basin (Becker, 1930). An unfaulted, gently-folded Permian section overlies the Pennsylvanian section in the study area.

Local Tectonic Setting

The Cement Anticline comprises a west-northwest trending anticline that is overturned slightly northward. A 2,500 foot (760 m) thick Lower (Wolfcampian) to Upper (Gaudalupean) Permian succession overlies a faulted and tightly-folded pre-Permian structure. A major south-dipping

reverse fault intersects the pre-Permian unconformity along the north flank of the anticline (Fig. 3). This fault parallels both the fold axis and a north-dipping normal fault system which has been truncated by the unconformity near the crest of the structure. The pre-Permian fold axis is also offset by several minor normal faults (Fig. 3). Minor structural deformation in post-Cloud Formation times produced a gentle near-symmetric upfold in the Permian units. As contoured on the top of the Rush Springs Formation, this anticline whose axis nearly coincices with that of the earlier Paleozoic structures is approximately 11 miles (18 km) long and 2 miles (3 km) wide (Reeves, 1921). Its crest is a topographic high dominated by two domes known as the East and West Cement Domes. These domes are spaced 4 miles (6.4 km) apart and are capped by the Moccasin Creek Gypsum Member of the Cloud Chief Formation (Fig. 4).

Stratigraphic Setting

The formations that compose the Permian section overlying the Cement Anticline are each described briefly below.

Permian System

Sumner Group

The Sumner Group comprises the Wellington Formation and the overlying Garber Sandstone (Fig. 4).

Wellington Formation. In this area the Ryan Sandstone bed forms the basal member of the Wellington Formation. Its thickness is approximately 80 feet (24 m). The basal sandstone has been described by Dott (1930) as massive, of medium hardness, and black to brown. Red shales

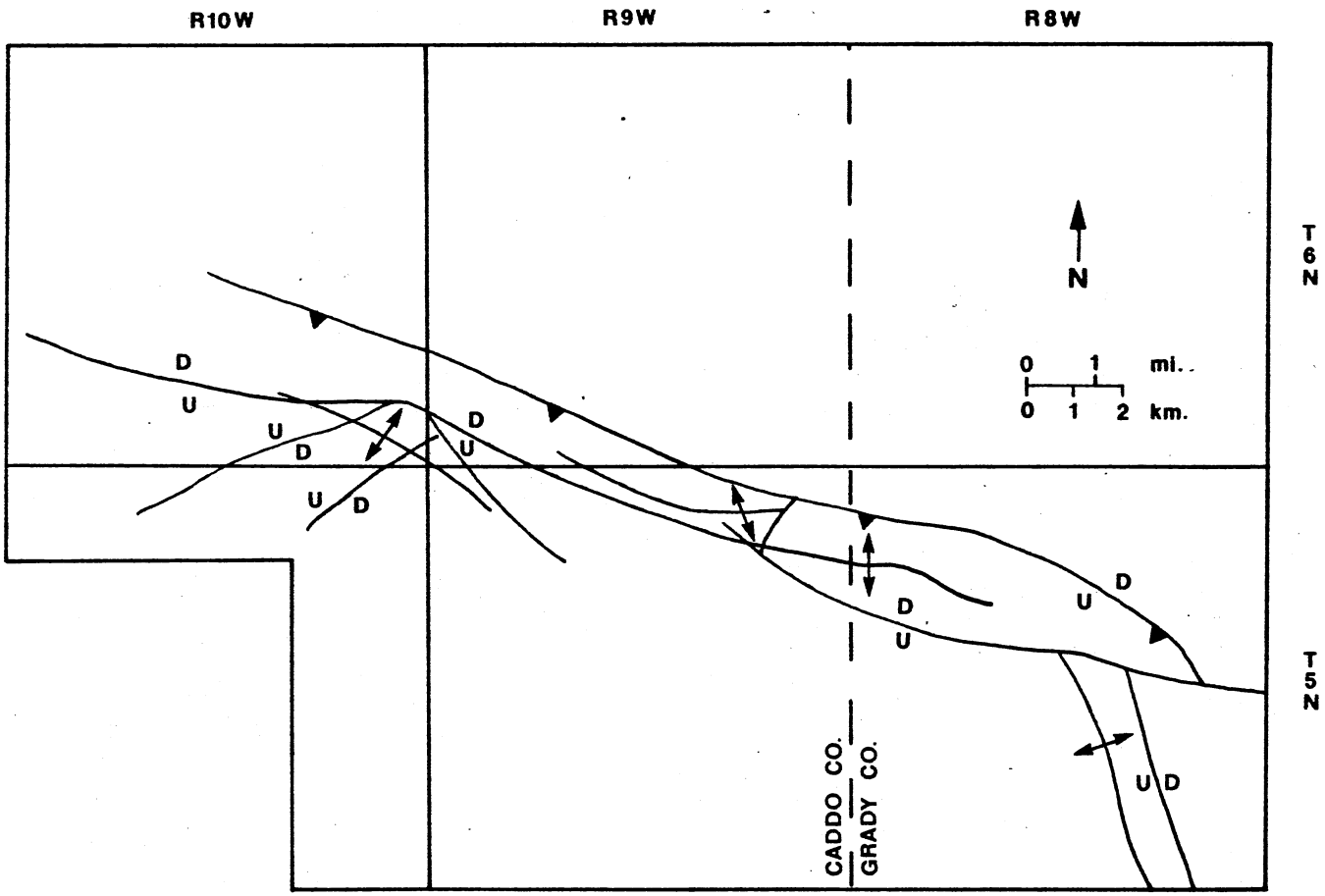

Fig. 3.--Pre-Permian structure.

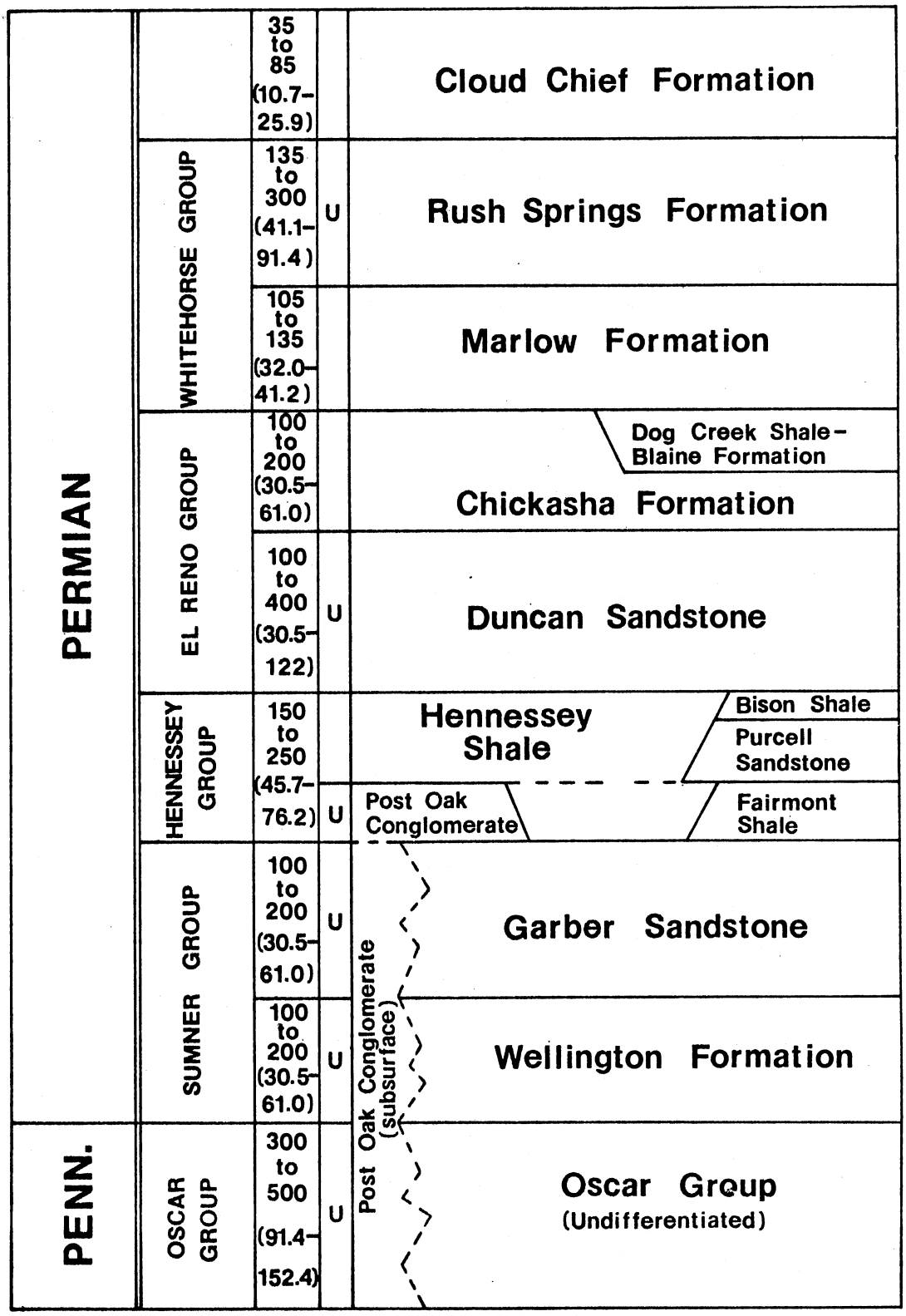

Fig. 4.--Columnar section.

containing several light-colored sandstone lenses overlie the Ryan Sandstone. The uppermost sandstone of the Ryan Sandstone Bed is thin-bedded, well cemented, and yellow, gray, or black in color. Shales of approximately equal thickness (80 feet, 24 m) overlie this sandstone member. These red shales also contain some thin, and locally a few massive, sandstone lenses. Local radiometric anomalies are associated with some of the sandstone members. The Wellington Formation is approximately 200 feet (61 m) thick.

Garber Sandstone. The reddish brown color of the sandstones within the Garber Sandstone Formation distinguish them from those of the underlying Wellington Formation. The Asphaltum Sandstone Bed (Bunn, 1930) is located at the base of the Garber sequence. Bunn (1930) described the Asphaltum Sandstone as a buff to gray, massive- to thin-bedded, calcareous sandstone which is locally asphaltic. It ranges from 20 to over 50 feet (7 to more than 16 m) in thickness. The coarsest grade members of the Asphaltum Sandstone Bed are separated by shale units and consist of carbonate- and clay-pebble conglomerate lenses.

Massive sandstone lenses occur locally within the Garber Sandstone. Generally, however, its constituent sandstone members are thin, hard, cross-bedded, and reddish brown, gray, or black (Dott, 1930). In the study area the Garber Sandstone is approximately 200 feet (60 m) thick.

Hennessey Group

Within the study area, the mappable argillaceous representative of the Hennessey Group is known as the Hennessey Shale Formation. The Hennessey Shale Formation contains the Fairmont Shale, Bison Shale, and Purcell Sandstone Members, undifferentiated. Close to the Wichita

Mountains Uplift the Hennessey Group is represented by the coarse distal stratigraphic equivalent of the Hennessey Shale known as the Post Oak Conglomerate (Fig. 4).

Hennessey Shale. The Hennessey Shale ranges in color from gray to reddish brown. Some light tan sandstone lenses occur locally within the Formation. The thickness of the Hennessey Shale in the study area is approximately 240 feet (70 m).

Towards the southwest of the study area the Hennessey Shale interdigitates laterally with the Post Oak Conglomerate (Fig. 4) which thickens toward the Wichita Mountains. At outcrop the thickness of the Post Oak Conglomerate is estimated as 500 feet (150 m), but in the subsurface (where it is known as "granite wash") it attains a maximum thickness of several thousand feet. The Post Oak Conglomerate is known to contain radiometric anomalies at outcrop and in the subsurface.

El Reno Group

The El Reno Group comprises the Duncan Sandstone and overlying Chickasha Formation, plus their lateral stratigraphic equivalents, the Dog Creek Shale and the Blaine Formation (Fig. 4). The Dog Creek Shale and the Blaine Formation are undifferentiated in the study area.

Duncan Sandstone. The Duncan Sandstone contains 2 to 3 massive, buff to gray-green, generally fine- to very fine-grained sandstones with some associated dolomitic lenses. The formation as a whole coarsens upward and its uppermost units are conglomeratic, cherty, and contain clay balls. Numerous siltstone and shale beds occur throughout the section. The Duncan Sandstone is approximately 250 feet (76 m) thick

in the study area. Radioactive anomalies occur in several of its constituent sandstones.

Chickasha Formation. The Chickasha Formation which consists of variegated sandstones, siltstones, shales, and mudstone conglomerates conformably overlies the Duncan Sandstone. The main distinguishing features of the Chickasha Formation relative to the Duncan Sandstone are its purple color and higher shale content.

Dog Creek Shale-Blaine Formation, Undifferentiated. Davis (1955) mapped the Dog Creek Shale and the Blaine Formation as an undifferentiated unit. The unit consists of red, blocky, silty shales. Fine-grained gypsiferous sandstones (locally, pure gypsum) are interbedded with the shales in the lower and middle portions of the sequence. The unit is approximately 70 feet (21 m) thick.

Whitehorse Group

The Marlow and Rush Springs Formation compose the Whitehorse Group (Fig. 4). They consist of fine-grained sandstones and siltstones interbedded with thin dolomite and gypsum beds.

Marlow Formation. The Marlow Formation is comprised of reddish brown, gypsiferous, silty shales together with fine-grained sandstones that contain gypsum concretions. Randomly oriented veins of satin-spar occur in the lower part of the formation. The middle of the Marlow Formation consists of light-brown lenticular sandstone called the Verden Lentil. Two thin-bedded dolomitic limestones, the Relay Creek and Emanuel Beds, separate the sandstones and shales in the upper part of

the formation. In the study area the Marlow Formation attains a thickness of 120 feet (37 m).

Rush Springs Formation. This formation consists predominantly of fine-grained, trough cross-bedded or horizontally-bedded quartzose sandstones. Normally these sandstones are red to light red due to the presence of iron-oxide coatings on the sand grains. In the study area the characteristic red color has been altered to buff, yellow, or white. The sandstones have been replaced with calcium carbonate in certain areas and concentrations of pyrite are found locally within these "limestones." The zone of sandstone alteration takes the form of an aureole overlying the pre-Permian Cement Anticline.

Outside the alteration aureole the Rush Springs Formation is remarkably homogenous. The poorly- to moderately-well sorted sandstones are generally fine-grained and are commonly friable despite the presence of moderate amounts of hematite and clay minerals which act as cementing agents. The quartz grains within these sandstones typically are subangular to subrounded. Siltstones and shales are minor constituents of the formation. Thickness of the Rush Springs Formation in the study area is approximately 250 feet (76 m).

Within its upper part, the Rush Springs Formation contains the Weatherford Gypsum Bed. The Weatherford Gypsum Bed is massive pink gypsum which, throughout most of Caddo County, is dolomitic with local variations to anhydrite or gypsum (Davis and Tanaka, 1963). Approximately 10 to 15 feet (3 to 5 m) of dolomitic sandstones and siltstones separate the Weatherford Gypsum Bed from the overlying Cloud Chief Formation. The Weatherford Gypsum Bed ranges from 1 to 40 feet (0.33 to 13.1) in thickness.

In several areas radiometric anomalies have been reported in the Rush Springs Formation, and a sandstone unit near the top of this formation acted as the host rock for the uranium ore body mined at Cement (Plate 14).

Cloud Chief Formation. The Cloud Chief Formation forms several outliers within the study area (Fig. 4). It consists of 60 to 120 feet (18 to 37 m) of gypsum and dolomite at the base overlain by 300 feet or more (100+ m) of siltstone, sandstone, and shale. The Moccasin Creek Gypsum Member is present at the base of the formation and is the only representative of this formation preserved within the study area. This basal member consists of massive pink to white gypsum which contains a few gray sandstone lenses. The Moccasin Creek Gypsum Member is approximately 85 feet (26 m) thick.

Environments of Deposition

The Permian red beds of southern Oklahoma were deposited in a variety of marine, marginal marine, and fluvio-deltaic environments (Davis, 1955).

The Anadarko Basin continually subsided through Permian time. Conglomerates, sandstones, siltstones, and shales plus carbonates and, locally, evaporites were deposited in the Basin. The Wichita Mountains provided the major source in terrigenous sediment (Fay, 1964). The Ouachita Mountains of southeast Oklahoma and northeast Texas constituted a minor source of clastic detrital material. The Wellington Formation, Garber Sandstone, and Hennessey Shale were deposited in deltaic, shallow marine, tidal flat, and supratidal environments (Davis, 1955) (Fig. 5).

The Ouachita Mountains are believed to have been the source area for most of the sediment comprising the Duncan and Chickasha Formations (Fay, 1964). These formations are considered to have been deposited in a fluvio-deltaic environment (Fay, 1964) (Fig. 5).

With the subsidence of the Chickasha Formation delta, the siltstones and sandstones of the Marlow Formation were deposited in a shallow transgressive sea (Fig. 5). Fay (1964) interpreted the Marlow Formation as being deposited in a brackish water to shallow marine environment, while MacLachlan (1967) interpreted the Marlow Formation as a tidal-flat deposit.

The Ouachita Mountains were uplifted in Late Permian time and formed the source area for Rush Springs Formation sediments (Fay, 1964). The depositional environment of the Rush Springs Formation has been interpreted as a shallow marine bay with sea level fluctuations exposing portions of the sands to aeolian reworking (Davis, 1955) (Fig. 5). Other interpretations include (1) coastal deposits where aeolian dunes are associated with marine strandline deposits (O'Brien, 1963), and (2) coastal dune deposits (MacLachlan, 1967). Rush Springs cross-bed orientations indicate polydirectional paleocurrents. The formation was probably deposited in several shallow marine, shoreface, and coastal plain environments. The constituent sand facies of the Rush Springs Formation may represent shallow marine offshore bars plus shoreface, beach-barrier, and localized backshore aeolian dunes. Climatic conditions during Rush Springs time were semi-arid to arid. Silts and shales within the formation represent the deposits of temporary coastal plain playa lakes or brackish backshore lagoons. The gypsum and dolomite beds may be coastal sabkha deposits whilst the thicker gypsum beds were probably precipitated after evaporative

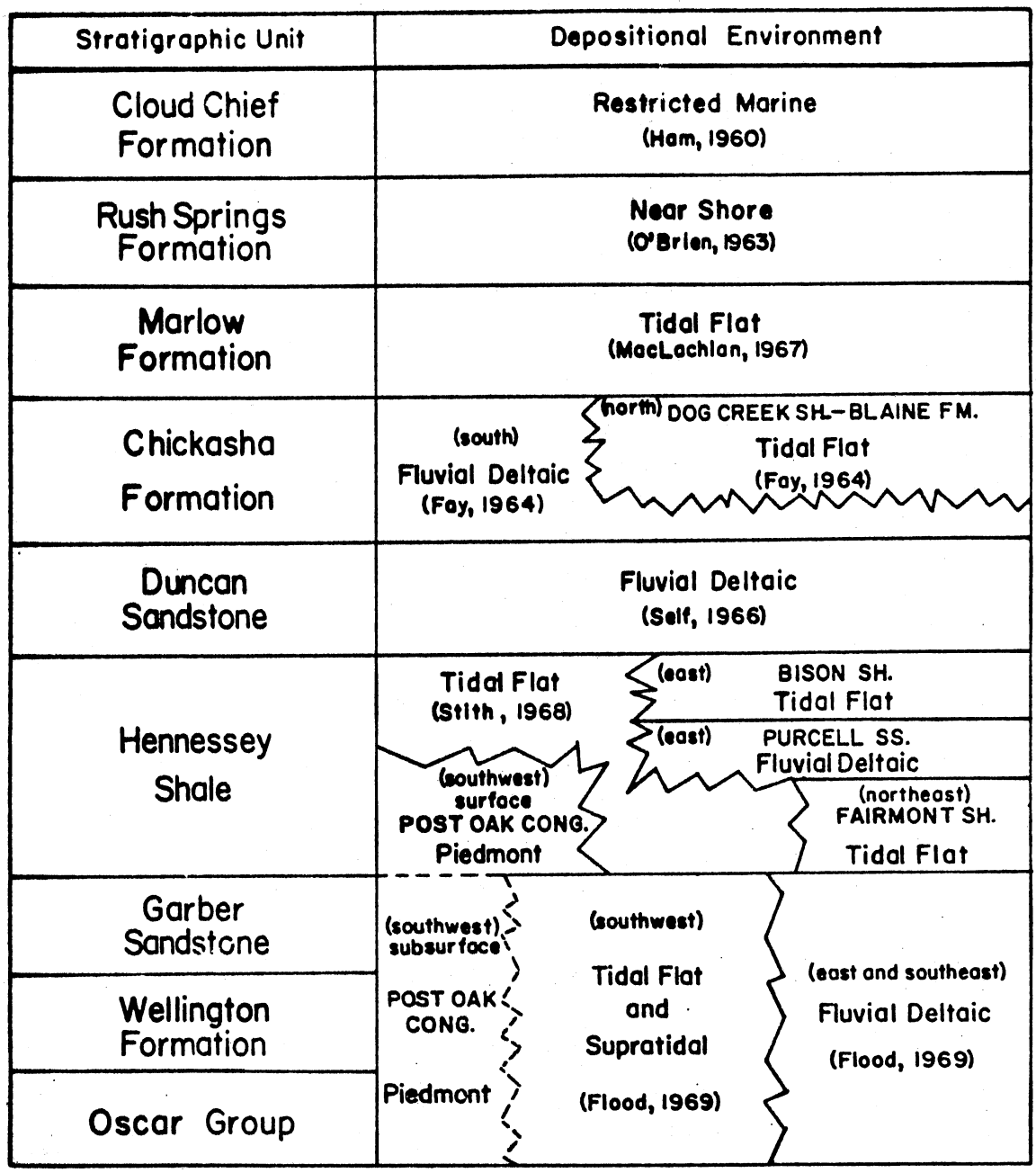

Fig. 5.--Stratigraphic unit and equivalent depositional environments, south-central Oklahoma (after Olmsted, 1975).

concentration from marine embayments of restricted circulation.

Deposition of the Cloud Chief Formation occurred within a restricted marine environment (Fig. 5). Ham (1960) believed deposition of the Cloud Chief Gypsum took place in a semi-enclosed arm of a sea into which influxes of sulfate-rich waters moved during minor transgressions.

CHAPTER IV

DIAGENETIC ALTERATION OF THE RUSH SPRINGS FORMATION IN THE CEMENT DISTRICT

One of the most remarkable features of the Cement Anticline is the marked alteration that has occurred (at outcrops and in the subsurface) in the coloration and mineralogy of the "normally" red-colored (hematite stained) Rush Springs Formation sandstones which overlie it (Plate 1). The outcrop distribution of this diagenetic alteration aureole was mapped in detail, and within it were identified six distinctive diagenetic zones (Plate 2). Petrologic and petrographic studies have been made of samples collected from Rush Springs Formation outcrops throughout the area. (Plate 3). An additional suite of surface samples was collected in order to determine the compositions of their clay mineral assemblages (Plate 3). The results of these studies were compared with those of earlier surface and subsurface investigations (Olmsted, 1975; Donovan, 1974; Al-Shaieb et al., 1977) in order to determine whether any new light could be shed upon the origin of the Rush Springs Formation diagenetic alteration and its relevance to the genesis of the Cement uranium ore body. The diagenetic zones were mapped in outcrops exposed along county roads and on private land where accessible. The distinguishing characteristics of each of the six diagenetic zones of the Rush Springs Formation are outlined briefly below.

The unaltered "normal" red-colored sandstone of the Rush Springs

Formation were designated as diagenetic zone one (Fig. 6), and served as a "background" against which the various diagenetic changes present within the alteration aureole could be compared (Plate 2). The "average" fine-grained, unaltered Rush Springs Formation sandstone is highly porous, subarkosic arenite composed of quartz (50 to 60 percent), orthoclase (8 to 12 percent), microcline and plagioclase (2 to 3 percent each), and chert fragments (up to 1 percent). The quartz grains are poorly- to moderately-well sorted and angular- to well-rounded (generally subangular to subrounded). Minor constituents include clay and silt fragments; detrital muscovite, biotite, chlorite, zircon, and sericite. Many pores are partially lined with authigenic illite and kaolinite, but hematite, which occurs as grain coatings and pore fillings, is the dominant cementing agent. Examples of clay mineral content are shown in Figure 7. Secondary silica overgrowths are present on a few quartz grains. Some sandstones contain superficial 1 to 5 mm diameter gypsiferous clots or pyrolusite or calcite nodules as broad as 1 cm in diameter. These are interpreted as the products of recent weathering processes.

Zone two is found north and south of the West Cement Dome and comprises unaltered Rush Springs Sandstone with hematite spotting (Plate 2, Fig. 8). The hematite spotting occurs as 0.5 to 1.0 cm diameter concretions of black hematite.

Rush Springs Sandstone altered to buff or yellow with limonite staining is mapped as diagenetic zone three (Fig. 9). Apart from a substantial loss of hematite, the overall petrologic makeup of the sandstone in zone three is similar to zones one and two. There is no carbonate cement present in zone three sandstones. A scanning electron

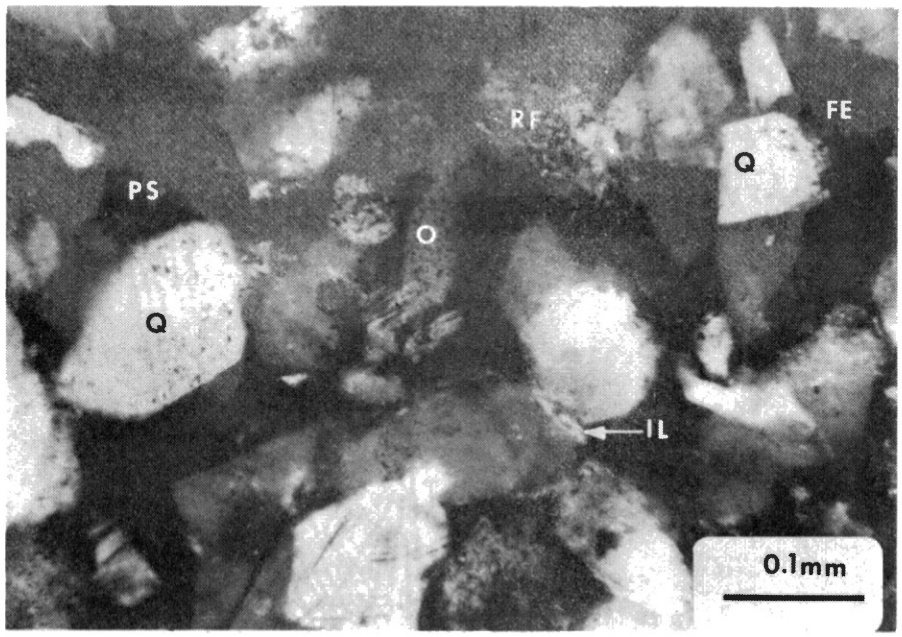

Fig. 6.--Photomicrograph of sample C-66 from diagenetic zone one. This sample of the "normal" red beds of the Rush Springs Formation is a subarkosic arenite. Note: hematite and illite (present as pore linings) are the dominant cementing minerals. Key: Q = quartz; O = orthoclase; RF = sedimentary rock fragment; HE = hematite; IL = illite; PS = pore space.

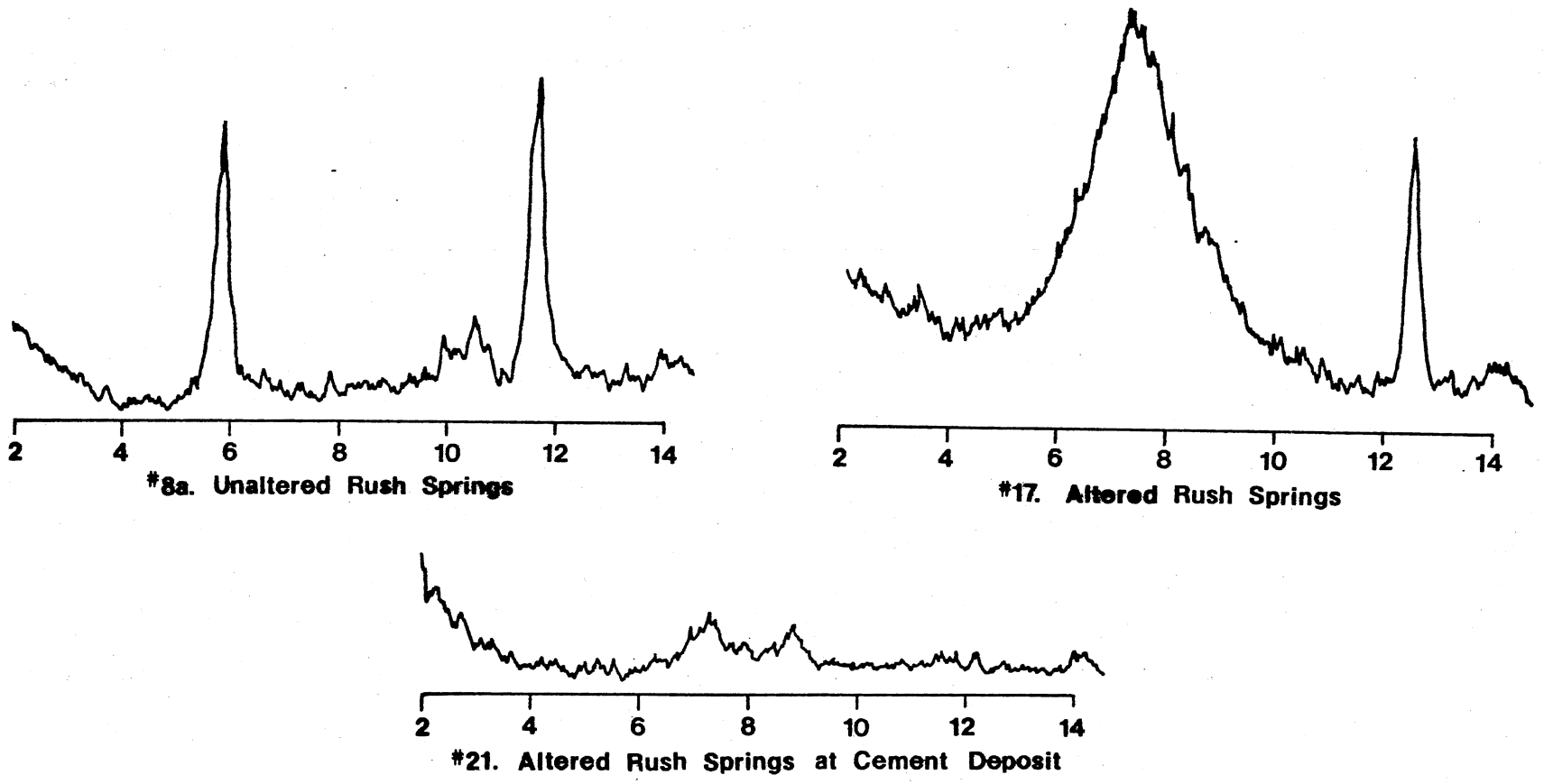

Fig. 7.--X-ray diffraction analysis for samples C-8a, C-17, and C-21. Analysis of sample C-8a, from zone 1, indicates smectite at 5.8° and chlorite at 11.7° as the dominant clay minerals. Analysis of sample C-17, from zone 3, indicates smectite at 7.1° and kaolinite at 12.4° as the dominant clay minerals. Analysis of sample C-21, from zone 4, indicates mixed layered clay minerals at 7.4° and 8.8°.

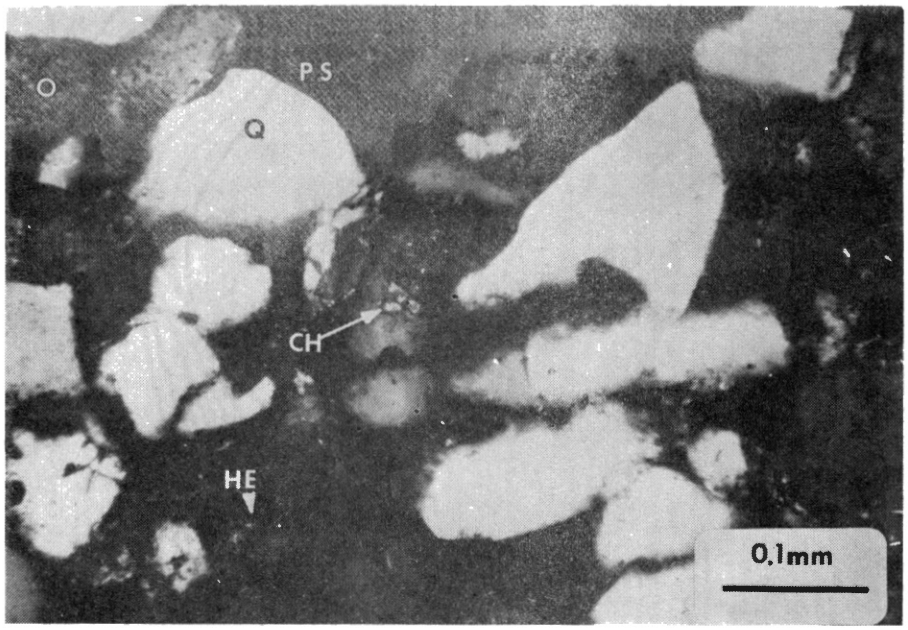

Fig. 8.--Photomicrograph of sample C-30 from diagenetic zone two. As in diagenetic zone one, this sample is a subarkosic arenite. Note: occurrence of clots of hematite granules and chlorite plates along grain boundary. Key: Q = quartz; O = orthoclase; HE = hematite; CH = chlorite; PS = pore space.

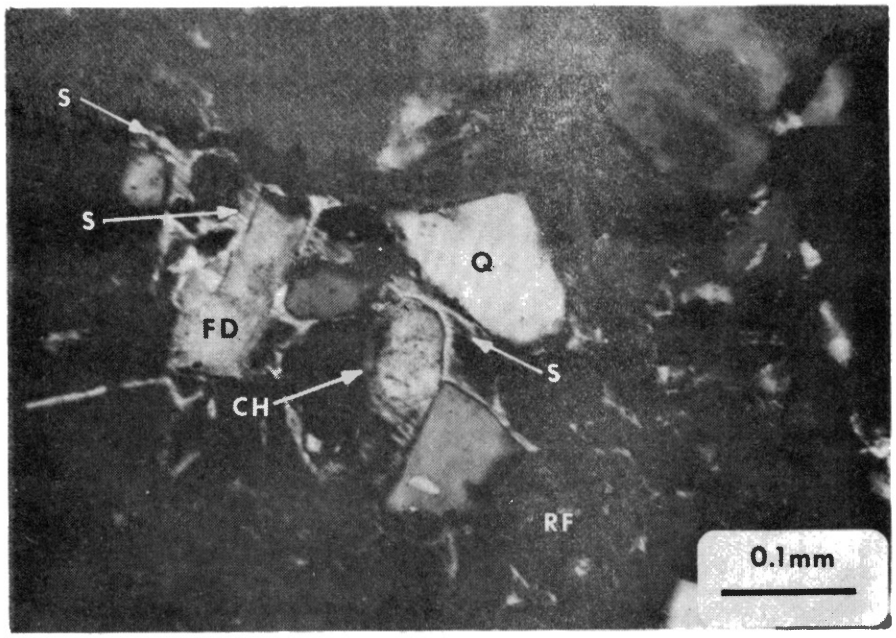

Fig. 9.--Photomicrograph of sample C-S-17 from diagenetic zone three. This sample of altered Rush Springs Sandstone is petrographically similar to those in zones one and two, except the presence of limonite instead of hematite. Note: chlorite present along pore lining and the presence of smectite along grain boundaries and in pore spaces. Key: Q = quartz; FD = feldspar; RF = rock fragment; CH = chlorite; S = smectite.

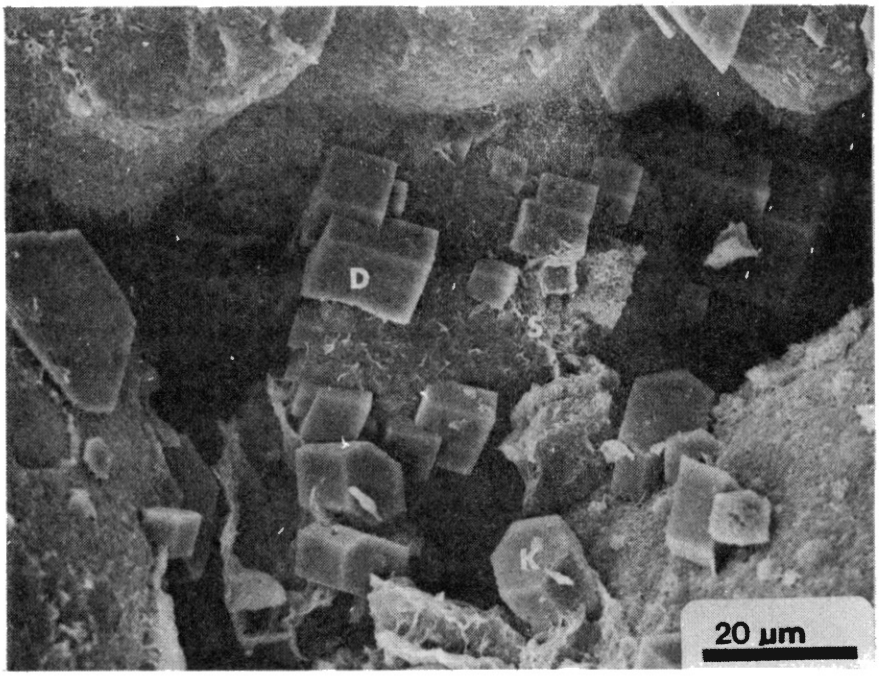

Fig. 10.--Scanning electron micrograph of sample C-S-17 from diagenetic zone three. As in Figure 9, smectite is present along grain boundaries. Note: presence of dolomite and kaolinite along pore linings. Key: D = dolomite; K = kaolinite; S = smectite.

micrograph from zone three is shown in Figure 10. The presence of smectite in zone three appears to have formed at the expense of illite indicated by the following reaction: Smectite + Al^{3+} + $K^{+} \rightleftarrows$ Illite + Si^{4+}. Zone three occupies a far larger surface area than any other diagenetic zones within the altered Rush Springs Formation outcrop. Generally, zone three is in contact with zone one.

Diagenetic zone four comprises altered Rush Springs Sandstone, similar to that of zone three, but is associated with sparry calcium carbonate cement (Plate 2, Fig. 11). The site of the Cement ore deposit, located at the East Cement Dome, lies within zone four. Two other areas are mapped as zone four. The first adjoins the east side of the West Cement Dome, while the second lies 1.5 miles (2.4 km) east of the East Cement Dome (Plate 2). The calcium carbonate is present in the pore spaces and as replacement of some of the detrital quartz and feldspar grains. Calcium carbonate comprises approximately 30 percent of the rock.

Zone five consists of "limestone" (Rush Springs Sandstone completely replaced with calcium carbonate) that contains pyrite (Fig. 12). Only one area, located 1.8 miles (2.9 km) east of the East Cement Dome, was mapped as zone five (Plate 2). The calcium carbonate in zone five has essentially totally replaced the detrital grains of the original sandstone and there are few pore spaces. The pyrite occurs as small (<1 to 10 mm diameter) concretions or in small veinlets throughout the rock. During mapping of the Rush Springs Formation it was noted that the Moccasin Creek Gypsum had also been replaced locally with calcium carbonate.

Diagenetic zone six is "limestone" (Rush Springs Sandstone completely replaced with calcium carbonate) containing no pyrite (Fig. 13). Only

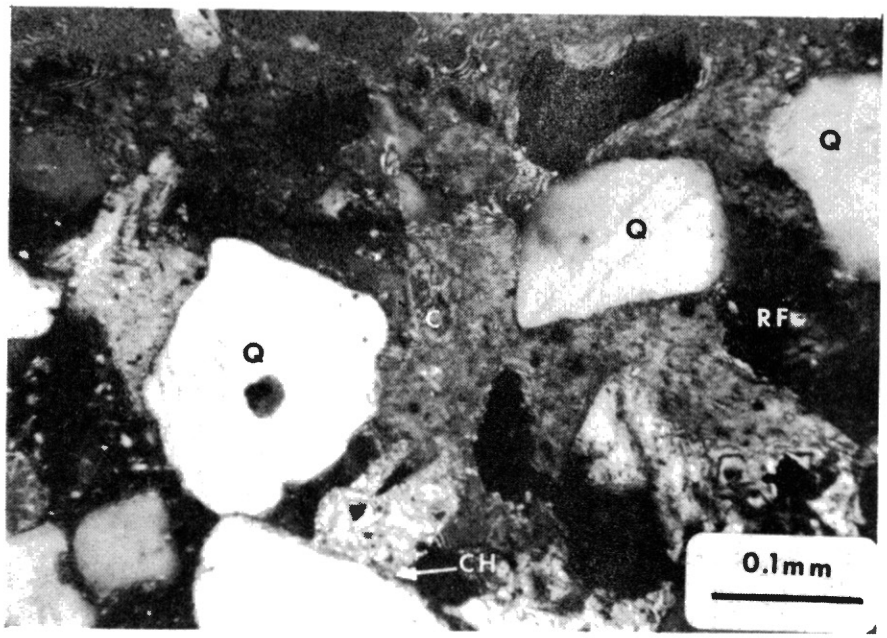

Fig. 11.--Photomicrograph of sample C-S-19B from diagenetic zone four. Altered Rush Springs near the Cement uranium deposit is shown in this sample. Note: calcium carbonate is the dominant cementing mineral, and the presence of chlorite along pore lining. Key: Q = quartz; RF = rock fragment; CH = chlorite; C = calcium carbonate.

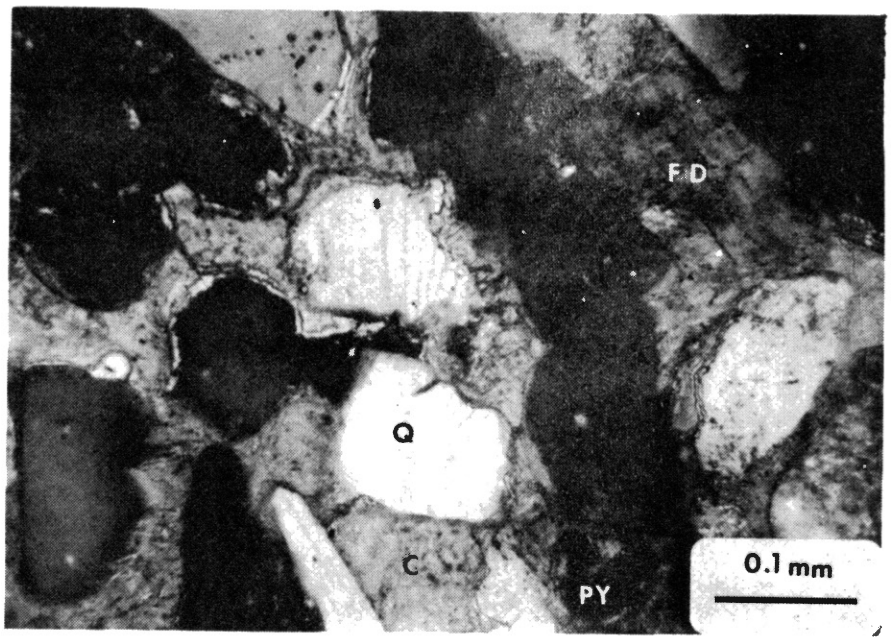

Fig. 12.--Photomicrograph of sample C-S-16 from diagenetic zone five. Rush Springs Sandstone being replaced by calcium carbonate is shown in this sample. Note: presence of pyrite. Key: Q = quartz; FD = feldspar; C = calcium carbonate; PY = pyrite.

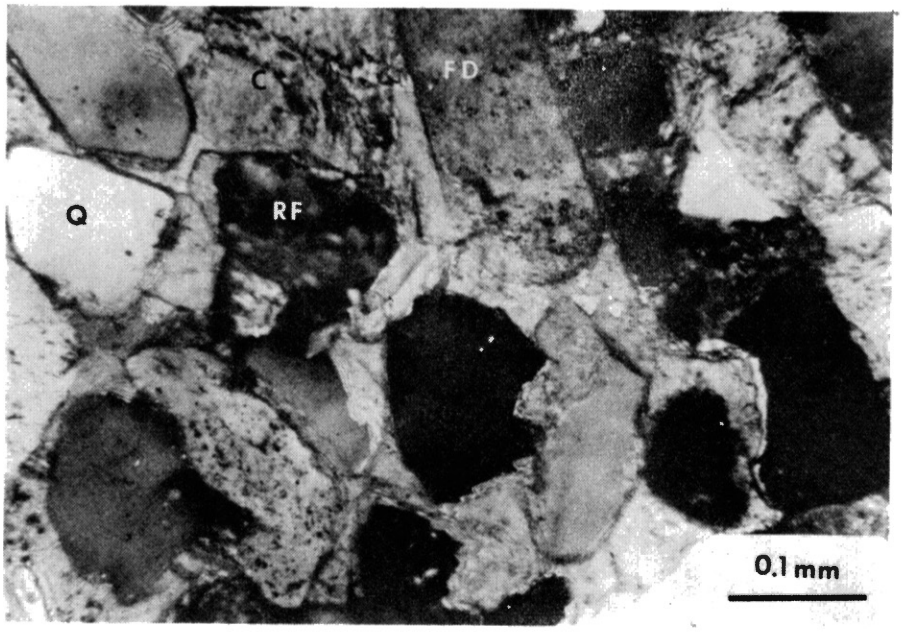

Fig. 13.--Photomicrograph of sample C-S-20 from diagenetic zone six. As in zone five, this sample shows calcium carbonate replacing Rush Springs Sandstone. Key: Q = quartz; FD = feldspar; RF = rock fragment; C = calcium carbonate.

one area, located at the Dolese Brothers, Inc. Quarry on the West Cement Dome, was mapped as zone six (Plate 2). As in zone five, zone six consists of sandstones whose original constituent grains have been totally replaced with calcium carbonate. The rocks are highly indurated and contain little pore space.

In the subsurface of the Cement District Donovan (1974) reported carbonate mineralization to a depth of 2,500 feet (760 m) in the sandstone of the Permian sequence. Approximately two-thirds of the distance up the flank of the Cement Anticline, the friable, reddish brown sandstones of the Rush Springs Formation showed a marked change to white, yellow, and pink (Donovan, 1974). Authigenic pyrite and magnetite have been recorded from subsurface samples of Permian sediments overlying the structure (Donovan et al., 1979).

The alteration of the gypsums (mainly the Moccasin Creek Gypsum Bed) and the sandstones of the Permian sequence has been attributed to hydrocarbon leakage (Donovan, 1974). Seepage was apparently controlled by the distribution of faults and the pre-Permian unconformity. The probable sources for the hydrocarbons were oil and gas reservoirs of Late Pennsylvanian (Missourian) age (Donovan, 1974). Calcium carbonate replacements of gypsum beds (originally anhydrite in parts of the Moccasin Creek Gypsum Bed) near the crest of the structure resulted from sulfates oxidizing the migrating hydrocarbons. Donovan (1974) stated that the reduction of the ferric oxides in the Rush Springs Formation was caused by hydrogen sulfide released either as a by-product of the sulfate-hydrocarbon reactions or associated with the escaping hydrocarbons. The change in the coloration of the sandstones was then produced by the breakdown of hematite which occurred with the removal of the soluble

ferrous ions. A general reaction of this process is: $Fe_2O_{3\,hematite} + 4S^{--}_{aq} + 6H^{+}_{aq} \rightleftarrows 2FeS_{2\,pyrite} + 3H_2O + 2e$. The soluble ferrous ions complexed with the sulfide anions to form pyrite. Subsequently, oxidation of the pyrite formed a hydrated limonitic complex which was readily removed in solution.

CHAPTER V

DESCRIPTION OF THE CEMENT URANIUM DEPOSIT AND ITS PROPOSED GENESIS

The site of the only once commercially mined uranium deposit in the study area is located at Cement near the crest of the Cement Anticline in the SW¼, NW¼, Sec. 3, T. 5 N., R. 9 W. (Plate 14). Ore minerals (carnotite and tyuyamunite) occurred disseminated within a series of poorly-defined, 3- to 5-foot-wide (1 to 1.5 m), and 3- to 6-foot-deep (1.5 to 2.0 m) "pods" along a 150-foot (46 m) length of the upper surface of a steeply southwest-dipping joint (McKay and Hyden, 1956). The mined trench gave radioactivity measurements ranging from 0.05 to 0.8 MR/HR (milliroentgens/hour). Approximately 13 tons (11.7 mt) of ore were mined, averaging 2.2 percent uranium. The host rock was a fine- to very fine-grained Upper Rush Springs Formation subarkosic sandstone composed primarily of quartz, orthoclase, plagioclase, microcline, and chert fragments. Both ore minerals occured as grain coatings and pore fillings within the sandstone. The average uranium:vanadium ratio of the ore was 2:1, and the average calcite content was 9 percent (McKay and Hyden, 1956). The sandstone was white with dark-brown, yellow-brown, and red stains along the ore zone. A halo of reddish brown sandstone was observed separating the ore zone from barren portions of the host. Away from the joint the sandstone was yellow with dark-brown staining. McKay and Hyden (1956) found non-radioactive pyrite nodules veined with

anhydrite of up to 6 inches (15 cm) in diameter within the yellow rock. The mineralized fracture is one of a system of joints trending N. 70°W. (McKay and Hyden, 1956). Stratigraphic controls are thought to have been unimportant in determining the orientation and geometry of the ore deposit.

Uranium in the Ground Water System

The transportation and precipitation of uranium in sandstones is dependent upon its interaction with the ground-water system. Ground water passing through the rock will tend to attain a uranium concentration which is approximately proportional to the uranium content of the rock. The amount of dissolved carbon dioxide, the pH, and the redox potential (Eh) of ground waters are the main parameters governing the types of soluble uranium complexes that form.

The ground-water system, at depth, may be considered a closed system that does, however, receive recurrent additions of CO_2 since atmospheric CO_2 has limited access to the system (Hostetler and Garrels, 1962; Langmuir, 1978). The carbonate content of the ground water will be reflected by the sum of the CO_2 within this closed system. An increase in the dissolved carbon dioxide will increase the stability field of the uranyl tricarbonate complex $[UO_2\ (CO_3)_3]^{-4}$ relative to the dicarbonate complex $[UO_2\ (Co_3)_2 \cdot 2H_2O]^{-2}$ (Fig. 14). However, when the total CO_2 decreases below $10^{-3.8}$M, the dominant species is the dicarbonate complex, and the uranyl tricarbonate complex is unstable and disassociates.

Uranium complexing is also controlled by the pH and the redox potential (Eh) of the ground waters. In the $U \cdot O_2 \cdot CO_2 \cdot H_2O$ system, uranium complexes are soluble in a wide range of pH (Hostetler and Garrels, 1962; Langmuir, 1978). Uranium occurs as the HUO_4^- ion in extremely alkaline

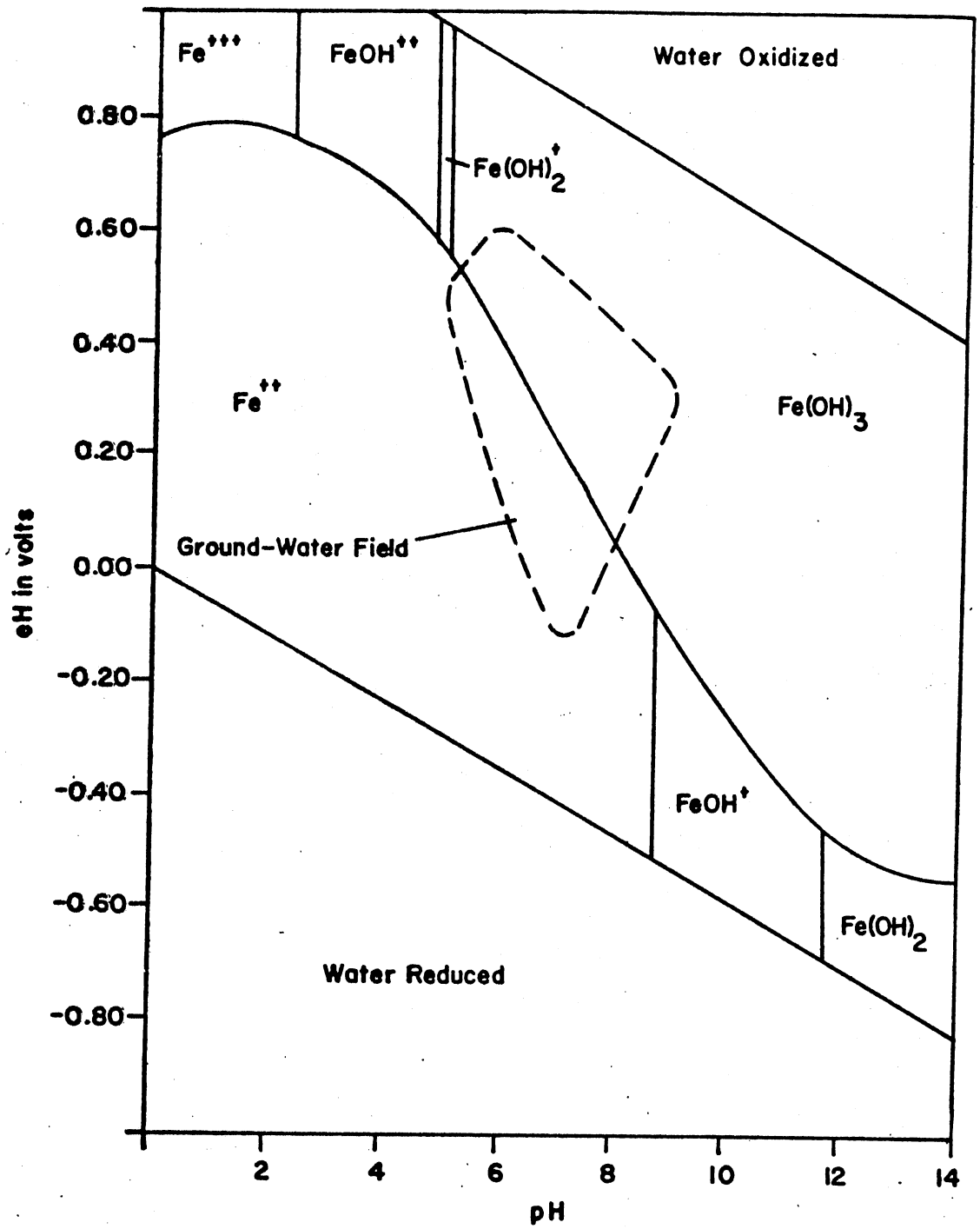

Fig. 14.--Stability field diagram for the aqueous ferric-ferrous system (after Olmsted, 1975; modified from Donovan, 1972).

solutions and the UO_2^{++} ion is found in strongly acidic solutions (Fig. 15). Stronger reducing agents are required to precipitate uranium with increasing alkalinity of the solution. The stability of carnotite is affected more by the ionic activities of potassium, uranium, and vanadium than by changes in the Eh and pH. Controlling factors in carnotite precipitation are the amounts of uranium, vanadium, and CO_2 dissolved in the ground water (Hostetler and Garrels, 1962; Langmuir, 1978).

Hostetler and Garrels (1962) found that sulfate and chloride ions will form complexes with uranyl and uranous ions. They determined that these complexes are negligible in most ground waters because they are only stable at very low pH ranges.

Genesis of the Cement Uranium Deposit

Uraniferous solutions, probably derived from the Wichita Mountain area, carried uranium to the Cement area as uranyl dicarbonate dihydrate $[UO_2(CO_3)_2 \cdot 2H_2O]^{--}$ and partly as uranyl tricarbonate $[UO_2(CO_3)_3]$ (Al-Shaieb et al., 1978).

As the uraniferous solutions passed through the sandstone of the Rush Springs Formation, precipitation of calcite stripped the carboante anion from the uranyl carbonate complex (Al-Shaieb et al., 1978). The abundance of carbonate replacements of quartz and feldspar in the sandstone near the ore body suggest that strongly alkaline conditions must have prevailed in the sandstone during deposition of the carbonate cement (Olmsted, 1975).

Hydrogen sulfide, which migrated upward along fracture systems and porous sandstones, reduced the freed uranyl cation. Diagenetic pyrite would indicate reducing conditions. The accumulation of uraninite

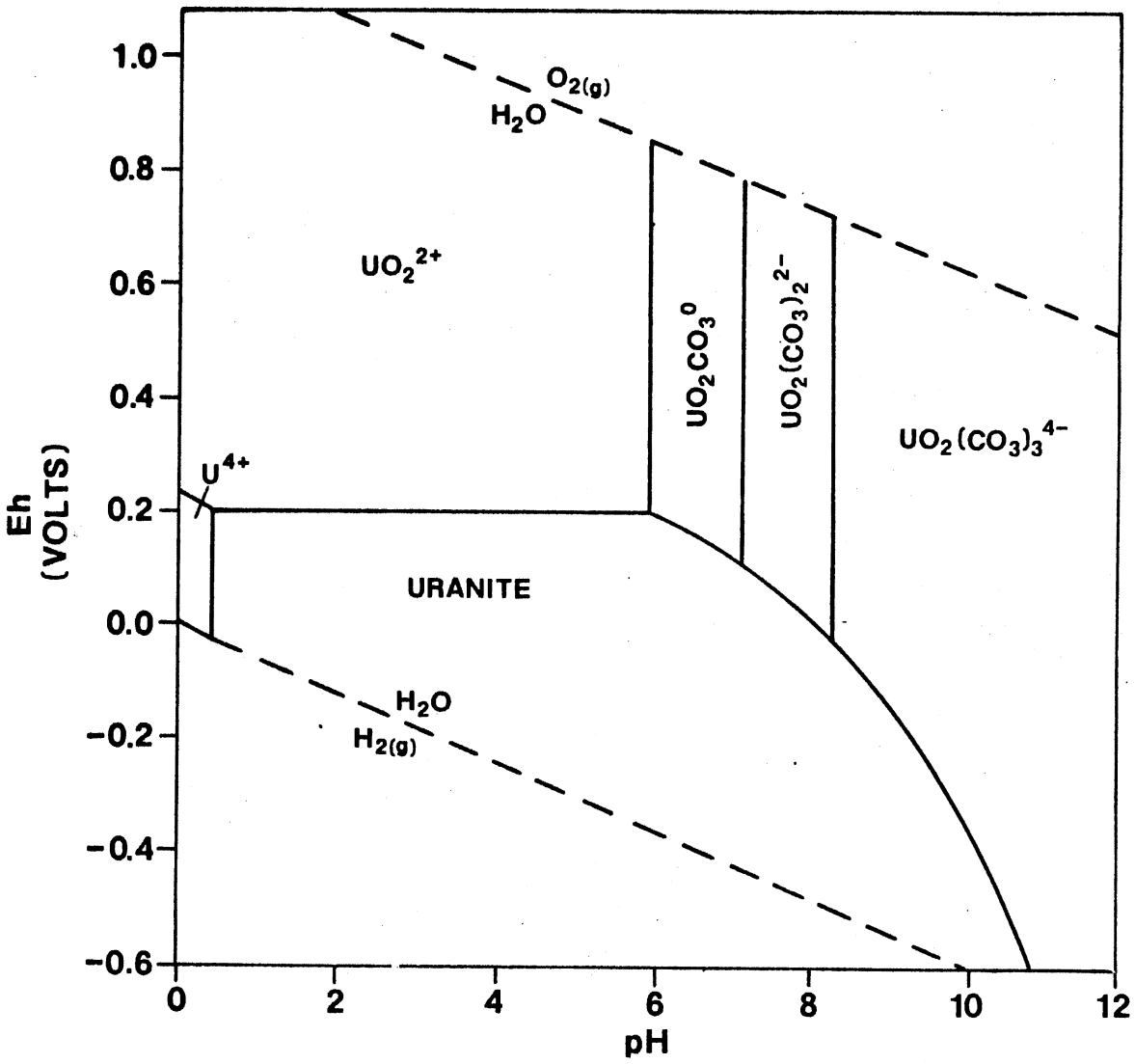

Fig. 15.--Uranite stability in typical ground water. Eh-pH diagram in the $U-O_2-CO_2-H_2O$ system at 25°C for $P_{CO_2}=10^{-2}$ ATM. Uranite $UO_{2(c)}$, solution boundaries are drawn at 10^{-6}M (0.24 ppm) dissolved uranium species (from Langmuir, 1978).

(UO_2) took place preferentially along the fracture because the reductants necessary for its precipitation in the prevailing, generally alkaline environment were at their most highly concentrated level along it. McKay and Hyden (1956) described diffusion bands of yellow, limonite-colored sandstone around the white host in the ore zone implying that the reduction effects diminished away from the fracture.

Oxidation resulting from a lowering of the water table at a later date resulted in the formation of carnotite [$K_2(UO_2)_2\ (VO_4)_2 \cdot 1\text{-}3\ OH_2O$] and tyuyamunite [$Ca(UO_2)_2\ (VO_4)_2 \cdot 7\text{-}10\text{-}\frac{1}{2}H_2O$]. The presence of these minerals suggest that calcium, potassium, and vanadium must have been present in the oxidizing solutions that passed through the host rock.

CHAPTER VI

INVESTIGATION OF THE URANIUM POTENTIAL IN THE CEMENT DISTRICT

Radiometric Anomalies

Four surface radiometric anomalies have been previously reported from the Rush Springs Formation in the Cement District. The most important of these is the Cement uranium deposit which was described in the preceding chapter. It is responsible for the only significant ^{214}Bi and $^{214}Bi/^{208}/T$ anomaly detected by the air-borne radiometric survey of the area undertaken by Geodata International in 1976. Radiometric readings at the deposit ranged from 0.05 to 0.80 MR/HR (milliroentgens/hour) (McKay and Hyden, 1956). Readings taken by the writer with a Scrintrex Model BGS-1s scintillation counter averaged 1,300 cps (counts per second) with a background of 150 cps. Mass spectrometer readings obtained at the site of the deposit were as follows: Total counts (per minute): 30190; K:1784; U:1810; and Th:58.

Olmsted (1975) reported two surface anomalies in the area. The first of these was associated with a Rush Springs Formation outcrop located in the SE¼, SW¼, Se. 2, T. 5 N., R. 9 W., where a radiometric reading of 0.03 MR/HR (milliroentgens/hour), against a normal background of 0.009 MR/HR (milliroentgens/hour), was recorded (Olmsted, 1975, p. 53). The anomally is along the contact between gray-green, thin-bedded, silty sandstone and an underlying massive, buff to gray, sandstone. The

second anomaly, located in the SE¼, SE¼, Sec. 31, T. 6 N., R. 9 W., is in a 1-foot (0.30 m) thick, reddish brown sandstone. Asphaltic concretions, some as much as 6 inches (15 cm) in diameter, were the most radioactive. Readings near the asphaltic sandstones averaged 0.07 MR/HR (milliroentgens/hour) against a background level of 0.009 MR/HR (milliroentgens/hour) (Olmsted, 1975).

The fourth anomaly was reported in 1968 by the United States Atomic Energy Commission. Fine to medium grained, well sorted sandstones of the Rush Springs Formation, which were red in places but bleached or limonite-stained, were exposed along a bulldozer cut. These sandstones gave readings ranging from 0.3 to 1.0 MR/HR (milliroentgens/hour) against a background radiation level of 0.03 MR/HR (milliroentgens/hour). This anomaly was located in Sec. 2, T. 5 N., R. 9 W. The third and fourth anomalies could not be located during the car-borne radiometric survey of the area.

Olmsted (1975) reported several anomalous zones in the subsurface, from his examination of gamma-ray logs of oil wells located in the area. According to Olmsted (1975) the gamma-ray log of Mobil Oil Company Surbeck No. 6 well, located in the NW¼, SE¼, Sec. 3, T. 5 N., R. 9 W., indicated the presence of three anomalous zones between 100 and 150 feet (29 to 49 m) below the surface. A second anomalous interval was apparent between 280 and 300 feet (92 and 98 m) below the surface, and a third anomaly was associated with a sandstone of the Hennessey Shale at a depth of 1,345 feet (441.3 m).

Olmsted (1975) also reported subsurface anomalies at several localities in Sec. 34 to 36, T. 6 N., R. 10 W., where the gamma-ray logs he examined indicated several anomalous zones within 2,900 feet (950 m)

of the surface. Gamma-ray logs from the following wells were reported as anomalous by Olmsted (1975): Ohio Oil Company Surbeck No. 4, Mobil Oil Company Surbeck No. 6, Palmer Oil Corporation Ulery No. 1 and No. 2, Palmer Oil Corporation Dixon No. 1 and No. 3, and Mobil Oil Company Lindsay No. 9. The locations of these wells and brief descriptions of their gamma-ray log anomalies are listed in Appendix B.

The car-borne radiometric survey using a Scrintrex Model BGS-1s scintillation counter resulted in the discovery of only one new minor anomaly, located in the NW¼, SW¼, Sec. 31, T. 6 N., R. 9 W. Scintillometer readings at this locality averaged 180 cps (counts per second) against a background level of 40 cps. This anomalous radioactivity was associated with a buff to yellow, fine-grained, massive-bedded sandstone of the Rush Springs Formation.

Additional radiometric readings were taken with an Exploranium Model GR 410 gamma-ray spectrometer at numerous sites throughout the area. The locations of these sites are shown on Plate 3, and the results obtained during this survey are listed in Appendix C. The following locations had uranium readings of approximately twice the normal background level: Numbers 33, 38, 42, 45, 50, 53, and 58.

Nine stratigraphic cross sections were constructed from electric and gamma-ray logs (Plates 4 through 12). The locations of the cross sections are shown in Figure 16. Two of the gamma-ray logs examined during this study were found to indicate previously unreported subsurface anomalies. The gamma-ray log of Stephens Petroleum Company Yule No. 5 well located in Sec. 1, T. 5 N., R. 9 W. showed a 20-foot thick (6.6 m) anomalous zone at a depth of 890 feet (290 m) below the surface. A 30-foot thick (10 m) anomaly at a depth of 2,560 feet (780 m) below the surface was found on

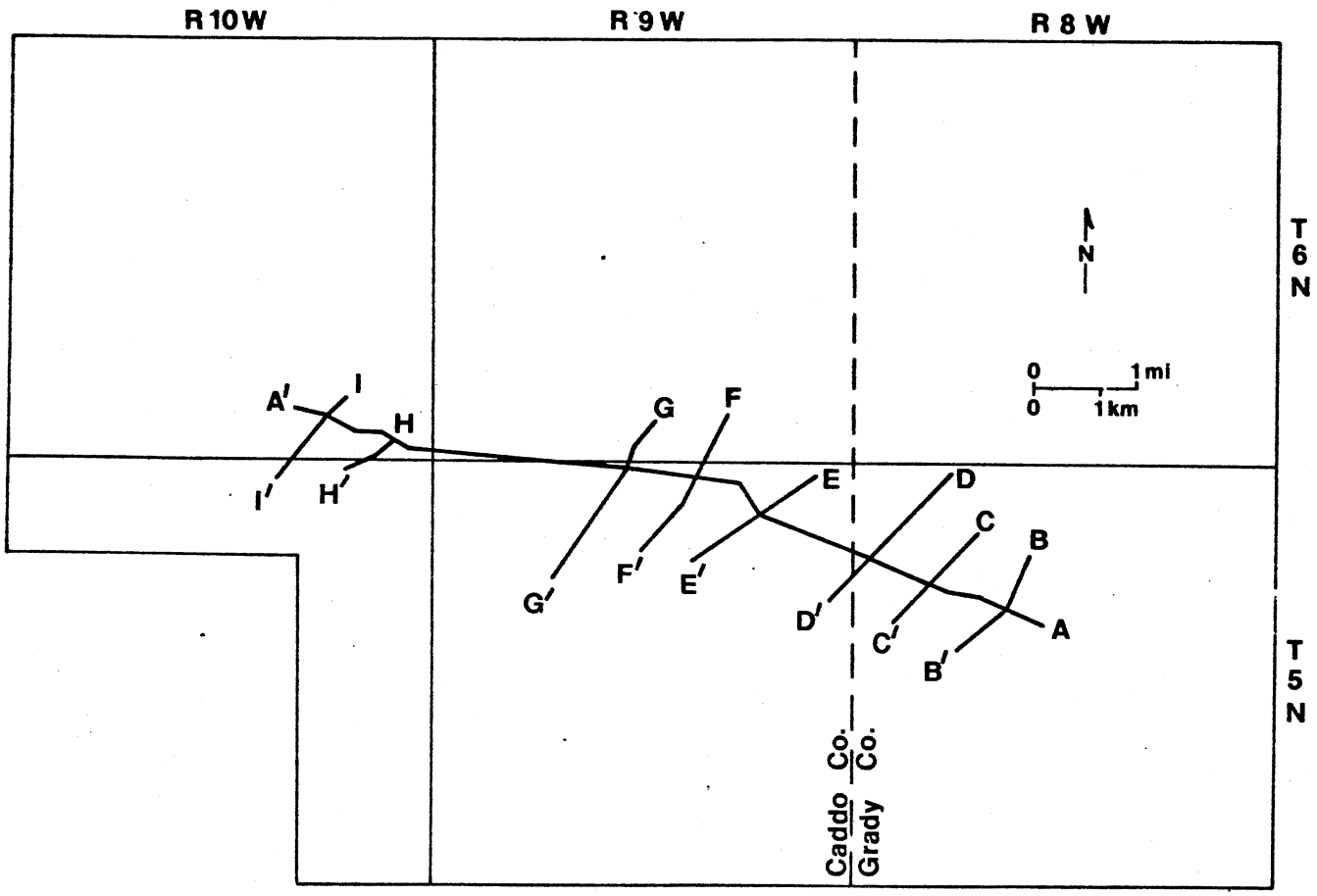

Fig. 16.--Locations of cross sections.

the log of Caddo Oil Company Vann No. 1 well located in the SW¼, SW¼, SW¼, Sec. 4, T. 5 N., R. 9 W.

Geochemical Anomalies

Sixty rock, 18 soil, and 2 stream sediment samples were collected for geochemical analysis. The locations of these samples are shown in Plate 3. Results for the 30 elements analyzed are listed in Appendix A. The only samples with an anomalously high uranium content were collected at the site of the Cement ore deposit. The following samples have anomalously high molybdenum contents: C-19, C-S-19b, C-S-19c, C-S-20a, and C-42 (Appendix D). Samples containing anomalously high values of other significant associated elements included: Vanadium - C-11a, C-12a, C-12b, C-S-13a, C-S-19c, C-33s, C-35s, C-45s, C-47s, and C-58s; Copper - C-S-13a and C-58s; Lead - C-33s (Appendix D).

Radon (Track-etch) Survey

Westinghouse Alpha 2 detectors were used in a radon (track-etch) survey in order to investigate any local anomalous radon-gas concentrations in the study area. Originally, 196 track-etch cups were planted. Of these cups, 150 were recovered and the resultant data were used to produce a contour map by employing a Symap Fortran computer program (Appendix E, Plate 13). Four major anomalies were defined by the computer contouring of the data. The most important anomaly (64 times background, with the statistical average background being 125 counts), is associated with the site of the Cement ore deposit, as is a further anomalous zone (16 times background) located directly north-northwest of the original mined trench. The second anomalous zone (16 times

background) is located approximately 2 miles (3.2 km) west of the East Cement Dome (mid-way between the East and West Cement Domes). The third anomalous area (16 times background) lies 1,000 feet (305 m) west of the West Cement Dome. A fourth anomalous area (16 times background) is located approximately 1.5 miles (2.4 km) northwest of the West Cement Dome (Plate 13).

Uranium Anomalies in Ground Water

The Rush Springs Formation is the principal aquifer in the area. Recharge to the Rush Springs was estimated by Davis and Tanaka (1963) as 10 percent of the average annual precipitation of 28.1 inches (71.4 cm). The range of depths to the water table in the Rush Springs Formation as a whole is 0 to 150 feet (0 to 46 m).

None of the ground water and stream sediment samples analyzed during the hydrogeochemical and stream sediment sampling reconnaissance (ORGDP, 1978), undertaken as part of the United States Department of Energy's National Uranium Resource Evaluation program, contained anomalous concentrations of uranium or associated trace metals. However, Olmsted (1975) reported several significant ground water uranium anomalies in the area (Fig. 17). Water samples collected by Olmsted (1975) from two wells located 200 feet (61 m) and 700 feet (213 m) north of the Cement ore deposit contained 120 to 160 ppb (parts per billion), and 465 to 860 ppb (parts per billion) uranium, respectively. Olmsted (1975) also reported high concentrations of uranium in water samples collected in Sec. 2, 4, and 11, T. 5 N., R. 9 W.

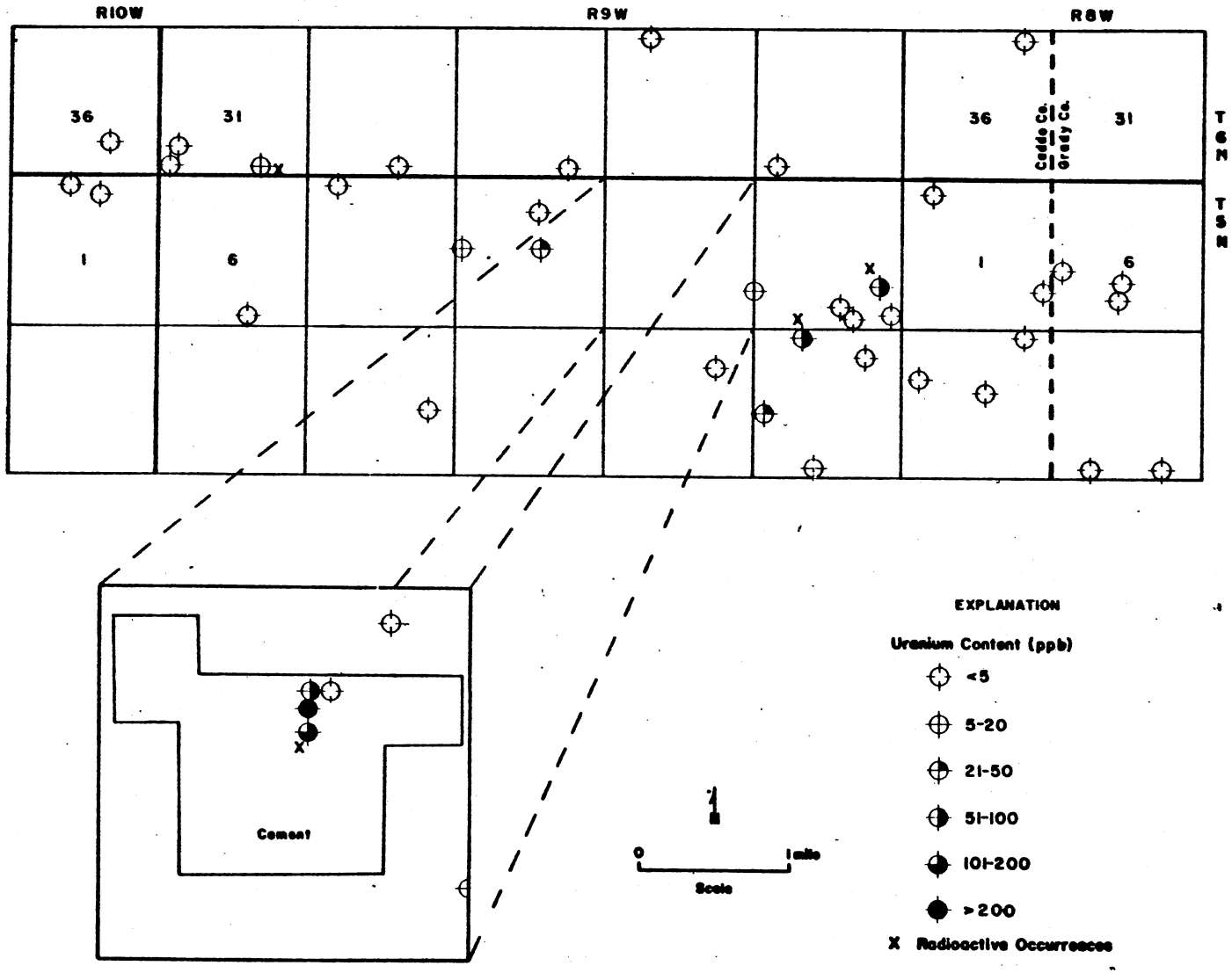

Fig. 17.--Ground water anomalies and radioactive occurrences in the Cement district (after Olmsted, 1975).

CHAPTER VII

EVALUATION OF FAVORABLE AREAS WITHIN THE CEMENT DISTRICT

Defining the areas within the Cement district adjudged most favorable for uranium accumulation was accomplished by integrating and interpreting the results of the previously described surveys and studies. While the Rush Springs Formation is the most promising environment for uranium deposition in the study area, clastic units within the majority of the undelrying Permian section are potentially favorable. Subsurface gamma-ray anomalies occur within the Duncan and Garber Sandstones, and are associated with sandstone bodies in the Chickasha Formation and the Hennessey Shale.

Favorable Areas

Three areas within the study area are considered especially favorable as potential locations of uranium accumulation (Plate 14). An evaluation of each of these areas is given below.

Area 1 (Plate 14), within which the original site of the Cement ore body is located, is regarded as the locality within the study area most likely to contain other uranium deposits. Four (previously described) surface anomalies are present within this area (Plate 14). Gamma-ray logs from several wells in this area contain zones of anomalous radioactivity (Plate 14). In particular, the gamma-ray log of the Mobil Oil

Company Surbeck No. 6 well shows a double kick at a depth of 90 feet (27 m) below the surface that is closely similar in character to a "typical" gamma-ray log in the vicinity of the "tails" of a "classic" roll-type uranium deposit as described by Gabelman (1977). Anomalous concentrations of the trace elements molybdenum and vanadium (which are commonly associated with uranium) are present within this area (Plate 14). The track-etch survey indicates a very strong radon anomaly (16 to 64 times background; background level being 125 cps) within Area 1 (Plate 14).

Similar criteria to those outlined above indicate that Area 2 (Plate 14) is a favorable environment for uranium deposits. A strong track-etch anomaly (16 times background) is present within Area 2. In addition, three surface radiometric anomalies occur within Area 2 and are associated with anomalous molybdenum values (Plate 14).

Finally, Area 2 is considered favorable because it exhibits three strong track-etch anomalies (all 16 times background; see Plate 14). Also, three gamma-ray logs from wells located within Area 3 show anomalously radioactive zones within 500 feet (152 m) of the surface. There is one surface radiometric anomaly located within Area 3 and it is associated with an anomalous vanadium value.

The three areas described above represent the most favorable areas for the accumulation of uranium ore deposits because of the presence within them of anomalous uranium concentrations in surface strata and ground water. In addition, they contain suitable host lithologies and, in the past, suitable reductants were available within them to promote uranium precipitation.

Discussion

The track-etch survey was used as a primary tool in the investigation of surface and subsurface anomalies and in the subsequent delineation of the above-outlined favorable areas. The use of track-etch surveys (which measure the amount of radon gas seeping from the subsurface) as indicators of uranium concentrations can be a valuable exploratory tool if the data they provide are interpreted properly.

Radon (^{222}Rn) is a part of the uranium (^{238}U) series decay chain and is associated with its parent, radium (^{226}Ra). Radon, which is a noble gas and has a half-life of 3,825 days, can migrate tens of meters before it decays, provided favorable porosity and permeability are available in the host rocks (Levinson, 1978). Radon gas is considered to migrate by either diffusion or by being transported in a fluid medium (air or water). The fluid transport method enables radon gas to migrate over large distances (up to several hundreds of meters) (Levinson, 1978).

Bloch (1979) has pointed out that sulfate-deficient oil field brines rich in radium (^{226}Ra) occur in Oklahoma and Kansas and that anomalous concentrations of radium do not necessarily indicate anomalous uranium concentrations. The transfer of radium from within individual mineral grains and away from grain boundaries to the pore solution can take place as a result of either solid diffusion through the grains or partial or complete dissolution of the grains (Bloch, 1979). Bloch (1979) showed that normal uranium concentrations in sandstone and shales can provide two-fold concentrations of radium. The writer believes that the Cement district's anomalous radon values (reflecting the concentration of radium) reported herein do reflect anomalous concentrations of uranium because (a) surface anomalies (radiometric and geochemical) occur

throughout the area, and (b) the Cement oil field does not produce sulfate-deficient brines.

The disequilibrium of $^{234}U/^{238}U$ of uranium ore bodies must be taken into account in the exploration and development of uranium deposits. Surface and subsurface uranium mineralization must be analyzed geochemically in order to determine its $^{234}U/^{238}U$ equilibrium ratio. The application of $^{234}U/^{238}U$ ratios in uranium exploration is an additional method of evaluating uranium mineralization (Levinson, 1978).

Conclusions

Surficial oxidized uranium deposits, similar to the original Cement ore deposit, are considered unlikely to be present within the three previously described favorable areas. However, the occurrence of oxidized (carnotite-type) deposits in the shallow subsurface (above the water table) cannot be ruled out. It is concluded that shallow (<200 feet, 61 m deep) joint-controlled uranite deposits are likely to occur (below the water table) within the strata of the Rush Springs Formation. Joint-controlled uranite deposits would be deposited under similar conditions as the Cement ore deposit (previously described) but not oxidized by ground water. Uranium present in such accumulations within these strata, could locally be remobilized by oxidizing ground waters. These uranium-bearing solutions percolating through the strata could have resulted in the formation of "classic" roll-type uranium deposits, provided that they encountered favorable reducing environments within the host sediments. Such environments would be characterized by suitable Eh and pH conditions (negative Eh, >6pH) and the presence of reductants such as pyrite or hydrogen sulfide gas. Sandstone bodies within the

Permian section overlying the Cement Anticline are interpreted as favorable host for "classic" roll-type uranium deposits.

Cement is the only town present within the study area, but unfortunately it represents a hindrance to an exploratory drilling program because it is located near the center of the most favorable area. Although the majority of the land in the Cement district is privately owned, virtually the entire area has been leased for oil and gas production. This would prove an additional obstacle in the path of any uranium exploration program.

BIBLIOGRAPHY

Adkinson, W. L., 1960, U.S.G.S. Oil and Gas Investigations Chart, OC 61.

Al-Shaieb, Z., et al., 1977, Evaluation of uranium potential in selected Pennsylvanian and Permian units and igneous rocks in southwestern and southern Oklahoma, GJBX-35-78: U.S. Department of Energy, Grand Junction, Colo., 240 p.

_____, _____, 1977, Uranium potential of Permian and Pennsylvanian sandstones in Oklahoma: Am. Assoc. of Petroleum Geologists Bull., v. 61, p. 360-375.

_____, _____, 1978, Guidebook to uranium mineralization in sedimentary and igneous rocks of Wichita Mountains region, southwestern Oklahoma: Published by Oklahoma City Geological Society, p. 61-73.

Bass, N. W., 1939, Verdes sandstone of Oklahoma, an exposed shoestring sand of Permian age: Am. Assoc. of Petroleum Geologists Bull., v. 23, p. 559-581.

Becker, C. M., Caddo County, in Oil and Gas in Oklahoma: Oklahoma Geological Survey Bull., v. 2, no. 40, p. 105-114.

Bolch, S., 1979, Origin of radium-rich oil field brines - a hypothesis, in Oklahoma Geology Notes: Oklahoma Geological Survey, v. 39, no. 5, p. 177-182.

Brown, O. E., 1937, Unconformity at base of Whitehorse Formation, Oklahoma: Am. Assoc. Petroleum Geologists Bull., v. 21, p. 1534-1556.

Bunn, J. R., 1930, Jefferson County, in Oil and Gas in Oklahoma: Oklahoma Geological Survey Bull., v. 2, no. 40, p. 341-381.

Chase, G. W., 1954, Occurrences of radioactive material in sandstone lenses of southwestern Oklahoma: Oklahoma Geological Survey Mineral Report, no. 25, p. 8.

Davis, L. V., 1955, Geology and ground water resources of Grady and northern Stephens Counties, Oklahoma: Oklahoma Geological Survey Bull., no. 73, p. 184.

_____, and Tanaka, H. H., 1963, Ground water resources of the Rush Springs sandstone in the Caddo County area, Oklahoma: Oklahoma Geological Survey Bull., no. 61, 63 p.

Degens, E. T., 1965, Geochemistry of sediments, a brief survey: Prentice-Hall, Inc., Englewood Cliffs, New Jersey, p. 14-54, 153-178.

De Voto, R. A., 1978, Uranium geology and exploration - lecture notes and references: Colorado School of Mines, Golden, Colo., 530 p.

Donovan, T. J., 1974, Petroleum microseepage at Cement, Oklahoma: evidence and mechanism: Am. Assoc. Petroleum Geologists Bull., v. 58, p. 429-446.

Donovan, T. J., et al., 1979, Aeromagnetic detection of diagenetic magnetite over oil fields: Am. Assoc. Petroleum Geologists Bull., v. 63, no. 2, p. 245-248.

Dott, R. H., 1930, Gavin County, in Oil and Gas in Oklahoma: Oklahoma Geological Survey Bull., v. 2, no. 40, p. 119-143.

Dyek-Willy, C., 1969, Uranium explroation using radon in soils: Canadian Mining Journal, v. 90, no. 8, p. 45-49.

Fay, R. O., 1964, The Blaine and related formations of northwestern Oklahoma and southern Kansas: Oklahoma Geological Survey Bull., no. 98, p. 238.

Fisher, R. P., and Stewart, J. H., 1961, Copper, vanadium and uranium deposits in sandstone - their distribution and geochemical cycles: Economic Geology, v. 56, p. 509-520.

Gabelman, J. W., 1977, Migration of uranium and thorium - exploration significance: Am. Assoc. Petroleum Geologists, Studies in Geology, no. 3, p. 40-76.

Geodata International, Inc., 1975, Aerial radiometric and magnetic survey of the Lawton National Topographic Map, Texas and Oklahoma: U.S. Energy Research and Development Administration, GJBY-34-76, Open-File Rept., v. 1 & 2, 61 p.

Green, D. A., 1936, Permian and Pennsylvanian sediments exposed in central and west-central Oklahoma: Am. Assoc. Petroleum Geologists Bull., v. 20, p. 1454-1475.

Grim, R. E., 1968, Clay Mineralogy: McGraw-Hill Book Company, New York,347p.

Gruner, J. W., 1956, Concentration of uranium in sediments by multiple migration-accretion: Economic Geology, v. 51, no. 6, p. 495-520.

Hagmaier, J. W., 1971, The relation of uranium occurrences to ground water flow systems: Bulletin of Earth Sciences, v. 4, no. 2, p. 19-24.

Ham, W. E., 1960, Middle Permian evaporites in southwestern Oklahoma, in Report of the Twenty-First Session Norden, Part 12, International Geological Congress, Copenhagen, p. 138-151.

Hansen, C., 1976, Subsurface Virgilian and Lower Permian arkosic facies, Wichita uplift - Anadarko basin, Oklahoma: Unpublished M. S. thesis, Oklahoma State University, 63 p.

Hart, D. L., 1974, Reconnaissance of the water resources of the Lawton quadrangle, southwestern Oklahoma: Oklahoma Geological Survey Hydrologic Atlas 3.

Herrman, L. A., 1961, Structural geology of Cement-Chickasha area, Caddo and Grady Counties, Oklahoma: Am. Assoc. of Petroleum Geologists Bull., v. 45, p. 1971-1993.

Hostetler, P. B., and Garrels, R. M., 1962, Transportation and precipitation of uranium and vanadium at low temperatures, with special references to sandstone-type uranium deposits: Economic Geology, v. 57, no. 2, p. 137-167.

Johnson, K. S., and Denison, R. E., 1973, Igneous geology of the Wichita Mountains and economic geology of Permian rocks in southwest Oklahoma: Geological Society of America Annual Meeting, Guide Book for Field Trip No. 6, Oklahoma Geological Survey, p. 33.

Krauskopf, K. B., 1979, Introduction to Geochemistry: McGraw-Hill Book Company, New York.

Langmuir, D., 1978, Uranium solution-mineral equilibria at low temperature with applications to sedimentary ore deposits: Geochimica Et Cosmochimica Acta, June, p. 136-149.

Levinson, A. A., and Coetzee, G. L., 1978, Implications of disequilibrium in exploration for uranium ores in the surficial environment using radiometric techniques - a review: Minerals Science Engr., v. 10, no. 1.

MacLachlan, M. E., 1967, Oklahoma, in Paleotectonic Investigations of the Permian System in the United States: U.S. Geological Survey Prof. Paper 515-E, p. 85-92.

McKay, E. S., and Hyden, H. J., 1956, Permian of north Texas and southern Oklahoma: U.S. Geological Survey TE I-640, p. 208-216.

Oak Ridge Gaseous Diffusion Plant, 1978, Hydro geochemical and stream sediment reconnaissance basic data for Lawton National Topographic Map Series Quadrangle, Oklahoma-Texas: U.S. Dept. of Energy Open-File Rept., p. 9-37.

O'Brien, B. E., 1963, Geology of east-central Caddo County, Oklahoma: Unpublished M. S. thesis, University of Oklahoma, 72 p.

Olmstead, R. W., 1975, Geochemical studies of uranium in south-central Oklahoma: Unpublished M. S. thesis, Oklahoma State University, 116 p.

Preliminary Reconnaissance for Uranium in Kansas, Nebraska and Oklahoma, 1951 to 1956, 1968, U.S. Atomic Energy Commission, Division of Raw Minerals, Grand Junction Office, AEC and U.S. Geological Survey, p. 44.

Reeves, R., 1921, Geology of the Cement Oil Field, Caddo County, Oklahoma: U.S. Geological Survey Bull., no. 726, p. 41-85.

Rigby, J. K., and Hamblin, W. K., ed., 1972, Recognition of ancient sedimentary environments; Society of Econ. Paleon. and Mineral., Spec. publ. no. 16.

Robinson, C. S., and Rosholt, J. N., Jr., 1961, Uranium migration and geochemistry uranium deposits in sandstone above, at and below the water table, Part II; relationship of uranium migration dates, geology, and chemistry of the uranium deposits: Economic Geology, v. 56, p. 1404-1420.

Stoever, E. C., Jr., 1957, Significant uranium deposit at Cement, Caddo County, Oklahoma: Oklahoma Geol. Notes, v. 17, no. 8, p. 77-78.

Sttawe, D. R., and Granger, H. C., 1965, Uranium ore rolls - an analysis: Economic Geology, v. 60, p. 240-250.

Symap, Laboratory for computer graphics and spatial analysis, Graduate School of Design, Harvard University, Cambridge, Mass.

Wedepohl, K. H., 1971, Geochemistry: Holt, Rinehart and Winston, Inc., New York, p. 106-155.

Weeks, A. D., and Eargle, D. H., 1963, Relation of diagenetic alteration and soil-forming processes to the uranium deposits of the southeast Texas coastal plain, in Clay and Clay Minerals, v. 10, Pergamon Press, New York, p. 24-41.

Wood, J. A., 1976, Basic data report on ground water levels in the Rush Springs sandstone area of southwestern Oklahoma, 1956-1976: Oklahoma Water Resources Board Publication No. 74, p. 3-13.

APPENDIXES

APPENDIX A

RESULTS OF ATOMIC ABSORPTION AND X-RAY FLUORESCENCE ANALYSES FOR THE CEMENT DISTRICT

	C-las	C-1a	C-2	C-2rs	C-3	C-4	C-5
U_3O_8	2.85	11.79	10.72	0.72	1.94	1.18	5.21
Ag	40	L10	L10	L10	L10	L10	L10
Al	339	272	167	230	190	278	280
As	L1	L1	L1	L1	L2	L1	L2
B	L10	15	L10	L10	L10	L10	L10
Ba	280	360	230	130	540	150	260
Be	L10	L10	L10	L10	L10	L10	L10
Ca	1052	1036	17738	1660	1881	257	1421
Co	7	5	4	6	5	5	5
Cr	13	10	7	6	8	10	12
Cu	7	10	12	3	11	5	8
Fe	220	156	43	66	87	118	136
La	11	ND	4.5	ND	ND	ND	4
Li	20	28	16	14	36	22	21
Mn	80	70	250	110	2140	100	120
Mo	L10	L10	L1)	L10	L10	L10	L10
Na	413	448	390	458	456	382	472
Nb	30	31	28	29	33	47	34
Ni	11	10	5	5	12	10	10
Pb	20	20	30	40	10	10	10
Sb	1.9	1.7	3.5	1.5	1.3	2.7	1.6
Sc	6.2	4	28	0.7	3.2	ND	4.8
Sn	3.2	2.5	9.1	ND	ND	6.1	2.5
Sr	100	140	270	ND	120	5	140
Ti	614	666	358	170	236	129	780
V	25	12	15	ND	ND	3	12
W	L10	L10	40	L10	L10	L10	L10
Y	28	28	24	24	27	44	29
Zn	24	26	22	32	76	25	26
Zr	416	390	349	342	201	413	515

L = Less than
ND = No data

	C-6	C-7	C-8	C-8a	C-9	C-S-9	C-10
U_3O_8	2.52	42.63	0.48	0.04	3.65	0.91	1.70
Ag	L10	L10	L10	L10	L10	20	L10
Al	279	115	215	6.8	268	219	249
As	L1	L1	L1	L1	L1	L2	L1
B	L10	L10	L10	L10	L10	L10	L10
Ba	330	230	110	240	370	300	300
Be	L10	L10	L10	L10	L10	L10	L10
Ca	800	1127	971	276	59	1080	1014
Co	5	4	3	6	4	3	5
Cr	9	9	7	10	11	8	11
Cu	8	10	6	4	6	6	9
Fe	114	29	73	64	136	66	145
La	ND	22	ND	6	ND	ND	ND
Li	17	6	11	12	18	12	30
Mn	50	1510	50	60	120	30	180
Mo	L10	L10	L10	L10	L10	L10	L10
Na	512	338	536	1583	496	543	488
Nb	31	24	31	22	31	32	32
Ni	10	11	8	9	11	7	11
Pb	10	20	10	10	10	10	12
Sb	1.7	6.2	1.6	4.5	1.8	1.7	1.6
Sc	1.9	56.7	ND	54	1.9	ND	3.1
Sn	2.1	17.2	1.9	12.6	2.4	2	1.9
Sr	150	260	160	ND	140	150	130
Ti	450	227	273	15	552	237	610
V	5	5	ND	ND	13	10	15
W	L10	L10	L10	L10	L10	L10	L10
Y	26	20	26	17	28	27	28
Zn	23	28	15	22	25	14	29
Zr	271	213	225	48	436	249	451

L = Less than
ND = No data

	C-S-10	C-10a	C-11	C-11a	C-11b	C-12	C-12a
U_3O_8	2.04	2.00	1.93	3.43	2.65	1.38	2.78
Ag	L10	L10	L10	L10	L10	L10	L10
Al	248	238	152	279	223	73	243
As	L2	L1	L1	L1	L2	L1	L1
B	L10	L10	L10	L10	L10	L10	L10
Ba	370	330	270	240	140	140	180
Be	L10	L10	L10	L10	L10	L10	L10
Ca	1566	56	15633	2832	7100	17715	12291
Co	6	5	4	9	7	4	8
Cr	13	8	9	21	13	10	13
Cu	15	9	7	18	7	9	8
Fe	100	156	127	37	16	36	139
La	10	ND	4	24	18	1.3	11.7
Li	35	27	15	63	32	7	53
Mn	420	70	180	270	320	110	200
Mo	L10	L10	L10	L10	L10	L10	L10
Na	570	438	761	583	751	408	632
No	34	30	31	29	32	28	30
Ni	10	12	9	22	17	12	12
Pb	10	10	10	10	ND	ND	20
Sb	2.0	2.0	2.0	1.9	1.5	2.6	2.1
Sc	5.4	5.8	17.2	10.6	10.3	31	16.2
Sn	2.9	3.1	3.8	2.5	2.6	6.9	4.0
Sr	150	150	280	75	10	560	110
Ti	702	461	583	1104	8	321	742
V	15	45	20	60	30	10	53
W	L10	L10	L10	L10	L10	L10	L10
Y	29	27	26	28	20	24	27
Zn	88	30	49	68	39	20	52
Zr	415	241	618	399	548	1332	329

L = Less than
ND - No data

	C-12b	C-13	C-S-13a	C-S-13b	C-14	C-15	C-S-15
U_3O_8	3.75	0.41	3.92	2.24	2.65	0.97	0.73
Ag	L10	L10	L10	L10	L10	L10	L10
Al	233	185	292	143	263	226	111
As	L1	L1	L1	L1	L2	L2	L1
B	L10	L10	10	L10	L10	L10	L10
Ba	230	260	270	150	290	150	170
Be	L10	L10	L10	L10	L10	L10	L10
Ca	12191	770	857	17345	1296	55	12665
Co	6	4	7	4	4	8	4
Cr	13	3	17	10	12	9	11
Cu	11	7	40	61	8	7	7
Fe	295	56	314	145	145	53	49
La	30	ND	31	14.4	18.5	ND	8.1
Li	33	12	33	33	15	19	6
Mn	400	30	230	1410	130	100	640
Mo	L10	L10	10	30	10	L10	L10
Na	515	459	522	412	443	387	511
Nb	29	32	30	29	33	33	30
Ni	18	9	14	11	8	8	8
Pb	ND	20	10	10	10	ND	20
Sb	2.1	1.5	1.8	3.6	1.8	1.9	ND
Se	18.4	ND	8.4	30.2	4.9	ND	ND
Sn	4.1	1.8	2.6	8.2	2.5	2.8	8.5
Sr	140	180	85	160	120	ND	200
Ti	885	194	953	492	929	284	184
V	60	ND	50	22	25	5	10
W	L10	L10	L10	L10	L10	L10	L10
Y	28	27	28	24	29	27	23
Zn	59	20	55	32	22	21	25

L = Less than
ND = No data

	C-16	C-S-16	C-17	C-S-17	C-18	C-18a	C-S-18
U_3O_8	1.47	0.57	0.78	2.07	7.56	8.49	4.81
Ag	L10	L10	L10	L10	L10	L10	L10
Al	189	81	192	256	251	244	253
As	L2	L1	L2	L2	L2	L2	L2
B	L10	L10	L10	L10	L10	L10	15
Ba	210	390	440	310	320	130	610
Be	L10	L10	L10	L10	L10	L10	L10
Ca	18408	17139	511	768	1292	1318	924
Co	3	4	4	5	3	10	3
Cr	14	5	4	9	20	11	17
Cu	6	6	7	12	24	6	49
Fe	79	39	52	139	125	229	108
La	ND	10.3	ND	ND	26	22	30
Li	11	4	22	21	26	22	30
Mn	1480	250	110	130	80	70	120
Mo	L10	L10	L10	L10	L10	10	40
Na	388	332	415	414	542	869	467
Nb	30	27	34	32	33	33	35
Ni	8	6	5	8	11	13	14
Pb	10	10	ND	ND	ND	10	ND
Sb	3.0	4.8	1.7	1.6	1.7	1.8	1.5
Se	20.3	39.7	ND	ND	6.6	2.1	4
Sn	6.4	12.1	2.2	1.9	2.5	2.6	1.9
Sr	135	365	165	135	130	5	170
Ti	400	94	100	414	799	827	831
V	13	ND	ND	17	35	40	40
W	L10	L10	L10	L10	L10	L10	L10
Y	26	21	28	26	29	27	28
Zn	15	22	20	67	32	19	766
Zr	202	92	118	205	1360	686	671

L = Less than
ND = No data

	C-19	C-S-19a	C-S-19b	C-S-19c	C-20	C-S-20	C-S-20a
U_3O_8	1.55	0.78	5.45	23.77	0.87	0.53	12.40
Ag	L10	20	20	L10	L10	L10	L10
Al	154	15	94	266	120	75	170
As	L1	L1	L1	L1	L1	L1	L2
B	10	20	10	15	L10	L10	L10
Ba	160	70	690	240	120	110	230
Be	L10	L10	L10	L10	L10	L10	L10
Ca	17671	17322	17254	4721	18721	17236	18174
Co	8	1	2	2	8	7	4
Cr	11	4	5	18	7	16	11
Cu	10	7	9	8	7	8	13
Fe	74	9	55	145	68	ND	46
La	14.4	47	10.4	11	6.3	ND	ND
Li	10	3	39	31	7	7	7
Mn	620	2230	280	420	590	770	350
Mo	4.6	L10	40	150	40	20	90
Na	399	281	361	353	421	421	437
Nb	29	20	25	30	31	30	30
Ni	13	12	9	13	8	9	6
Pb	25	ND	10	10	10	10	10
Sb	4.3	10.1	5.3	2.6	3.5	3.6	3.1
Sc	34	94.4	45.7	17	27.6	35	19
Sn	10.6	30.3	13.8	5.8	7.9	9.1	6.7
Sr	150	1390	430	155	230	270	200
Ti	373	24	62	787	280	124	338
V	32	5	5	165	10	4	5
W	L10	L10	L10	L10	L10	L10	L10
Y	23	14	19	27	24	23	24
Zn	19	17	29	28	20	31	16
Zr	192	29	70	681	193	125	240

L = Less than
ND = No data

	C-21	C-S-21	C-22	C-30	C-30s	C-32s	C-33s
U_3O_8	17.28	1.84	1.95	1.72	2.17	3.00	3.73
Ag	20	L10	L10	L10	L10	L10	L10
Al	23	186	187	243	240	224	240
As	L1	L1	L2	L2	L2	L2	L1
B	L10	L10	20	L10	L10	L10	L10
Ba	80	270	20	300	15	10	10
Be	L10	L10	L10	L10	L10	L10	L10
Ca	1424	18787	873	835	834		8397
Co	2	3	5	5	6	13	9
Cr	11	9	4	8	6	8	8
Cu	7	10	21	8	9	16	13
Fe	82	74	9	36	106	253	157
La	ND	12	ND	ND	ND	30	30
Li	14	20	10	15	20	30	30
Mn	320	1280	120	160	260	330	310
Mo	20	L10	L10	L10	L10	L10	L10
Na	427	340	886	884	831	670	520
Nb	32	29	36	32	33	28	30
Ni	14	10	11	9	10	13	30
Pb	ND	10	ND	10	10	20	30
Sb	2.0	3.1	1.8	1.8	1.6	2.3	1.6
Sc	ND	25	ND	1.9	1.9	10.8	6.4
Sn	2.6	7.4	2.5	2.5	1.8	4.0	3.2
Sr	645	255	20	140	15	35	10
Ti	299	524	117	464	603	722	515
V	25	18	15	25	20	50	60
W	L10	L10	L10	L10	L10	L10	L10
Y	27	23	28	27	28	26	28
Zn	19	52	17	25	34	38	39
Zr	205	578	136	306	525	525	490

L = Less than
ND = No data

	C-34	C-35s	C-39s	C-41s	C-42	C-44	C-45s
U_3O_8	2.10	3.18	2.31	2.00	9.57	2.83	3.19
Ag	L10	L10	L10	L10	30	20	L10
Al	265	226	269	197	283	286	281
As	L1	L2	L2	L2	L1	L2	L2
B	L10	L10	L10	L10	L10	L10	30
Ba	290	10	20	25	240	350	10
Be	L10	L10	L10	L10	L10	L10	L10
Ca	1625	1561	622	43	1436	1013	999
Co	4	8	5	8	3	4	6
Cr	9	6	7	5	13	8	8
Cu	8	13	8	6	7	189	20
Fe	109	202	138	66	145	81	239
La	18	20	10	ND	10	ND	20.3
Li	18	20	10	ND	24	22	30
Mn	160	250	200	140	110	30	360
Mo	L10	L10	L10	L10	90	30	L10
Na	413	746	829	791	422	453	861
Nb	31	33	32	31	31	32	33
Ni	9	14	19	17	13	11	11
Pb	10	20	ND	ND	10	10	20
Sb	1.8	1.7	1.6	1.4	1.7	1.5	1.8
Sc	4.6	4.8	2.4	ND	4.6	ND	4.7
Sn	2.6	2.5	2.1	1.4	2.4	2.1	2.7
Sr	146	30	20	60	135	155	15
Ti	672	836	472	269	864	312	895
V	33	55	30	30	13	10	50
W	L10	L10	L10	L10	L10	L10	L10
Y	28	29	28	28	30	29	28
Zn	31	44	35	22	41	110	46
Zr	537	840	385	419	662	260	497

L = Less than
ND = No data

	C-47s	C-48s	C-50s	C-51	C-52	C-53s	C-54
U_3O_8	4.06	1.53	2.23	4.69	1.76	1.87	0.88
Ag	L10	30	L10	L10	L10	L10	L10
Al	236	57	190	270	277	215	273
As	L2	L1	L2	L2	L2	L2	L1
B	L10	L10	L10	L10	L10	L10	L10
Ba	10	20	30	350	330	30	300
Be	L10	L10	L10	L10	L10	L10	L10
Ca	934	29619	1340	816	1480	3345	1366
Co	7	6	5	15	19	9	13
Cr	8	10	7	9	9	4	5
Cu	15	54	11	5	5	10	6
Fe	132	45	84	117	91	96	6
La	ND	11.3	ND	ND	ND	ND	ND
Li	10	10	ND	18	29	ND	34
Mn	150	260	240	210	340	170	180
Mo	20	L10	L10	L10	L10	L10	L10
Na	880	758	800	412	512	809	419
Nb	32	24	32	30	32	30	32
Ni	9	ND	8	11	13	5	9
Pb	20	20	20	20	10	10	ND
Sb	1.4	3.7	1.3	1.7	1.8	1.7	1.3
Sc	2.2	40.5	ND	1.1	2.8	2.6	ND
Sn	2.1	9.8	1.4	2.3	2.4	2.1	1.5
Sr	20	190	140	150	120	60	170
Ti	603	187	465	411	610	451	163
V	50	ND	ND	10	28	10	ND
W	L10	L10	L10	L10	L10	L10	L10
Y	28	20	30	28	29	28	29
Zn	32	31	32	30	88	17	18
Zr	613	203	711	314	528	460	181

L = Less than
ND = No data

	C-55s	C-56	C-57	C-58s	C-63	C-64	C-64s
U_3O_8	1.85	0.78	0.54	4.65	1.81	3.98	1.97
Ag	L10	L10	L10	L10	L10	L10	L10
Al	219	222	269	328	231	277	291
As	L1	L2	L1	L2	L1	L2	L1
B	L10	L10	15	30	L10	10	30
Ba	ND	340	250	10	310	290	30
Be	L10	L10	L10	L10	L10	L10	L10
Ca	1879	692	1435	1881	794	627	2884
Co	4	20	13	6	10	8	ND
Cr	2	6	10	12	8	11	6
Cu	2	6	9	106	7	6	8
Fe	147	97	169	465	150	202	278
La	2.7	ND	ND	38.7	ND	18.5	19.2
Li	25	27	21	60	25	12	10
Mn	150	160	270	400	300	300	220
Mo	L10	L10	L10	L10	L10	L10	L10
Na	898	550	401	839	469	482	838
Nb	30	32	30	28	30	29	30
Ni	2	8	5	11	14	10	5
Pb	20	10	10	20	ND	ND	ND
Sb	1.6	1.3	1.9	1.7	1.8	1.8	1.9
Sc	3.2	ND	3.1	10.6	1.1	3.2	7.2
Sn	2.1	1.5	2.5	2.8	2.3	2.8	3.0
Sr	40	135	60	20	140	110	70
Ti	550	212	440	1241	561	1078	934
V	20	10	10	55	20	30	ND
W	L10	L10	L10	L10	L10	L10	L10
Y	29	28	24	28	26	31	29
Zn	26	28	31	119	39	67	11
Zr	402	154	414	399	460	958	669

L = Less than
ND = No data

	C-64sx	C64x	C-65	C-65s	C-66soc	C-66-unx	C-67
U_3O_8	1.46	2.13	0.94	1.61	5.38	1.46	2.02
Ag	L10	L10	L10	L10	L10	L10	L10
Al	180	274	218	233	263	189	256
As	L2	L2	L2	L2	L2	L2	L2
B	L10	L10	L10	L10	L10	L10	L10
Ba	ND	ND	270	10	310	ND	160
Be	L10	L10	L10	L10	L10	L10	L10
Ca	660	823	1282	1065	1132	1167	877
Co	7	3	9	ND	11	3	9
Cr	7	8	7	7	11	3	12
Cu	12	6	5	7	13	ND	10
Fe	79	188	53	56	177	68	114
La	ND	9.5	ND	ND	ND	18.5	ND
Li	30	10	18	10	20	20	14
Mn	190	180	180	110	380	180	200
Mo	L10	L10	L10	L10	L10	L10	L10
Na	758	806	859	801	809	610	504
Nb	31	29	31	31	30	30	31
Ni	13	14	11	16	15	3	10
Pb	10	10	10	20	ND	ND	10
Sb	1.2	1.9	1.5	1.6	1.6	1.4	1.6
Sc	1.8	2.9	ND	ND	3.4	ND	1.4
Sn	1.3	2.5	1.8	2.0	2.6	1.4	2.1
Sr	60	20	180	10	20	80	30
Ti	332	613	176	381	1062	306	511
V	ND	20	10	ND	35	10	25
W	L10	L10	L10	L10	L10	L10	L10
Y	28	27	27	28	30	28	28
Zn	10	18	28	12	32	23	15
Zr	491	364	167	366	840	404	372

L = Less than
ND = No data

	C-67str	C-68x	C-68a-str	C-68s	C-69	C-70	C-71s
U_3O_8	1.70	0.67	1.03	2.46	1.74	2.05	2.40
Ag	L10	L10	L10	L10	L10	20	L10
Al	235	265	149	302	258	274	244
As	L2	L2	L1	L2	L2	L2	L2
B	L10	L10	L10	20	L10	L10	L10
Ba	10	310	20	10	350	340	ND
Be	L10	L10	L10	L10	L10	L10	L10
Ca	988	1168	928	800	680	1049	1383
Co	6	10	4	3	7	5	3
Cr	5	8	4	8	10	10	9
Cu	7	8	5	14	8	21	7
Fe	98	71	44	208	114	151	136
La	ND	ND	ND	8.1	ND	ND	5.9
Li	10	29	ND	30	13	21	10
Mn	180	220	160	200	410	250	330
Mo	L10	L10	L10	L10	L10	L10	L10
Na	845	411	741	789	439	439	783
Nb	31	30	31	30	30	31	35
Ni	19	13	9	10	20	8	10
Pb	10	ND	30	25	ND	ND	20
Sb	1.5	1.3	1.2	1.7	2.0	1.6	1.7
Sc	ND	ND	ND	4.1	2.4	3.2	2.1
Sn	1.8	1.5	ND	2.4	2.5	2.1	2.6
Sr	25	110	120	10	130	95	20
Ti	459	218	158	783	425	598	663
V	15	11	10	ND	10	20	30
W	L10	L10	L10	L10	L10	L10	L10
Y	28	27	25	29	27	28	28
Zn	10	15	6	18	20	57	27
Zr	368	192	260	482	211	416	89

L = Less than
ND = No data

	C-72	C-73
U_3O_8	1.49	1.49
Ag	L10	L10
Al	279	230
As	L2	L1
B	L10	L10
Ba	350	270
Be	L10	L10
Ca	752	609
Co	9	7
Cr	11	6
Cu	40	13
Fe	165	108
La	ND	ND
Li	21	35
Mn	170	160
Mo	L10	L10
Na	411	456
Nb	30	30
Ni	4	5
Pb	ND	20
Sb	1.9	1.7
Sc	2	ND
Sn	2.8	2.2
Sr	90	125
Ti	494	393
V	12	15
W	L10	L19
Y	27	27
Zn	42	22
Zr	214	285

L = Less than
ND = No data

APPENDIX B

GAMMA-RAY LOGS IN THE CEMENT DISTRICT INDICATING SUBSURFACE MINERALIZATION

Operator, Well No. & Location	Depth to Anomaly in Feet (Meters)	Thickness in Feet (Meters)	Lithology
Stephens Petr. Co. Yule No. 5 NE-SW, 1-5N-9W	890 (271.3)	20 (6.1)	sandstone
Ohio Oil Co. Surbeck No. 4 NE-NW-SW, 2-5N-9W	90 (27.4)	30 (9.1)	sandstone
	2430 (740.7)	70 (21.3)	sandstone
Mobil Oil Co. H. Sunbeck No. 6 NW-SE-SE, 3-5N-9W	106 (32.3)	5 (1.5)	sandstone
	130 (39.6)	7 (2.1)	sandstone
	141 (43.0)	3 (0.9)	sandstone
	290 (88.4)	4 (1.2)	sandstone
	1345 (410.0)	3 (0.9)	sandstone
Caddo Oil Co. Vann No. 1 SW-SW-SW, 4-5N-9W	2560 (780.3)	30 (9.1)	shale
Palmer Oil Corp. Ulery No. 1 SE-NE-NE, 34-6N-10W	393 (119.8)	3 (0.9)	sandstone
	437 (133.2)	10 (3.0)	sandstone
	1000 (304.8)	34 (10.7)	shale
	1810 (551.7)	7 (2.1)	sandstone
Palmer Oil Corp. Ulery No. 2 SW-NE-NE, 34-6N-10W	412 (125.6)	5 (1.5)	sandstone
	465 (141.7)	10 (3.0)	sandstone
	524 (159.7)	5 (1.5)	sandstone
	1040 (317.0)	30 (9.1)	shale
	2810 (856.5)	30 (9.1)	shale
Palmer Oil Corp. Dixon No. 1 35-6N-10W	975 (297.2)	30 (9.1)	shale
	1100 (335.3)	25 (7.6)	sandstone
	2525 (769.6)	12 (3.7)	sandstone
Palmer Oil Corp. Dixon No. 3 35-6N-10W	15 (4.6)	12 (3.7)	sandstone
	258 (78.6)	3 (0.9)	silty sandstone
	1025 (312.4)	18 (5.5)	shale
Mobil Oil Co. O Lindsay No. 9 NW-NE-NE, 35-6N-10W	1920 (585.2)	10 (3.0)	sandstone

APPENDIX C

MASS SPECTROMETER READINGS

SAMPLE LOCATION	READINGS			
Number	Total Counts	Potassium	Uranium	Thorium
7	30,190	1,784	1,810	58
30	4,020	500	65	35
31	2,860	349	34	14
32	4,435	485	79	58
33	4,560	454	115	69
34	3,505	431	47	39
35	3,845	369	68	57
36	3,770	365	79	55
38	4,450	529	108	27
39	3,410	430	56	26
40	3,300	390	42	24
41	3,280	410	53	26
42	4,380	506	115	45
43	3,850	493	58	28
44	3,790	460	54	29
45	4,530	476	93	66
46	4,310	511	86	58
47	4,140	492	81	49
48	1,470	51	18	14
49	3,110	380	35	14
50	4,020	413	94	43
51	3,670	524	56	17
52	3,790	475	47	32
53	4,050	371	101	34
54	3,460	425	42	32
55	3,810	457	67	30
56	4,070	534	76	48
57	3,240	423	28	27
58	4,480	445	90	67
59	2,890	353	36	21
60	1,370	45	13	8
61	3,510	429	54	33
62	4,090	452	72	50
63	3,280	376	45	30
65	3,260	383	39	26
66	3,380	482	38	18
67	3,770	457	60	35
68	3,340	462	41	26
69	4,230	626	51	29
70	3,350	374	51	34
71	4,260	553	62	46
72	3,560	504	36	28
73	3,330	395	33	25

APPENDIX D

GEOCHEMICAL ANOMALIES IN THE CEMENT DISTRICT

Sample Number	Total Gamma-Ray Count (cps)*	Track-Etch Values (Times Background)**	U_3O_8 (Neutron-Delay Activation) (ppm)	V (ppm)	V/U Ratio	Significant Associated Elements (ppm)
C-11a	50	***	3.43	60	17.5	
C-12a	40	***	2.78	53	19.1	
C-12b	40	***	3.75	60	16.0	
C-S-13a	115	4	3.92	50	12.8	Cu (40)
C-19	50	4	1.55	32	20.6	Mo (40)
C-S-19b	1300	64	5.45	5	0.9	Mo (40)
C-S-19c	240	64	23.77	165	6.9	Mo (150)
C-S-20a	120	4	12.40	5	4.0	Mo (90)
C-33s	50	4	3.73	60	16.1	PB (30)
C-35s	35	***	3.18	55	17.3	
C-42	120	8	9.58	13	1.4	Mo (90)
C-45s	45	4	3.19	50	15.7	
C-47s	40	4	4.06	50	12.3	
C-58s	45	4	4.65	55	11.8	Cu (106)

*Background = 30-40 cps (counts per second)
**Background = 125 counts
***Outside track-etch survey

APPENDIX E

SYMAP COMPUTER PROGRAM

SYMAP, VERSION 5.20

LABORATORY FOR COMPUTER GRAPHICS AND SPATIAL ANALYSIS
GRADUATE SCHOOL OF DESIGN
HARVARD UNIVERSITY
CAMBRIDGE, MASSACHUSETTS 02138
UNITED STATES OF AMERICA

TIME = 0.0

A-OUTLINE

DOWN COORDINATE DIVIDED INTERNALLY BY 8.00
ACROSS COORDINATE DIVIDED INTERNALLY BY 10.00

VERTEX	DOWN	ACROSS
	ISLAND	1
(1)	1.00	15.00
(2)	1.00	76.00
(3)	20.00	76.00
(4)	20.00	131.00
(5)	26.00	131.00
(6)	26.00	192.00
(7)	39.00	192.00
(8)	39.00	285.00
(9)	78.00	285.00
(10)	78.00	305.00
(11)	91.00	305.00
(12)	91.00	285.00
(13)	128.00	285.00
(14)	128.00	272.00
(15)	72.00	272.00
(16)	72.00	240.00
(17)	84.00	240.00
(18)	84.00	170.00
(19)	71.00	170.00
(20)	71.00	57.00
(21)	50.00	57.00
(22)	50.00	15.00

AREA= 13856.98 CENTER=(50.03, 150.38)

A-OUTLINE PACKAGE EXTREME COORDINATES ARE
0.13 1.50 TOP-LEFT CORNER
16.00 30.50 BOTTOM-RIGHT CORNER

B-DATA POINTS

DOWN COORDINATE DIVIDED INTERNALLY BY 8.00
ACROSS COORDINATE DIVIDED INTERNALLY BY 10.00

POINT	DOWN	ACROSS
(1)	2.00	17.00
(2)	2.00	23.00
(3)	2.00	29.00
(4)	2.00	36.00
(5)	2.00	41.00
(6)	2.00	49.00
(7)	2.00	56.00
(8)	2.00	62.00
(9)	2.00	67.00
(10)	7.00	35.00
(11)	7.00	41.00
(12)	8.00	68.00
(13)	12.00	18.00
(14)	13.00	23.00
(15)	13.00	35.00
(16)	12.00	41.00
(17)	13.00	68.00
(18)	17.00	18.00
(19)	17.00	23.00
(20)	19.00	40.00
(21)	19.00	69.00
(22)	24.00	41.00
(23)	24.00	48.00
(24)	24.00	54.00
(25)	24.00	61.00
(26)	24.00	68.00
(27)	23.00	95.00
(28)	23.00	101.00
(29)	23.00	108.00
(30)	23.00	115.00
(31)	23.00	121.00
(32)	29.00	41.00
(33)	30.00	68.00
(34)	28.00	95.00
(35)	28.00	121.00
(36)	34.00	42.00
(37)	34.00	57.00
(38)	35.00	68.00
(39)	34.00	97.00
(40)	33.00	133.00
(41)	32.00	144.00
(42)	32.00	160.00
(43)	33.00	166.00
(44)	33.00	171.00
(45)	40.00	42.00
(46)	40.00	56.00
(47)	40.00	61.00
(48)	40.00	69.00
(49)	39.00	98.00
(50)	39.00	112.00

(51)	40.00	118.00
(52)	38.00	150.00
(53)	38.00	166.00
(54)	39.00	171.00
(55)	38.00	186.00
(56)	44.00	29.00
(57)	44.00	35.00
(58)	44.00	48.00
(59)	44.00	55.00
(60)	44.00	62.00
(61)	43.00	68.00
(62)	43.00	75.00
(63)	43.00	81.00
(64)	43.00	87.00
(65)	43.00	94.00
(66)	45.00	101.00
(67)	44.00	107.00
(68)	43.00	114.00
(69)	43.00	119.00
(70)	43.00	125.00
(71)	43.00	138.00
(72)	43.00	144.00
(73)	43.00	154.00
(74)	43.00	160.00
(75)	43.00	165.00
(76)	43.00	180.00
(77)	43.00	186.00
(78)	44.00	192.00
(79)	44.00	200.00
(80)	43.00	208.00
(81)	42.00	215.00
(82)	42.00	228.00
(83)	42.00	234.00
(84)	42.00	241.00
(85)	42.00	247.00
(86)	42.00	254.00
(87)	42.00	267.00
(88)	41.00	278.00
(89)	50.00	69.00
(90)	49.00	99.00
(91)	49.00	120.00
(92)	48.00	133.00
(93)	48.00	146.00
(94)	49.00	192.00
(95)	47.00	272.00
(96)	47.00	279.00
(97)	56.00	68.00
(98)	51.00	99.00
(99)	53.00	146.00
(100)	52.00	177.00
(101)	53.00	186.00
(102)	52.00	253.00
(103)	52.00	279.00
(104)	61.00	69.00
(105)	61.00	121.00
(106)	59.00	146.00
(107)	61.00	192.00
(108)	58.00	253.00
(109)	65.00	69.00
(110)	65.00	77.00
(111)	65.00	91.00
(112)	65.00	97.00
(113)	65.00	102.00
(114)	65.00	107.00
(115)	65.00	113.00
(116)	65.00	120.00
(117)	65.00	127.00
(118)	65.00	133.00
(119)	65.00	140.00
(120)	65.00	146.00
(121)	65.00	152.00
(122)	65.00	159.00
(123)	65.00	165.00
(124)	65.00	172.00
(125)	65.00	180.00
(126)	65.00	199.00
(127)	65.00	211.00
(128)	64.00	219.00
(129)	65.00	225.00
(130)	64.00	253.00
(131)	62.00	279.00
(132)	65.00	180.00
(133)	69.00	227.00
(134)	67.00	278.00
(135)	74.00	187.00
(136)	74.00	193.00
(137)	72.00	278.00
(138)	81.00	226.00
(139)	77.00	279.00
(140)	83.00	278.00
(141)	83.00	285.00
(142)	83.00	291.00
(143)	83.00	297.00
(144)	88.00	279.00
(145)	93.00	279.00
(146)	104.00	279.00
(147)	108.00	279.00
(148)	114.00	279.00
(149)	119.00	279.00
(150)	125.00	279.00

B-DATA POINTS PACKAGE EXTREME COORDINATES ARE

0.25	1.70	TOP-LEFT CORNER
15.63	29.70	BOTTOM-RIGHT CORNER

E-VALUES

DATUM	VALUE
(1)	72.00
(2)	95.00
(3)	51.00
(4)	53.00
(5)	43.00
(6)	49.00
(7)	296.00
(8)	273.00
(9)	175.00
(10)	1553.00
(11)	45.00
(12)	76.00
(13)	835.00
(14)	1355.00
(15)	2025.00
(16)	78.00
(17)	82.00
(18)	177.00
(19)	263.00
(20)	68.00
(21)	295.00
(22)	104.00
(23)	144.00
(24)	46.00
(25)	172.00
(26)	264.00
(27)	115.00
(28)	56.00
(29)	181.00
(30)	287.00
(31)	64.00
(32)	48.00
(33)	121.00
(34)	243.00
(35)	67.00
(36)	174.00
(37)	1110.00
(38)	136.00
(39)	277.00
(40)	500.00
(41)	625.00
(42)	525.00
(43)	450.00
(44)	555.00
(45)	296.00
(46)	152.00
(47)	2640.00
(48)	197.00
(49)	71.00
(50)	73.00
(51)	406.00
(52)	590.00
(53)	408.00
(54)	850.00
(55)	2556.00
(56)	71.00
(57)	281.00
(58)	109.00
(59)	90.00
(60)	135.00
(61)	113.00
(62)	115.00
(63)	133.00
(64)	85.00
(65)	166.00
(66)	108.00
(67)	411.00
(68)	524.00
(69)	303.00
(70)	95.00
(71)	113.00
(72)	68.00
(73)	126.00
(74)	42.00
(75)	130.00
(76)	1440.00
(77)	1116.00
(78)	85.00
(79)	147.00
(80)	319.00
(81)	137.00
(82)	69.00
(83)	48.00
(84)	68.00
(85)	44.00
(86)	19.00
(87)	121.00
(88)	47.00
(89)	217.00
(90)	157.00
(91)	1565.00
(92)	356.00
(93)	206.00
(94)	119.00
(95)	518.00
(96)	71.00
(97)	139.00
(98)	146.00
(99)	165.00
(100)	208.00
(101)	7842.00
(102)	171.00
(103)	52.00
(104)	331.00
(105)	242.00
(106)	74.00
(107)	2274.00
(108)	370.00
(109)	232.00
(110)	150.00
(111)	350.00
(112)	112.00
(113)	345.00
(114)	179.00
(115)	164.00
(116)	62.00
(117)	407.00
(118)	165.00
(119)	79.00
(120)	115.00
(121)	210.00
(122)	129.00
(123)	88.00
(124)	84.00

(125)	123.00
(126)	2754.00
(127)	374.00
(128)	346.00
(129)	291.00
(130)	358.00
(131)	312.00
(132)	142.00
(133)	61.00
(134)	151.00
(135)	271.00
(136)	135.00
(137)	171.00
(138)	157.00
(139)	142.00
(140)	135.00
(141)	202.00
(142)	112.00
(143)	167.00
(144)	108.00
(145)	39.00
(146)	237.00
(147)	235.00
(148)	83.00
(149)	164.00
(150)	112.00

F-MAP

CONTOUR OF TRACK ETCH DATA AT CEMENT OIL FIELD, OKLA.

ELECTIVE

6 RANGES OF VALUE CLASS INTERVALS ARE PROPORTIONED 1) 125.50 2) 500.50 3) 1000.50 4) 2000.50 5) 6000.50

8 SUPPRESSION OF CONTOUR LINES OR BOUNDARIES
9 SUPPRESSION OF HISTOGRAM

0.350000 MINUTES FOR INPUT

MAP 1

CONTOUR OF TRACK ETCH DATA AT CEMENT OIL FIELD, OKLA.

MAP WINDOW DISPLAYED IS
(0.125, 1.500) (TOP-LEFT CORNER)
(16.019, 30.500) (BOTTOM-RIGHT CORNER)

MAP SCALE = 0.4483 (INCHES ON OUTPUT MAP)/(UNITS ON SOURCE MAP)

MAP SHOULD BE PRINTED AT 8.0 ROWS PER INCH AND 10.0 COLUMNS PER INCH

TRANSFORMATION FROM SOURCE COORDINATES TO PRINT CHARACTER LOCATION IS
ROW = (DOWN COORDINATE - 0.13) * 3.5862
COLUMN = (ACROSS COORDINATE - 1.50) * 4.4828

THERE ARE 150 VALID DATA VALUES

MINIMUM AND MAXIMUM VALID DATA VALUES ARE 19.000 AND 7842.000

MEAN OF VALID DATA IS 367.987

STANDARD DEVIATION OF VALID DATA IS 773.897

THERE ARE 150 VALID DATA VALUES

MINIMUM AND MAXIMUM VALID DATA VALUES ARE 19.000 AND 7842.000

MEAN OF VALID DATA IS 367.987

STANDARD DEVIATION OF VALID DATA IS 773.897

DATA POINTS FOR MAP

POINT	ROW	COLUMN	DATUM	VALUE	LEVEL
1)	0	1	1	72.00	1
2)	0	4	2	95.00	1
3)	0	6	3	51.00	1
4)	0	9	4	53.00	1
5)	0	12	5	40.00	1
6)	0	15	6	49.00	1
7)	0	18	7	296.00	2
8)	0	21	8	273.00	2
9)	0	23	9	175.00	2
10)	3	9	10	1550.00	4
11)	3	12	11	45.00	1
12)	3	24	12	76.00	1
13)	5	1	13	835.00	3
14)	5	4	14	1395.00	4
15)	5	9	15	2025.00	4
16)	5	12	16	70.00	1
17)	5	24	17	82.00	1
18)	7	1	18	177.00	2
19)	7	4	19	263.00	2
20)	8	11	20	68.00	1
21)	8	24	21	295.00	2
22)	10	12	22	104.00	2
23)	10	15	23	144.00	2
24)	10	17	24	46.00	1
25)	10	21	25	172.00	2
26)	10	24	26	204.00	2
27)	10	36	27	115.00	2
28)	10	39	28	56.00	1
29)	10	42	29	183.00	2
30)	10	45	30	287.00	2
31)	10	48	31	64.00	1
32)	13	12	32	48.00	1
33)	13	24	33	121.00	2
34)	12	36	34	243.00	2
35)	12	48	35	67.00	1
36)	15	12	36	174.00	2
37)	15	15	37	1110.00	3
38)	15	24	38	136.00	2
39)	15	37	39	277.00	2
40)	14	53	40	500.00	3
41)	14	58	41	625.00	3
42)	14	65	42	585.00	3
43)	14	68	43	450.00	3
44)	14	70	44	595.00	3
45)	17	12	45	290.00	2
46)	17	18	46	152.00	2
47)	17	21	47	2040.00	4
48)	17	24	48	197.00	2
49)	17	37	49	71.00	1
50)	17	43	50	73.00	1
51)	17	46	51	406.00	2
52)	17	65	52	530.00	3
53)	17	66	53	408.00	2
54)	17	70	54	890.00	3
55)	17	77	55	2550.00	5
56)	19	6	56	71.00	1
57)	19	9	57	281.00	2
58)	19	15	58	109.00	2
59)	19	18	59	90.00	1
60)	19	21	60	135.00	2
61)	19	24	61	113.00	2
62)	19	27	62	115.00	2
63)	19	30	63	133.00	2
64)	19	32	64	85.00	1
65)	19	35	65	166.00	2
66)	20	39	66	108.00	2
67)	19	41	67	411.00	2
68)	19	44	68	534.00	3
69)	19	47	69	303.00	2
70)	19	49	70	95.00	1
71)	19	55	71	113.00	2
72)	19	58	72	68.00	1
73)	19	62	73	126.00	2
74)	19	65	74	42.00	1
75)	19	67	75	130.00	2
76)	19	74	76	1440.00	4
77)	19	77	77	1116.00	4
78)	19	79	78	85.00	1
79)	19	83	79	147.00	2
80)	19	87	80	319.00	2

81)	18	90	81	137.00	2
82)	18	95	82	69.00	1
83)	18	98	83	48.00	1
84)	18	101	84	68.00	1
85)	18	104	85	44.00	1
86)	18	107	86	19.00	1
87)	18	113	87	121.00	2
88)	18	116	88	47.00	1
89)	22	24	89	217.00	2
90)	22	38	90	157.00	2
91)	22	47	91	1585.00	4
92)	21	53	92	356.00	2
93)	21	59	93	206.00	2
94)	22	76	94	119.00	2
95)	21	115	95	518.00	3
96)	21	118	96	71.00	1
97)	25	24	97	138.00	2
98)	23	38	98	146.00	2
99)	23	59	99	165.00	2
100)	23	73	100	208.00	2
101)	23	77	101	7842.00	5
102)	23	107	102	171.00	2
103)	23	118	103	52.00	1
104)	27	24	104	331.00	2
105)	27	48	105	242.00	2
106)	26	59	106	74.00	1
107)	27	79	107	2274.00	4
108)	26	107	108	370.00	2
109)	29	24	109	232.00	2
110)	29	28	110	150.00	2
111)	29	34	111	350.00	2
112)	29	37	112	112.00	2
113)	29	39	113	345.00	2
114)	29	41	114	179.00	2
115)	29	44	115	164.00	2
116)	29	47	116	62.00	1
117)	29	50	117	407.00	2
118)	29	53	118	165.00	2
119)	29	56	119	79.00	1
120)	29	59	120	115.00	2
121)	29	61	121	210.00	2
122)	29	65	122	129.00	2
123)	29	67	123	88.00	1
124)	29	70	124	84.00	1
125)	29	74	125	123.00	2
126)	29	82	126	2754.00	5
127)	29	88	127	374.00	2
128)	28	91	128	346.00	2
129)	29	94	129	291.00	2
130)	28	107	130	358.00	2
131)	27	118	131	312.00	2
132)	30	74	132	142.00	2
133)	30	95	133	61.00	1
134)	30	116	134	151.00	2
135)	33	77	135	271.00	2
136)	33	80	136	135.00	2
137)	32	118	137	171.00	2
138)	36	95	138	157.00	2
139)	34	118	139	142.00	2
140)	37	118	140	135.00	2
141)	37	121	141	202.00	2
142)	37	124	142	112.00	2
143)	37	126	143	167.00	2
144)	39	118	144	108.00	2
145)	41	116	145	39.00	1
146)	46	118	146	237.00	2
147)	46	118	147	235.00	2
148)	51	118	148	80.00	1
149)	53	118	149	164.00	2
150)	56	118	150	112.00	2

STANDARD SEARCH RADIUS IS 2.7402

0.137000 MINUTES FOR INITIAL CALCULATIONS

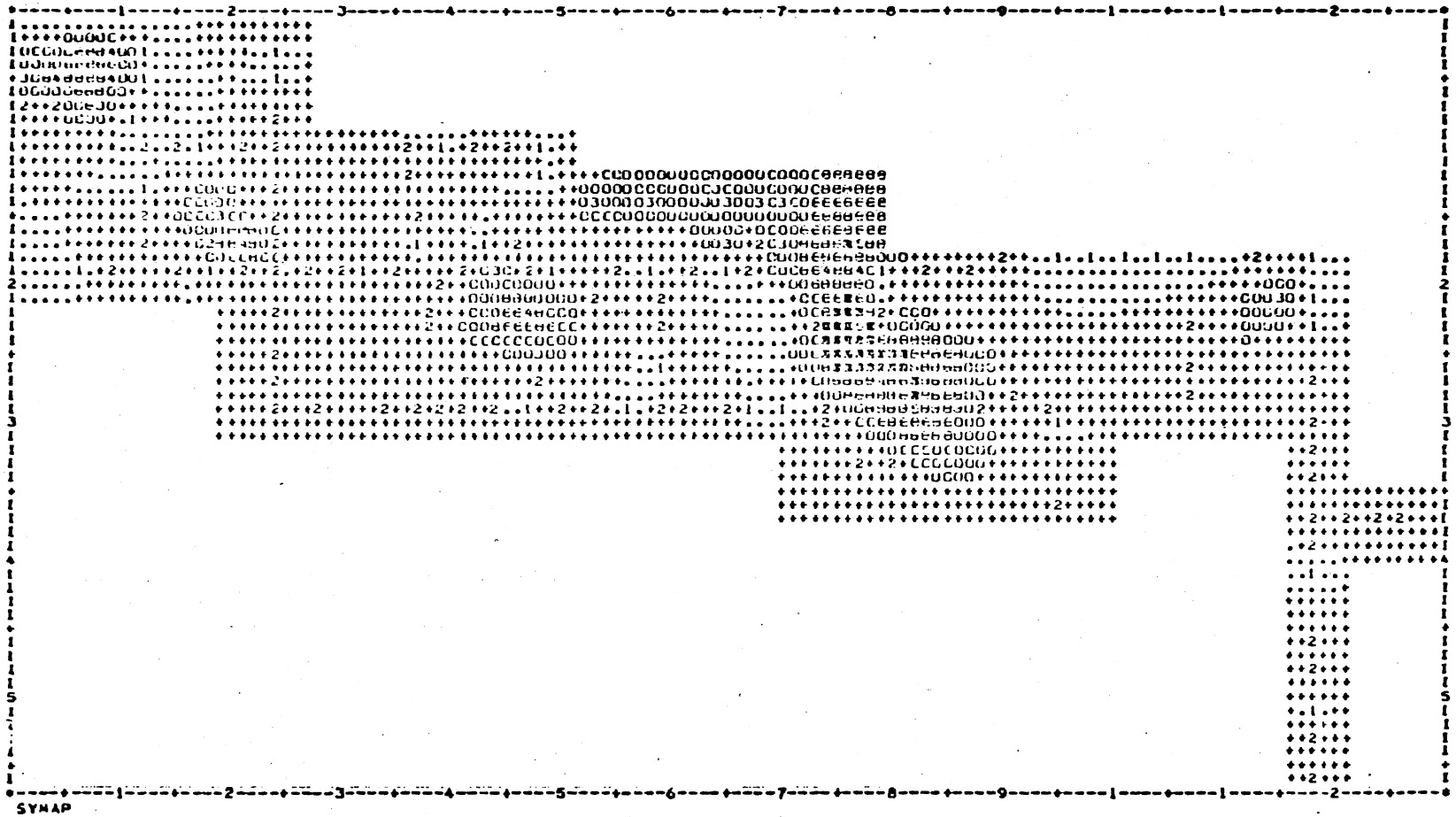

SYMAP

1.11500 MINUTES FOR MAP

CONTOUR OF TRACK ETCH DATA AT CEMENT OIL FIELD, OKLA.

DATA VALUE EXTREMES ARE 19.00 7842.00

ABSOLUTE VALUE RANGE APPLYING TO EACH LEVEL
('MAXIMUM' INCLUDED IN HIGHEST LEVEL ONLY)

MINIMUM	19.00	103.44	440.17	1113.31	2459.25
MAXIMUM	103.44	440.17	1113.31	2459.25	7842.00

PERCENTAGE OF TOTAL ABSOLUTE VALUE RANGE APPLYING TO EACH LEVEL

1.08	4.30	8.60	17.20	68.81

FREQUENCY DISTRIBUTION OF DATA POINT VALUES IN EACH LEVEL

LEVEL	1	2	3	4	5
	.....	+++++++++	OOOCCOOCC	EEEEEEEEE	[illegible]
	.....	+++++++++	CCCCOOOCC	EEEEEEEEE	[illegible]
SYMBOLS	....1....	++++2++++	OOOCCCCCC	EEEEEEEEE	[illegible]
	.....	+++++++++	OOOCCCCCC	EEEEEEEEE	[illegible]
	.....	+++++++++	OOCCCCCCC	EEEEEEEEE	[illegible]
FREQ.	41	67	11	8	3

0.030003 MINUTES FOR HISTOGRAM

1 MAPS HAVE BEEN PRODUCED
END OF JOB

VITA

Roy Frank Allen

Candidate for the Degree of

Master of Science

Thesis: URANIUM POTENTIAL OF THE CEMENT DISTRICT, SOUTHWESTERN OKLAHOMA

Major Field: Geology

Biographical:

Personal Data: Born in Anderson, South Carolina, February 21, 1952, the son of Mr. and Mrs. Roy L. Allen.

Education: Graduated from Enid High School, Enid, Oklahoma, in May, 1970; completed the requirements for a Bachelor of Science degree in Geology from Texas A & M University, College Station, Texas, in December 1974; completed requirements for the Master of Science degree in Geology at Oklahoma State University in May, 1980.

Professional Experience: Geological technician, Chevron Resources Company, Karnes City, Texas, September 1975 to December, 1976; Geological technician, Chevron Resources Company, San Antonio, Texas, January, 1977 to September, 1978; Geological assistant, R & J Consultants, October, 1978 to June, 1979; Research assistant, Department of Geology, Oklahoma State University, Stillwater, Oklahoma, February, 1979 to February, 1980; Teaching assistant, Department of Geology, Oklahoma State University, Stillwater, Oklahoma, August, 1979 to December, 1979; junior member of the American Association of Professional Geologists; member of the American Institute of Mining, Metallurgical, and Petroleum Engineers; student member of the Geological Society of America.

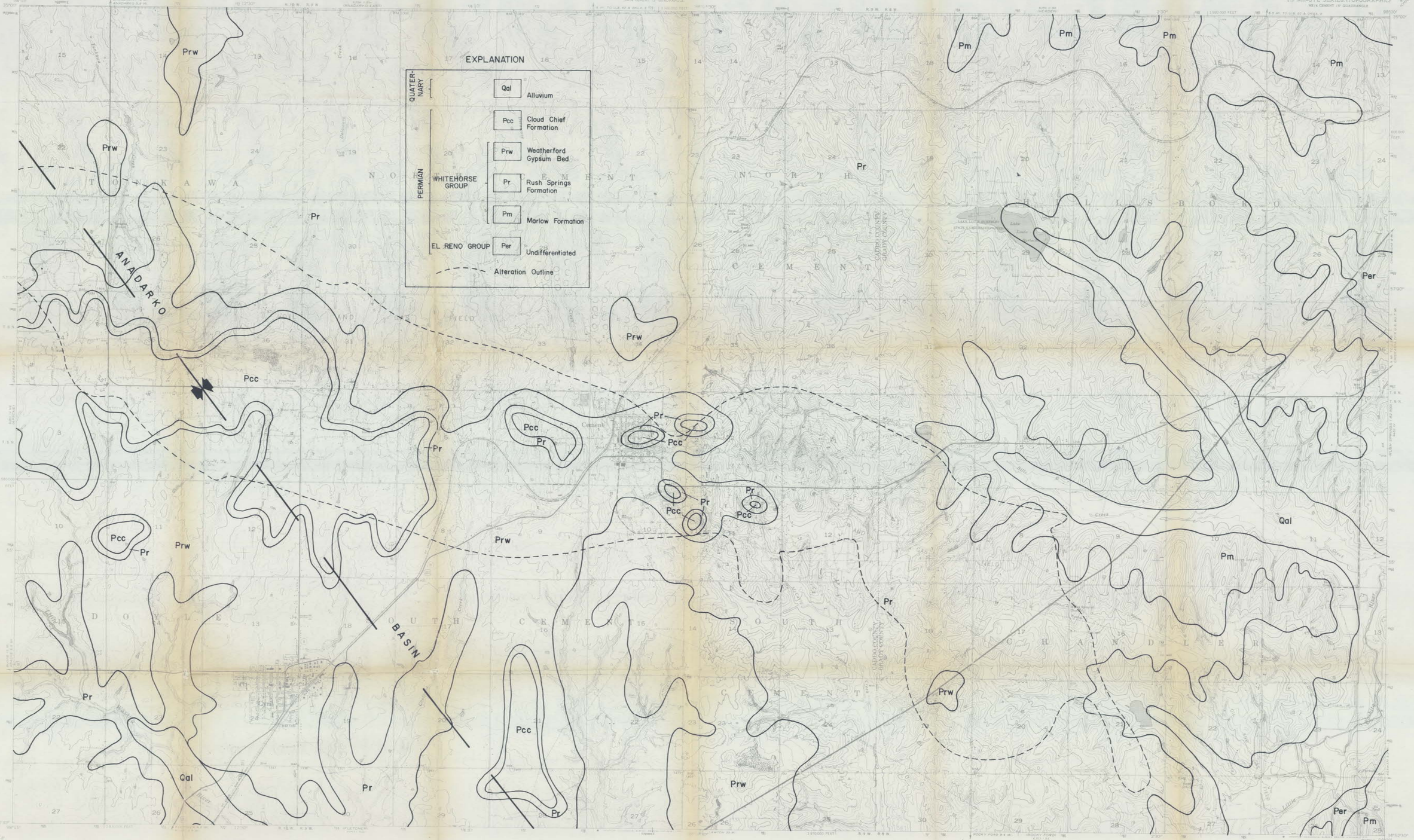

Plate I. GEOLOGIC AND SURFACE ALTERATION MAP OF THE CEMENT DISTRICT

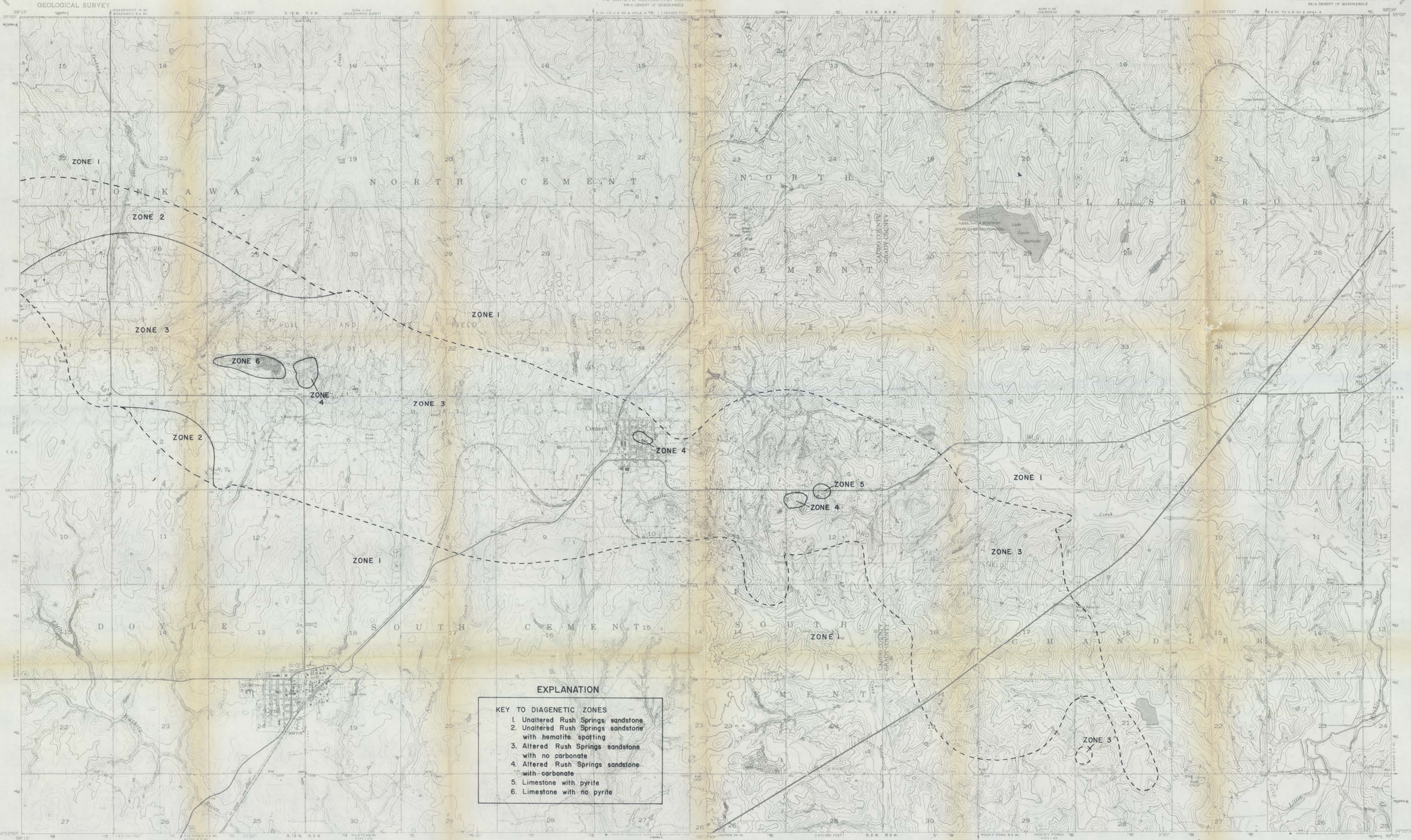

Plate 2. DIAGENETIC MAP OF THE CEMENT DISTRICT

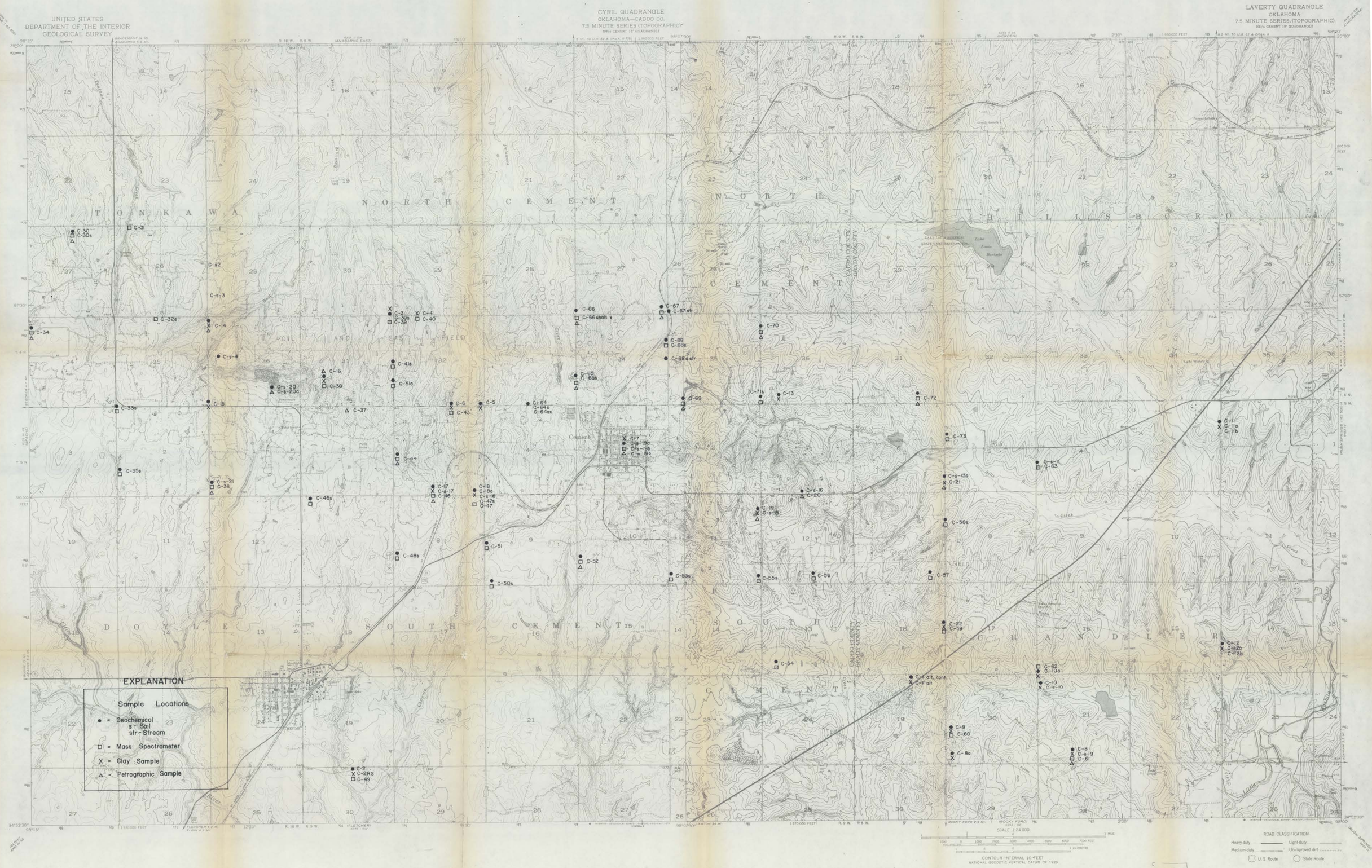

Plate 3. LOCATIONS OF GEOCHEMICAL, MASS SPECTROMETER, PETROGRAPHIC, AND CLAY MINERAL SAMPLES

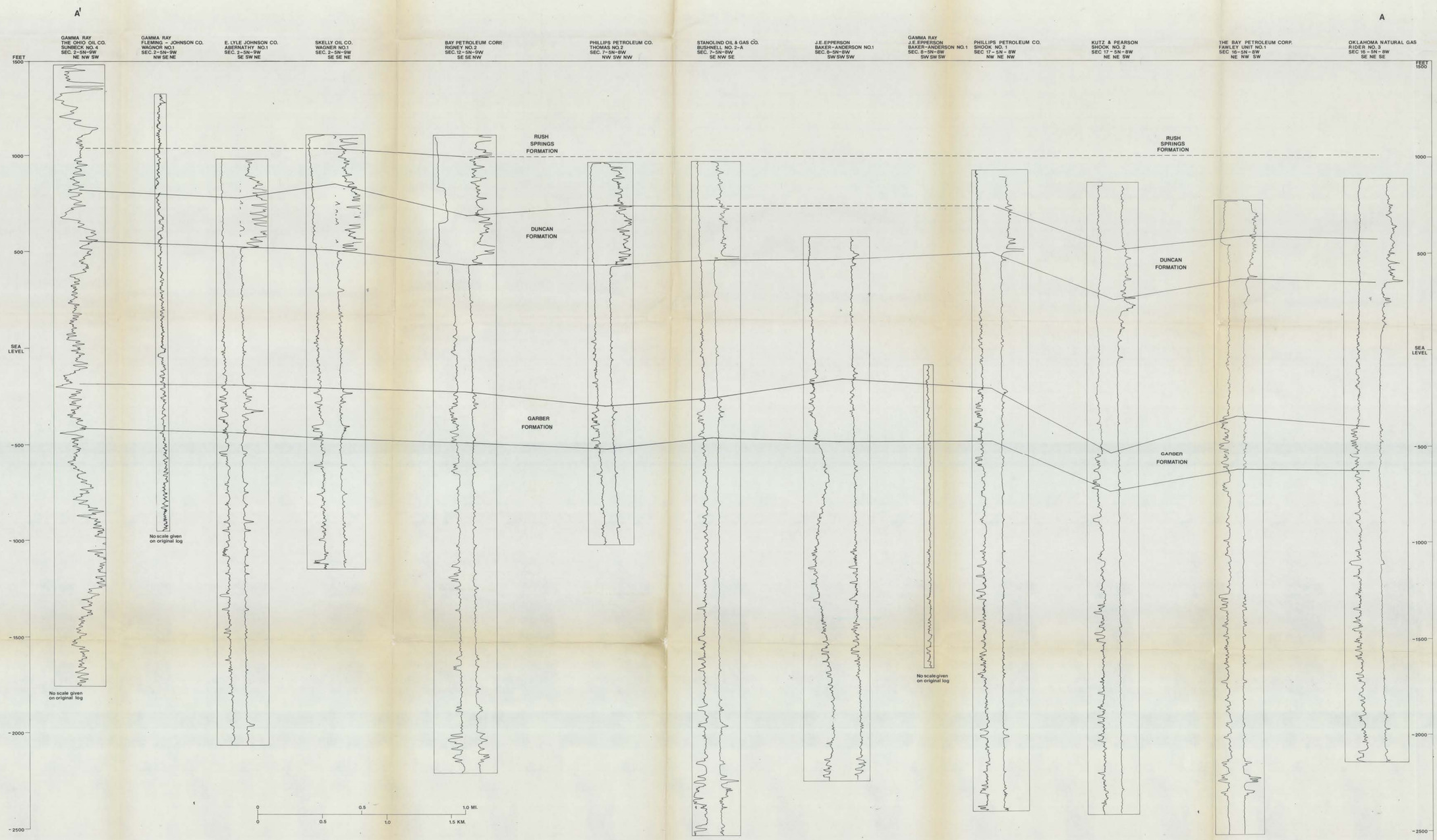

Plate 4. EASTERN PORTION OF EAST-WEST CROSS-SECTION (A'-A) OF THE PERMIAN SEQUENCE OVERLYING THE CEMENT ANTICLINE (CONTINUED)

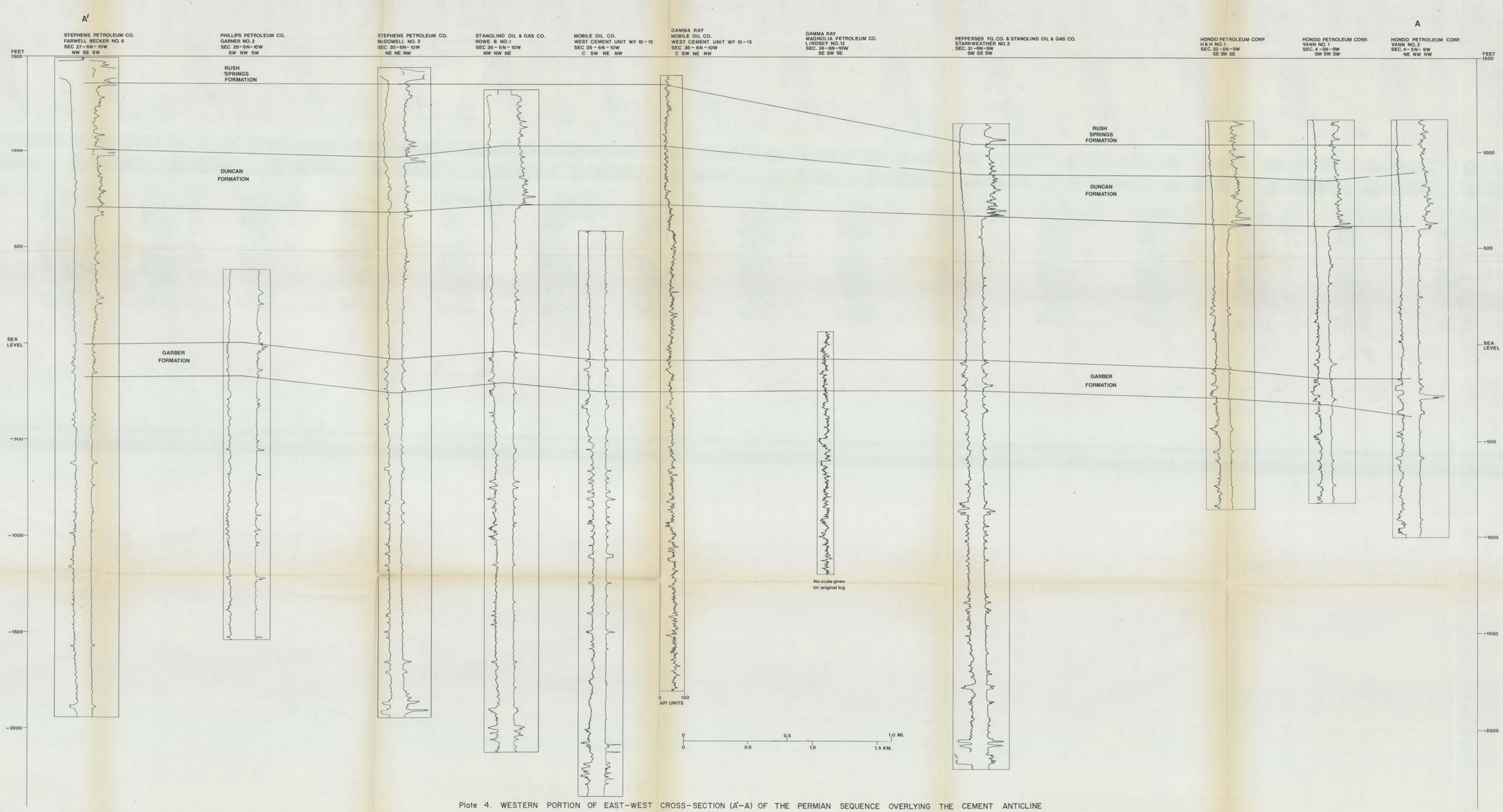

Plate 4. WESTERN PORTION OF EAST-WEST CROSS-SECTION (A'-A) OF THE PERMIAN SEQUENCE OVERLYING THE CEMENT ANTICLINE

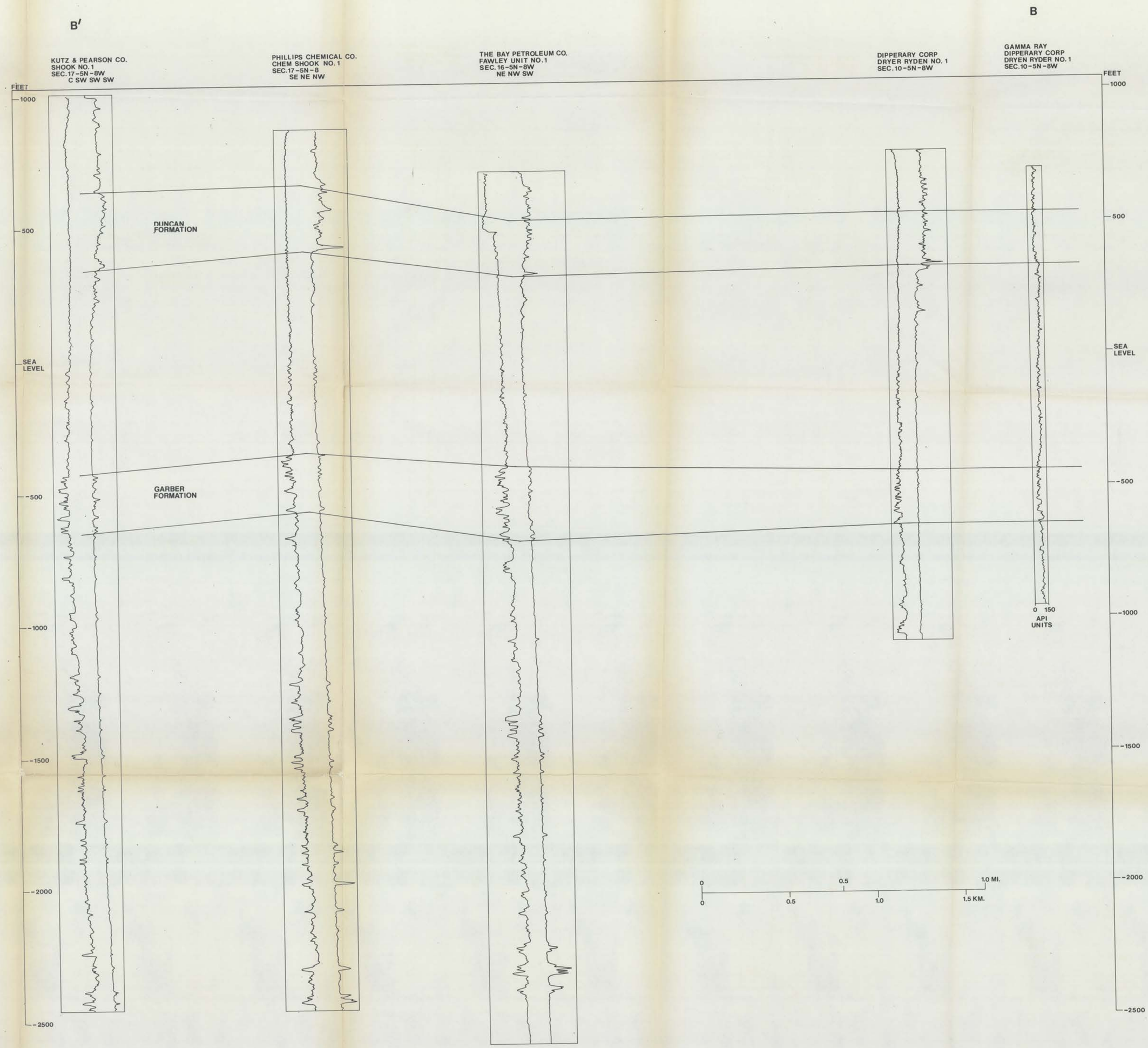

Plate 5. NORTH-SOUTH CROSS-SECTION (B′-B) OF THE PERMIAN SEQUENCE OVERLYING THE EASTERN END OF THE CEMENT ANTICLINE

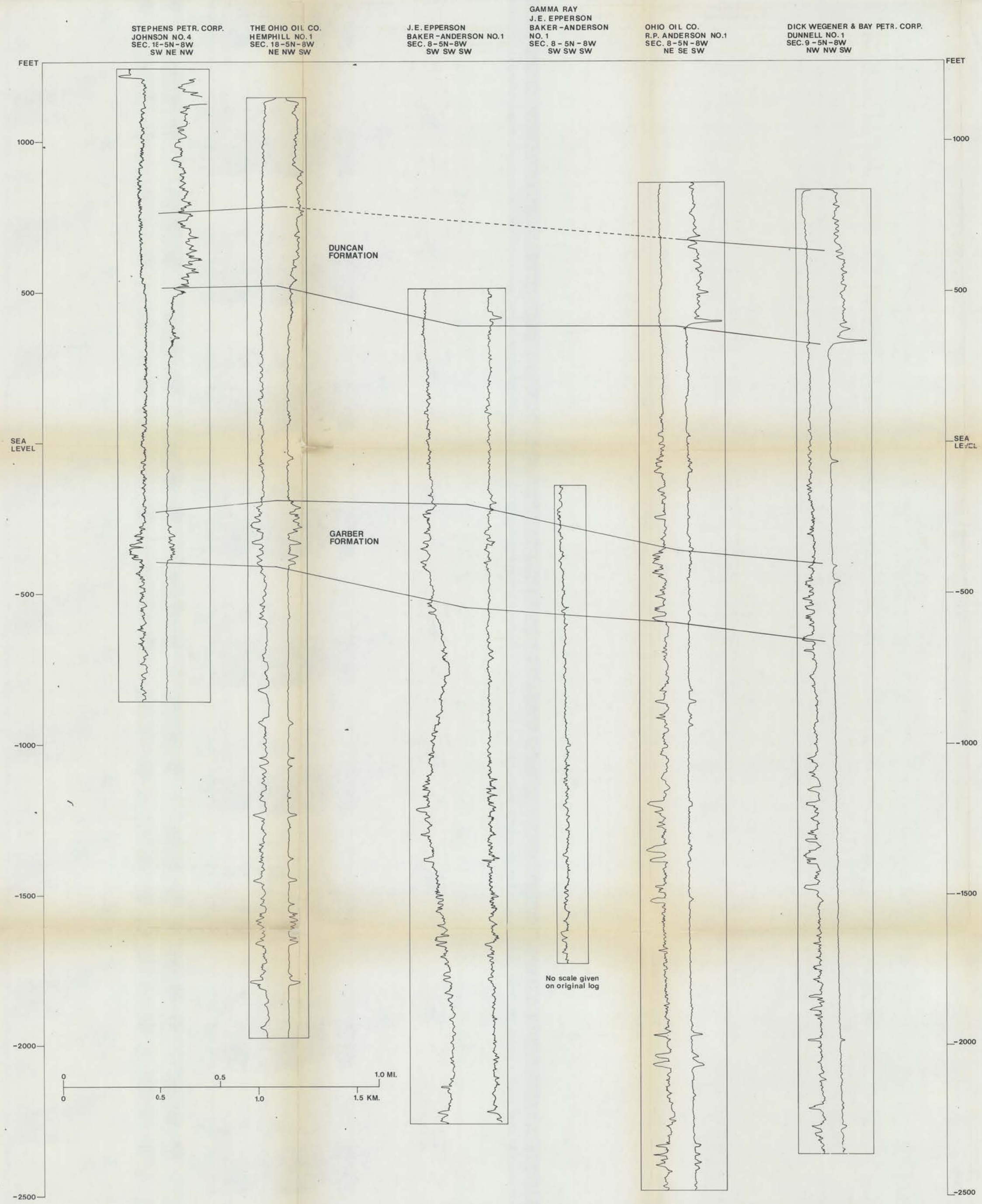

Plate 6. NORTH-SOUTH CROSS-SECTION (C'-C) OF THE PERMIAN SEQUENCE OVERLYING THE EASTERN END OF THE CEMENT ANTICLINE

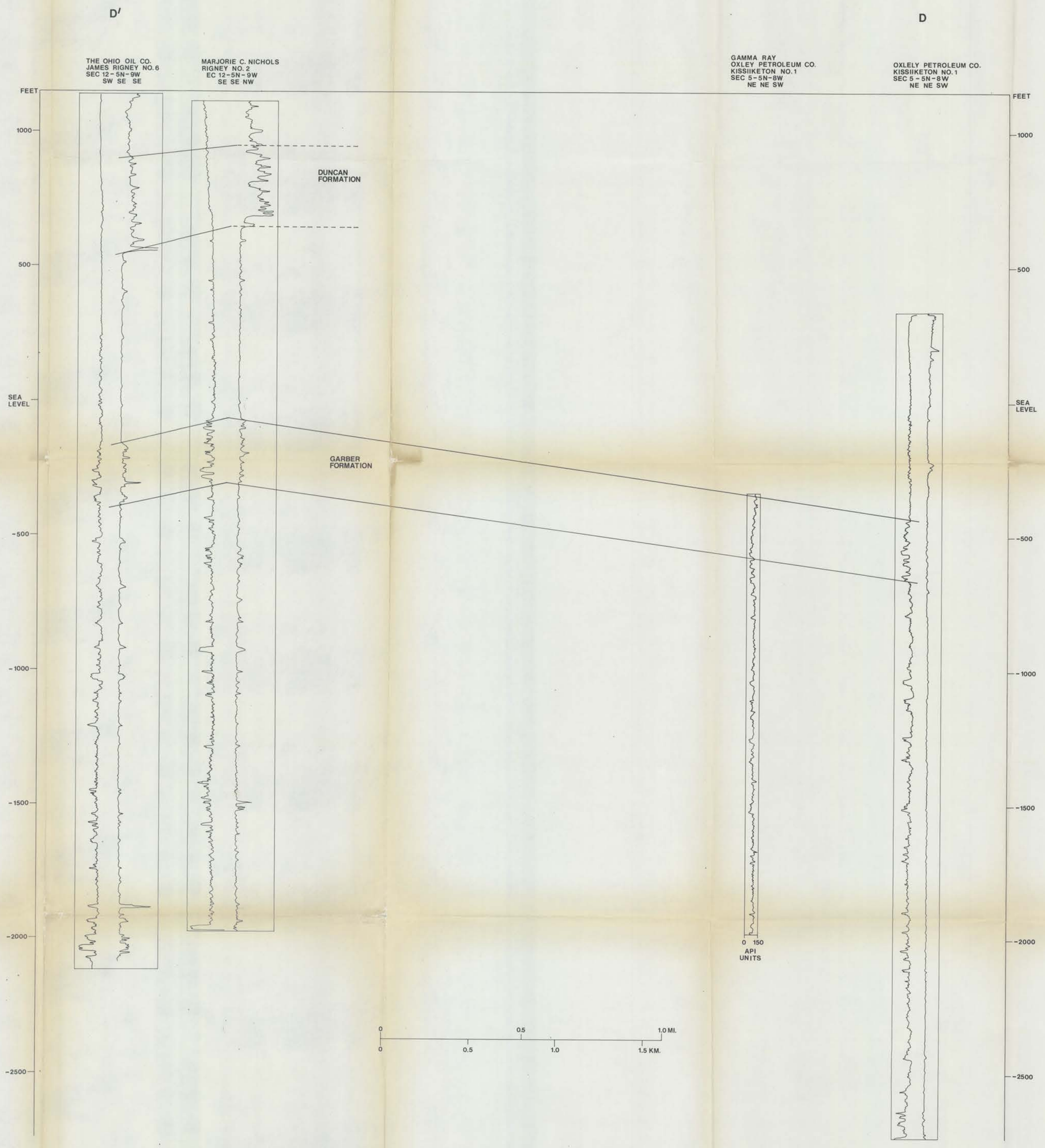

Plate 7. NORTH-SOUTH CROSS-SECTION (D'-D) OF THE PERMIAN SEQUENCE OVERLYING THE EASTERN END OF THE CEMENT ANTICLINE

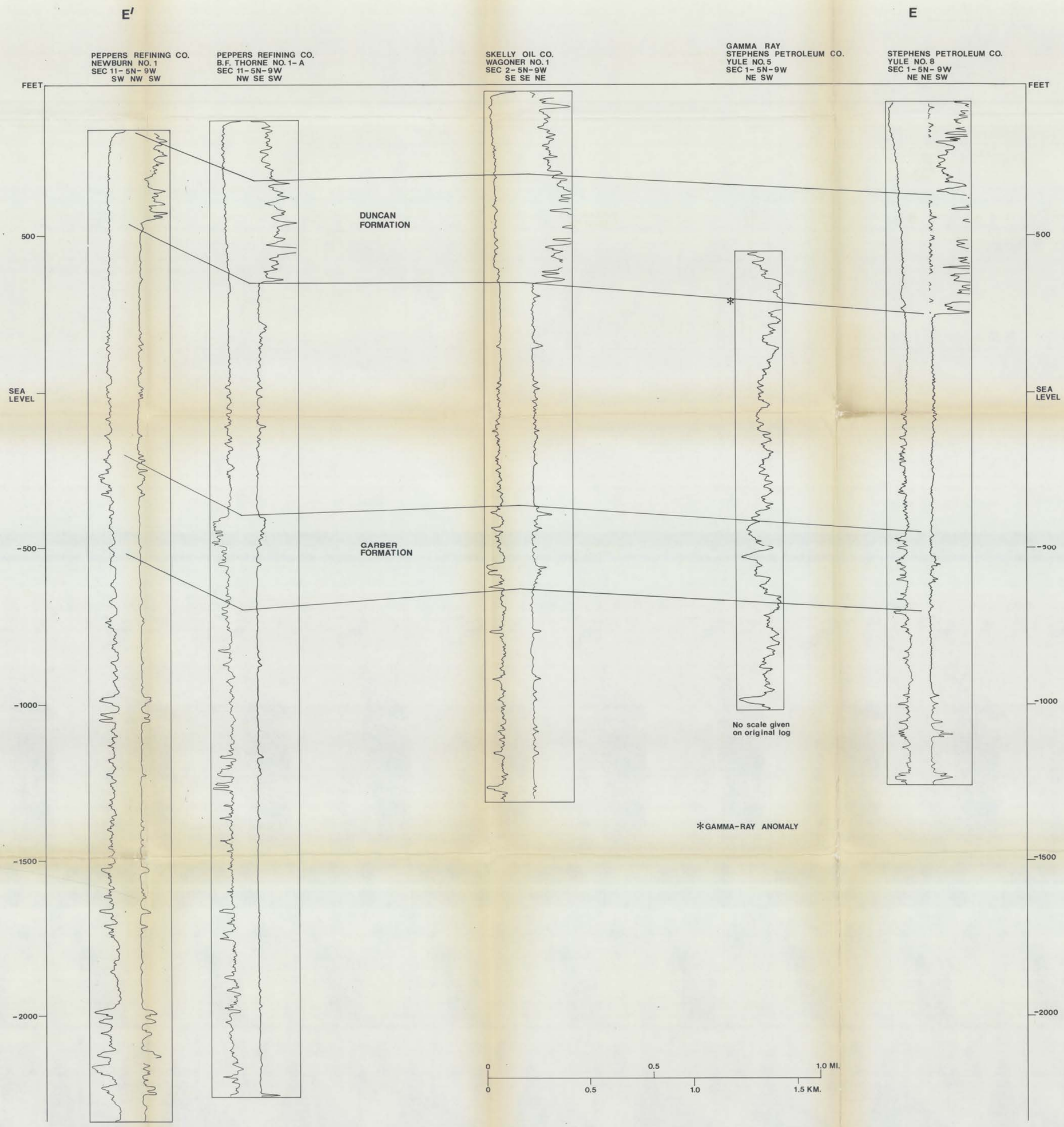

Plate 8. NORTH-SOUTH CROSS-SECTION (E'-E) OF THE PERMIAN SEQUENCE OVERLYING THE CENTRAL PORTION OF THE CEMENT ANTICLINE

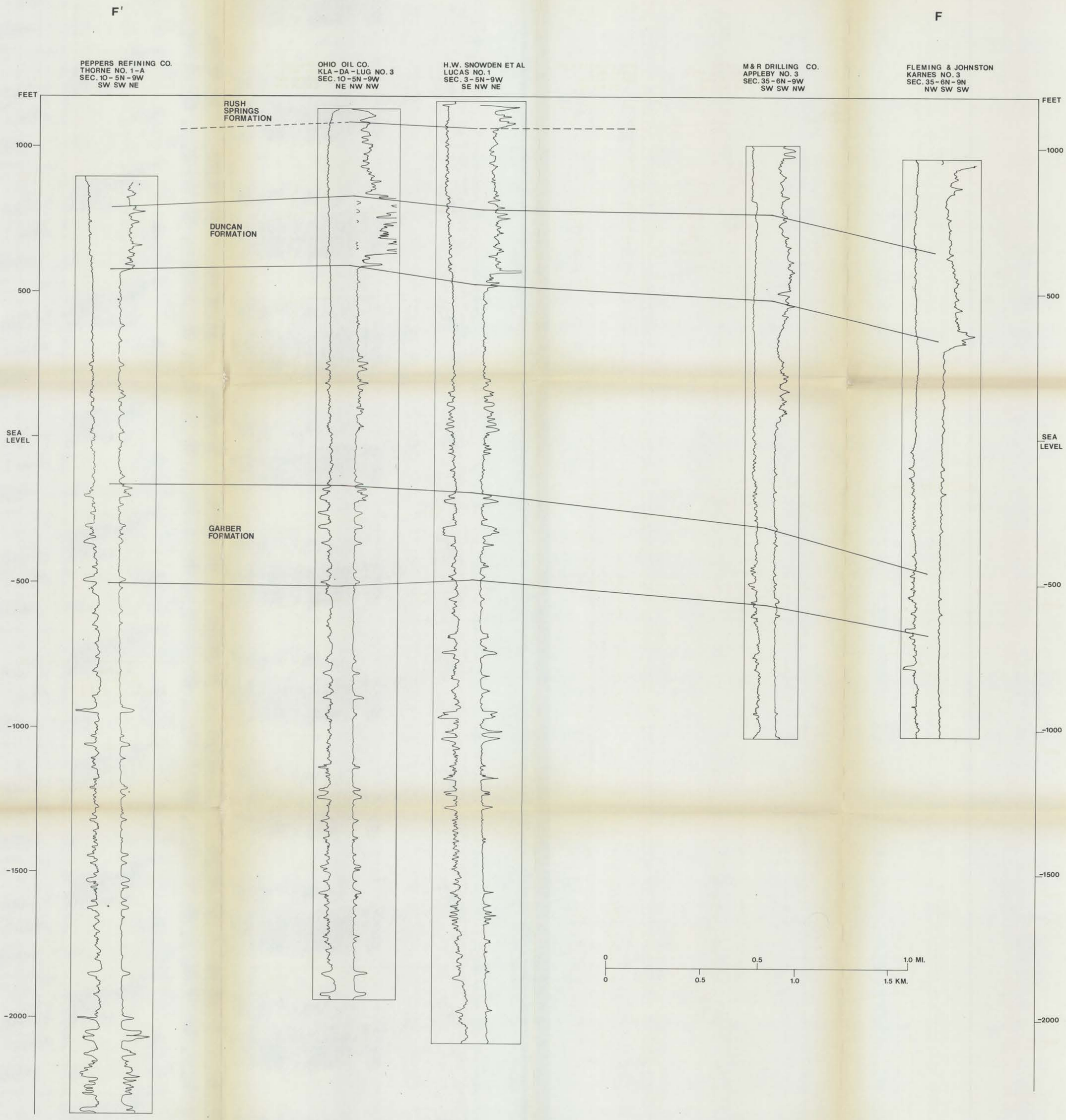

Plate 9. NORTH-SOUTH CROSS-SECTION (F'-F) OF THE PERMIAN SEQUENCE OVERLYING THE CENTRAL PORTION OF THE CEMENT ANTICLINE

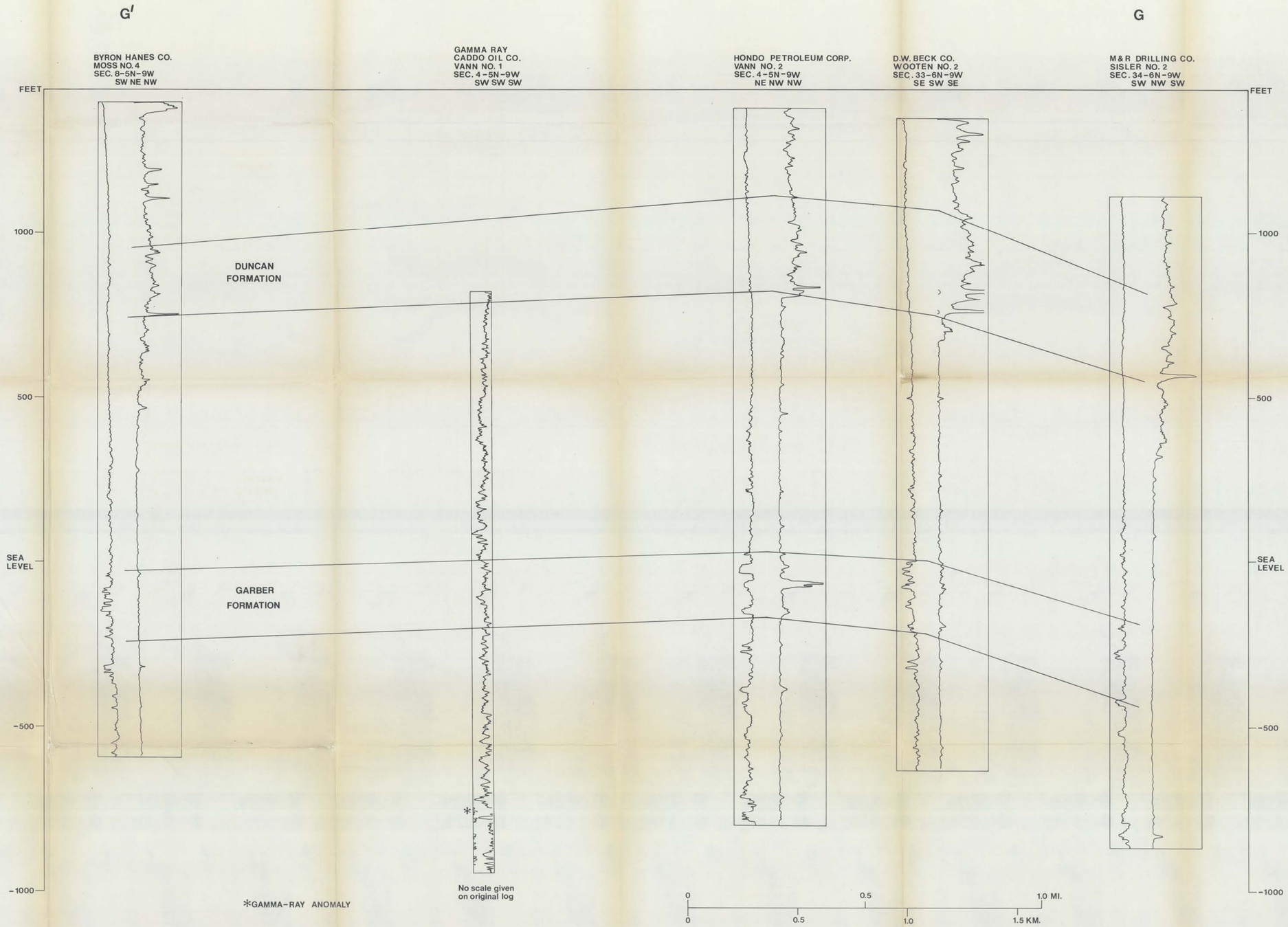

Plate 10. NORTH-SOUTH CROSS-SECTION (G'-G) OF THE PERMIAN SEQUENCE OVERLYING THE WESTERN END OF THE CEMENT ANTICLINE

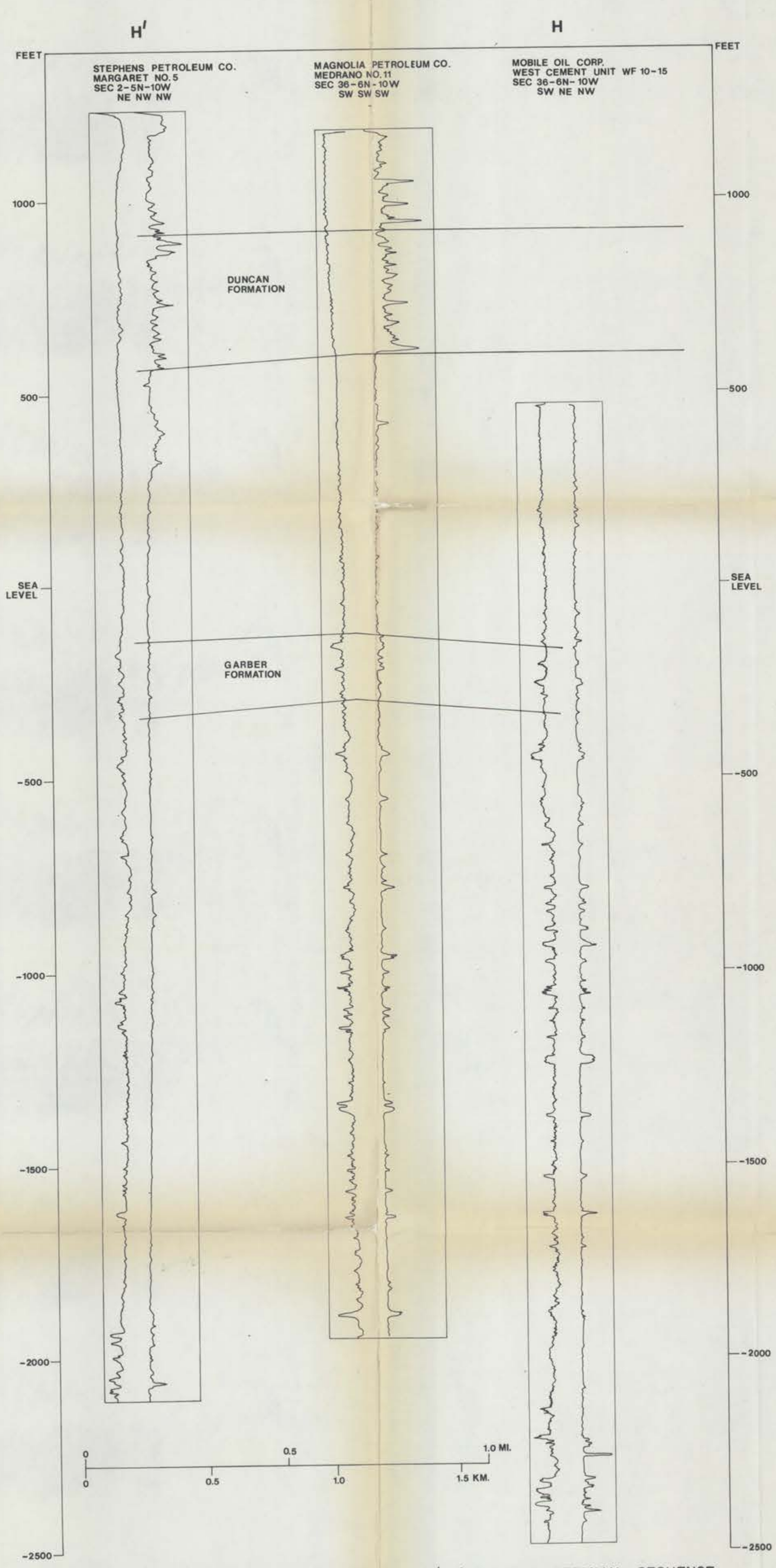

Plate 11. NORTH-SOUTH CROSS-SECTION (H'-H) OF THE PERMIAN SEQUENCE OVERLYING THE WESTERN END OF THE CEMENT ANTICLINE

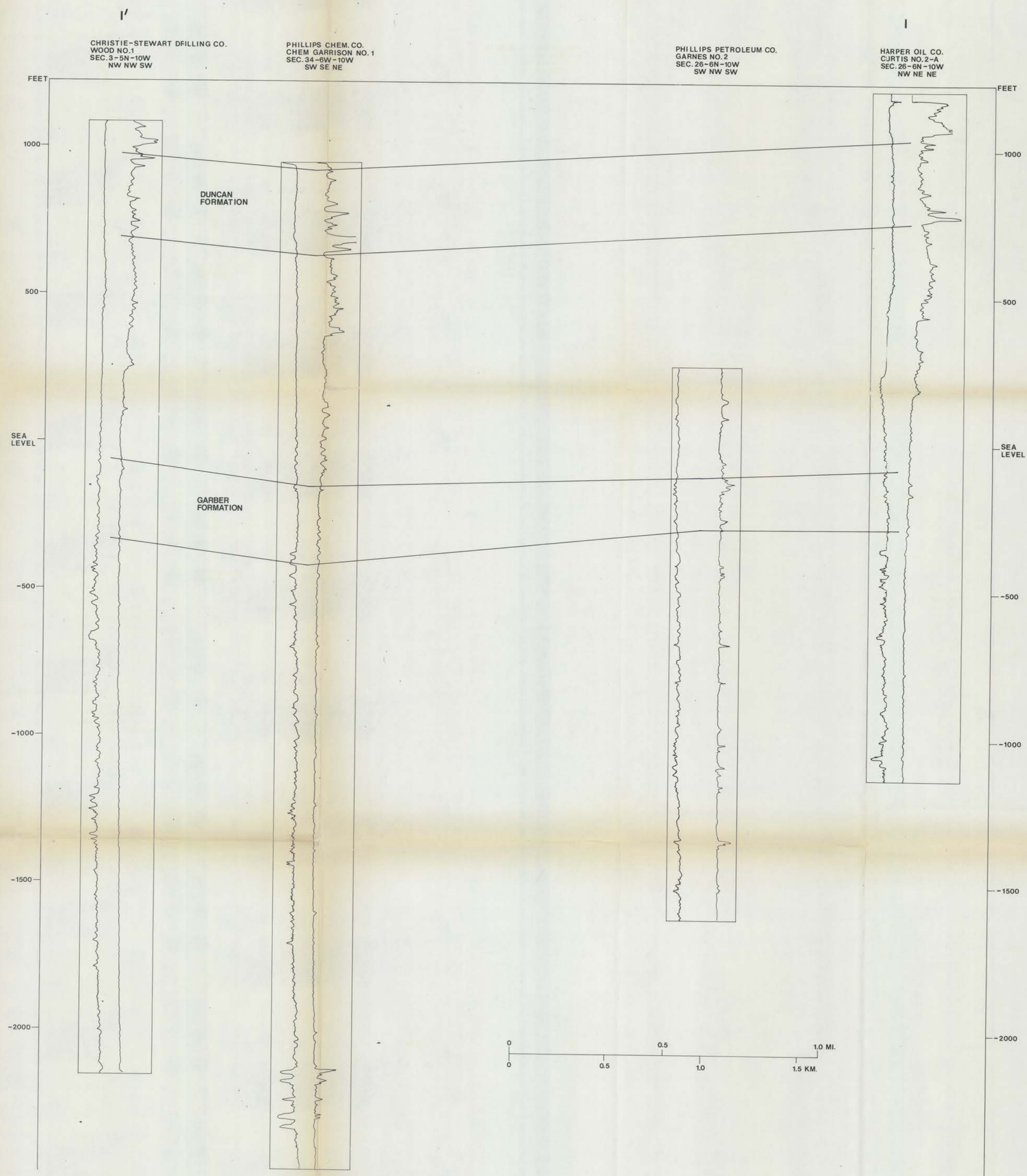

Plate 12. NORTH-SOUTH CROSS-SECTION (I'-I) OF THE PERMIAN SEQUENCE OVERLYING THE WESTERN END OF THE CEMENT ANTICLINE

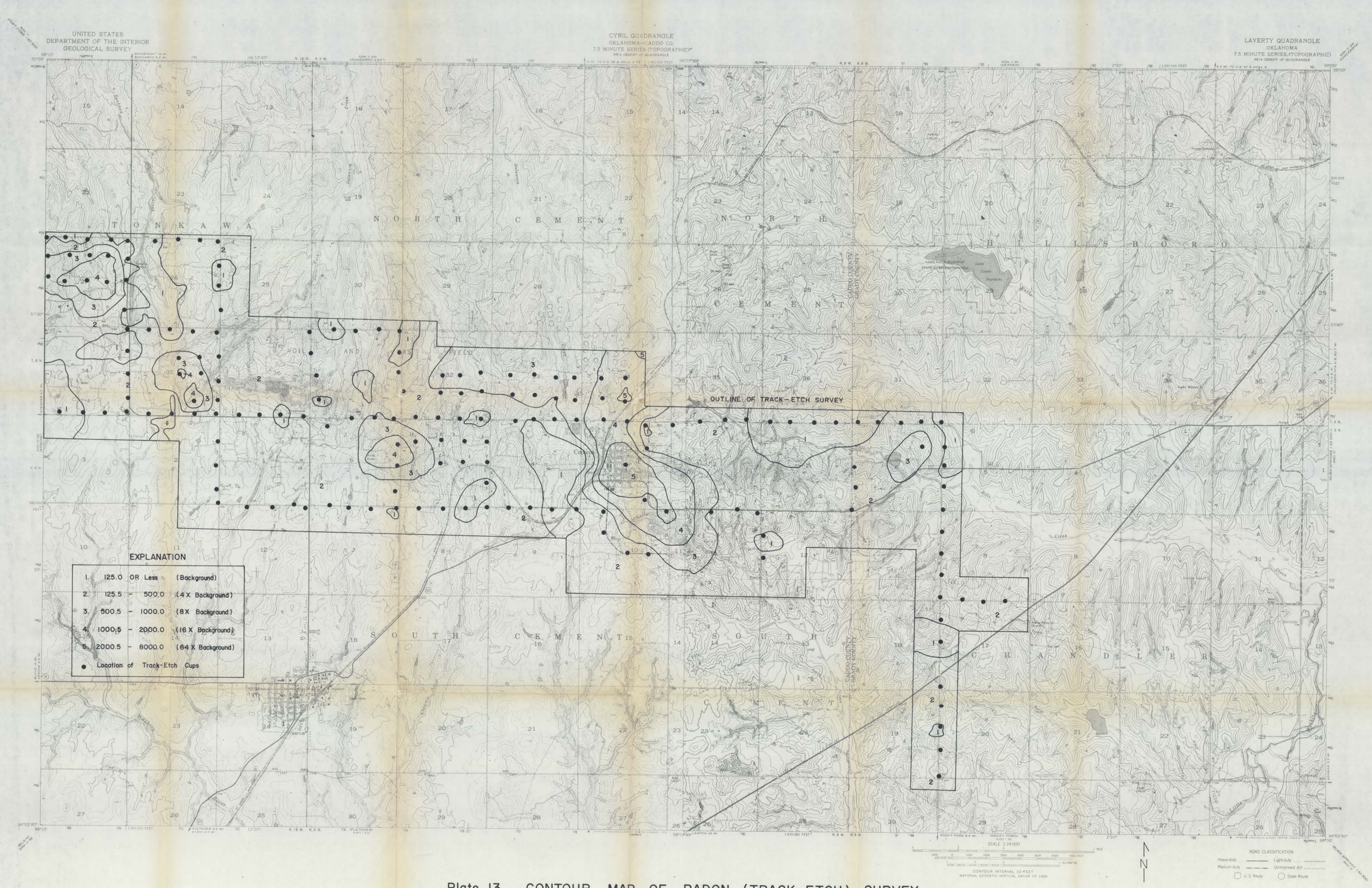

Plate 13. CONTOUR MAP OF RADON (TRACK-ETCH) SURVEY

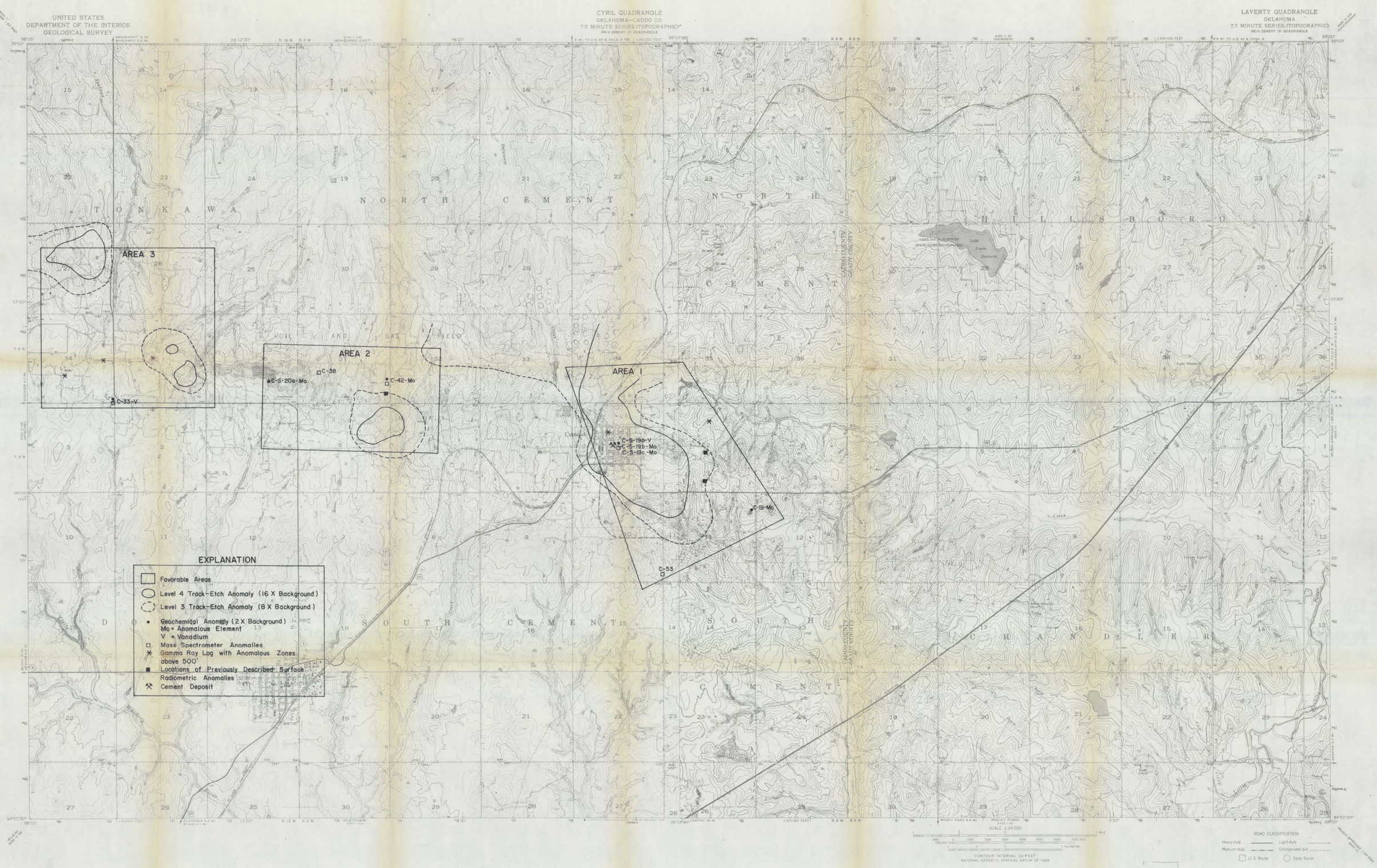

Plate 14. FAVORABLE AREAS, RADIOMETRIC, MASS SPECTROMETER, GAMMA-RAY LOG WELLS (≤ 500 FEET ; ≤ 152 METERS), GEOCHEMICAL ANOMALIES, AND THE LOCATION OF THE CEMENT ORE DEPOSIT